Technische Universität München
Lehrstuhl für Technische Chemie II

Deactivation Routes in Zeolite Catalyzed Isobutane/2-Butene Alkylation and Regeneration Procedures

Iker Zuazo

Vollständiger Abdruck der von der Fakultät für Chemie der Technischen Universität München zur Erlangung des akademischen Grades eines

Doktors der Naturwissenschaften

genehmigten Dissertation.

Vorsitzender: Univ.-Prof. Dr. Thorsten Bach

Prüfer der Dissertation:

1. Univ.-Prof. Dr. Johannes A. Lercher
2. Univ.- Prof. Dr. Frank H. Köhler

Die Dissertation wurde am 06.05.2004 bei der Technischen Universität München eingereicht und durch die Fakultät für Chemie am 27.05.2004 angenommen.

Acknowledgments

Everything comes to an end and, as somebody sang, “nothing lasts forever”. I have to say...yes, nothing lasts forever...but these three years of my life will stay always deep inside me, and nobody can take them out. Besides that, time run like hell...but, of course, that would not be in this way without all the good moments (in- and outside the Uni) with my (already missed) colleagues.

First of all, I would like to give one million thanks to the great group dealing with alkylation at TCII. Johannes, it was a great experience to work with you. We went through easier and more difficult times, times full of stress and also more relaxed times, but at the end of the day, you were always very fair with me, you took always all the time I needed to discuss, and you trusted in me from the beginning. I think we did a good job together and we were successful with our tasks. I had quite a lot of fun with your secret feeling for science (“aus dem Bauch heraus...”) but I have to recognize that it worked many of the times. You were the guide I needed and you showed me how to work as a professional and, therefore, I feel indebted to you. Following with the group of alkylation…Alex and Andreas...well...what can I say about you two, guys? If I could choose a team for my future working life...both of you would be in my team, no doubt about it. It was really a pleasure to work with you. We had a lot of fun, we learned a lot together, and I think we were somehow something more than only “lab-colleagues”. I will miss you a lot, and I hope we can see each other in the next (but not too far...) future. I enjoyed very much all these conversations about similarities-dissimilarities among our countries. Alex, I will never forget these couple of beers at the “Scharfes-Eck” in Garching at the beginning of the times...and now, going to more recent times, I would like to thank Hitri for her huge help. It was not only a pleasure but also very funny to work with you. Without your help I would have needed even the next life to finish all the experiments I wanted to do. Try not to forget all the Spanish that you learned from me, ok? I also want to thank Carsten for the MALDI measurements. Roberta, thank you for all the important corrections you did.

I would also like to say thanks to Xaver Hecht and Andreas Marx. I have never seen so nice setups as the ones you built. You are a genius in this topic and, well, without your

help there would be no way to run reactions. Thanks a lot.

I am also very indebted to all these people that talked to me in German even when it was completely impossible to understand what I wanted to say, and specially Andreas, Christian, Philipp(s), Hendrik (vielen Dank für die Korrektur!), Maria, Su, Jan Olaf, Peter, Josef...and all the rest. Danke euch! Ihr habt mir aber viel geholfen! (Phillip und Peter, es war super mit euch joggen zu gehen...).

I know that with my legendary memory I would forget to thank a couple of you and, that is why, I would like to do it in a more general way. Thank you, TCII group, it was really a pleasure to share this time with you.

I would also like to thank my Spanish friends from München...you gave me the necessary support to finish the thesis.

And now, going a bit more to the inside...I do not know if “thanks” is the right word, but somehow I would like to say something like that to all my family (Aita, Ama, Laika, Javi, Maite, Gonzalo, Ana, June) for all the mountains of love and help you gave me in these past years. Esti, I would specially like to thank you for all your help during the thesis and for all your support during this (sometimes hard) time. I will never forget the nights that I had to spend in the Lab doing reactions/regenerations...it was more than a dream to see you coming with the dinner and a glass of wine...thank you again four your support and for your love.

Iker

Chapter 1

General Introduction

1.1 Introduction to the alkylation process

In chemistry, the term alkylation comprises a variety of reactions, which have in common that an alkyl group of an arbitrary (but usually well defined) carbon number is introduced into an arbitrary substrate by means of an alkylating agent, typically alkene, an alcohol, or an alkyl halide [1]. Alkylation within the petroleum refining industry more specifically refers to a process positioned downstream of the fluid catalytic cracking unit (FCCU, [2]) and is meant to convert part of the C_4 hydrocarbons formed as by-products in the FCCU into the so-called "alkylate", a most valuable component in the refinery's gasoline pool [1].

Alkylate is made up of a complex mixture of branched alkanes which are excellent blending components for gasoline showing a high octane number (research and motor) and a low Reid vapour pressure and being free of aromatics, alkenes and sulphur and therefore, providing benefits in each of its properties versus gasoline specifications. Since the factors that determine gasoline emissions levels are complex, the solutions adopted typically involve controlling the content of sulphur, aromatics, olefins and oxygen.

The alkylation reaction is catalysed by strong acids, of which only sulphuric and hydrofluoric acid, are commercially used [3]. Both acid catalysts commercially used suffer from a variety of safety and environmental drawbacks. Hydrofluoric acid is a corrosive and highly toxic liquid with a boiling point close to room temperature. Refineries based on HF are therefore under pressure to install security systems to minimize dangers from possible HF leaks, and the authorities of many industrialized countries have ceased to license new HF alkylation plants. Sulphuric acid, although being also a corrosive liquid, it is not volatile which makes its handling easier. Its main disadvantage is the high acid consumption required, being about one third of the total operating costs of alkylation units using H_2SO_4 attributed to acid consumption [4]. Equipment corrosion, transport, and handling hazards and environmental liability associated with the disposal of spent acid are disadvantages of both processes [5].

Zeolites, being noncorrosive, non-toxic and rather inexpensive materials, were the first solid acids tested as alternatives to sulphuric and hydrofluoric acid in iso-butane/alkene alkylation [6]. The main drawback in the use of zeolites for iso-butane/butene alkylation is its rapid deactivation, which up to date has impeded its industrial application. Thus, in order to achieve an economically feasible industrial process, the catalysts must be frequently regenerated. The patent literature suggests that multiple regenerations (as many as several hundred) are needed for processes based on solid catalysts to be competitive with existing processes based on H_2SO_4 and HF [1]. Therefore a deep knowledge on the alkylation mechanism and on the deactivation route seems to be mandatory in order to enlarge the lifetime of the catalyst in a single reaction or to be able to continuously perform over a reaction/regeneration procedure over long periods of time with a high productivity, which makes the process economically feasible.

1.2 Reaction / side-reactions mechanism overview

There is general agreement about the mechanism that takes place during the iso-butane/alkene alkylation which is believed to proceed via carbenium type species, both in liquid acids and in the surface of solid acids [1,6-12]. The key elementary steps during the iso-butane/butene alkylation on zeolites would include:

- The alkylation reaction is initiated by the activation of the alkene through its protonation (reaction 1). A Brønsted acid site of the catalyst is considered to be the source of the proton in solid acid alkylation. Thus, the carbenium type species will be bound to the acid site by an alkoxy linkage.

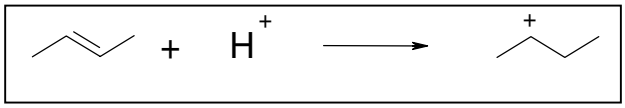

(1)

A secondary carbenium ion would be formed in case of using n-butene as the alkylating agent. The carbenium ion formed may isomerize via a methyl-shift (reaction 2) or receive a hydride transfer from iso-butane to form a tertiary butyl (reaction 3). When iso-butane is used as the alkylation agent a tertiary carbocation would be directly formed.

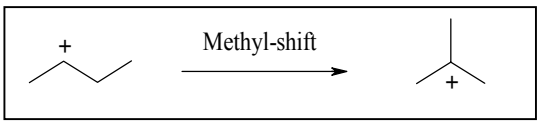

(2)

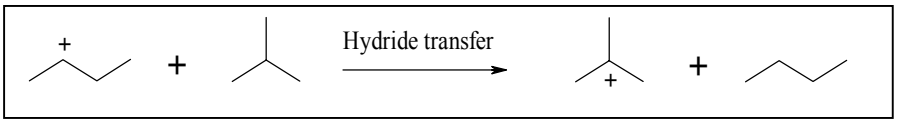

(3)

The skeletal rearrangement needed for reaction 2 is believed not to occur under the typical alkylation conditions due to the high activation energy required. Moreover, double bond shifts between 1-butene and 2-butene, and even more so cis/trans isomerization in 2-butene, are usually very rapid reactions that occur under alkylation reaction even at mildly acidic sites. Therefore, and regardless of whether the *n*-butene used in the feed, an equilibrium or near-equilibrium mixture of them will be available, strongly prevailing 2-butene among them.

- The alkylation itself involves the electrophilic addition of the tertiary butyl species to a butene to form a trimethylpentyl species at the acid site (reaction 4). A fast isomerization of the TMP-cation through hydride- and methyl- shifts occurs, and although the equilibrium composition is not reached, long residence times favour these rearrangements [13]. Therefore different TMPs will be also obtained from the primary product of alkylation (2,2,3-TMP) as a consequence of these hydride- and methyl- shifts. On the other hand, depending on the isomer and the type of carbenium ion involved the addition will lead to different iso-octyl cations, resulting afterwards in a big variety of iso-alkanes [5].

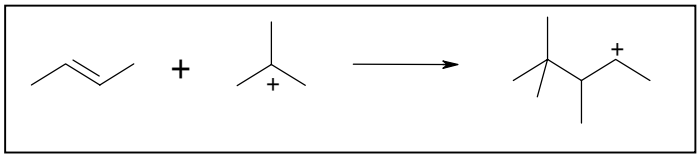

(4)

- The transformation of the ions into the corresponding alkanes is done though intermolecular hydride transfer (reaction 5), typically from iso-butane to an alkyl-carbenium ion, regenerating the tert-butyl cation to continue the chain sequence. Hydride transfer is the crucial step in the reaction sequence. It ensures the perpetuation of the catalytic cycle and leads to the exclusive desorption of saturated compounds. Hydride transfer is a relatively rapid process if both the reactant and the product carbenium ion are tertiary whereas it is

much less favoured if a chemisorbed tertiary carbenium ion reacts with an alkane, which can only give a secondary or a primary carbenium ion [14,15].

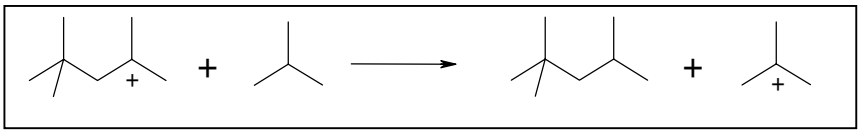

(5)

- Oligomerization and cracking are responsible for the formation of light and heavy-ends, *i.e.*, of iso-alkanes with odd carbon numbers and also partially responsible of some of the C_8 compounds produced during the alkylation reaction. A general oligomerization scheme is presented in Figure 1.

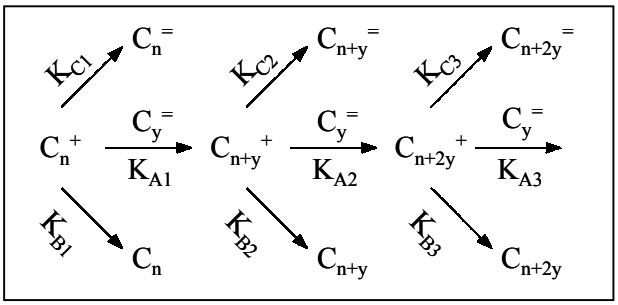

Figure 1. Pathway to oligomerization products with the corresponding rate constants. Adapted from [16].

In the oligomerization scheme K_A defines the rate of alkene addition, K_B defined the hydride transfer rate and K_C the rate of deprotonation. The ratio between hydride transfer and the combined olefin addition and deprotonation is one of the main parameters that determines the lifetime of a catalyst under defined reaction conditions. C_n^+ refers to any carbocation present in the reaction media coming either from the classical alkylation reaction or from any other source as, *i.e.*, cracking, that can undergo oligomerization, alkylation or deprotonation reactions. $C_y^=$ refers to any olefin present in the reaction media coming either from the feed or as a product of cracking or deprotonation reactions.

Cracking of hydrocarbons under typical alkylation conditions is solely produced by β-scission. Weitkamp et al. introduced a useful classification of different modes of β-scission, as shown in Figure 2.

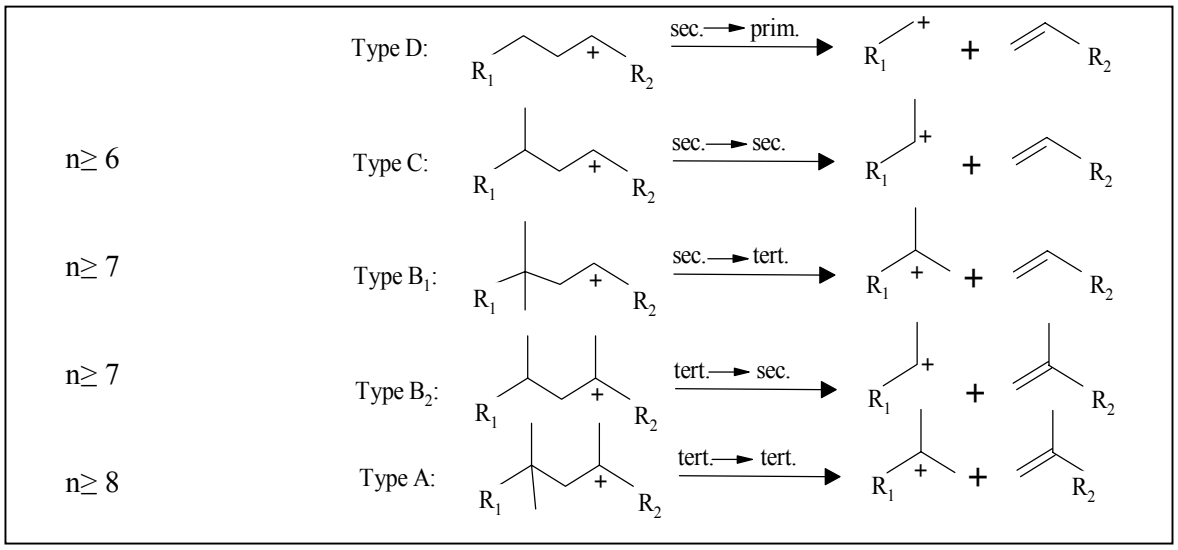

Type A β-scission, which is the most rapid, starts from a tertiary carbenium ion to give again a tertiary carbenium ion and al alkene. Type B β-scission, which is slower than type A β-scission, starts from a tertiary to give a secondary or vice versa. Type C β-scission, which is still slower, starts from a secondary carbenium ion to give another secondary carbenium ion. Type D β-scission, which is the slowest mechanism, start from a secondary carbenium ion and yield a primary carbenium ion.

1.3 Deactivation/regeneration of zeolites

The most common deactivation mechanisms in industrial processes catalyzed by zeolites are [17]:

- Poisoning of the active sites by feed components and impurities, or by non-desorbed heavy products (coke).
- Blockage of the access of the reactant to the active sites (or of the adsorbate to the pores) by coke, by extra-framework species resulting from dealumination, etc.
- Structure alterations.
- Sintering of supported metals (e.g., in bifunctional catalysts).

In the case of iso-butane/butene alkylation the main cause for deactivation is the formation of coke molecules (carbonaceous deposits), which can either poison the active sites or block their entrances. Although the formation of carbonaceous deposits during zeolite-based

alkylation has been the main impediment to its industrial application, characterization of carbonaceous deposits and regenerability of these materials has been only scarcely reported. Guisnet *et al.* [18] are responsible of some of the most interesting studies on the composition of coke and deactivation effect during iso-butane/butene alkylation. The carbonaceous deposits were extracted with methylene chloride, after dissolution of the deactivated catalyst in hydrofluoric acid, and analyzed with GC, IR, ^{1}H-NMR and GC/MS coupling. The authors concluded that the carbonaceous deposits are mainly constituted by aliphatic, highly branched molecules with one or several double bonds. Weitkamp *et al.* [19] characterized the carbonaceous deposits during iso-butane/butene alkylation on LaY zeolite by ^{13}C CP/MAS NMR, concluding that the carbonaceous deposits were essentially paraffinic, perhaps with some multiring naphthenes. Flego *et al.* [20,21] characterized the carbonaceous deposits during iso-butane/butene alkylation on LaHY by *in situ* UV/VIS, FT-IR and ^{13}C CP/MAS NMR. The authors concluded that deactivation was due to acid site poisoning by high molecular weight oligomers as alkenyl carbenium ions. Feller *et al.* [22] proposed the formation of a highly unsaturated and highly branched polymer, which is strongly adsorbed on the acid sites and fills the pores at the end of the reaction. Several authors [23,24] also proposed pore mouth plugging as one of the main effects leading to deactivation.

Several authors focused their studies on the regeneration procedure over the past few years. Querini [25] studied the regeneration of the catalyst by several methods, *i.e.* in air, in ozone, in hydrogen, by using combined treatments and in hydrogen peroxide. The author found hydrogen peroxide to be active for coke oxidation already at 90°C and a successful regeneration was achieved when the ozone treatment was followed by a hydrogen treatment. Ginosar *et al.* [26] studied the regeneration of the catalyst by using supercritical fluids, *i.e.* n-butane, iso-butane, n-pentane and isopentane. They found supercritical fluids more effective than near-critical fluids for the regeneration of the catalyst. Besides that, they found iso-butane to be the most effective among them with the added advantage that iso-butane is an alkylation reactant. Guisnet *et al.* [17,27] and Stöcker *et al.* [28] investigated the regeneration by oxidative treatments. They found that temperatures as high as 600°C are needed to completely oxidize the deposited coke during the alkylation reaction. He *et al.* [29] investigated a regeneration process in which regeneration with dissolved H_2 in iso-butane, as well as regeneration with H_2 in the gas phase, was done with time length from 0.2 to 24 h, regeneration temperature from 25 to 300°C and pressure from 1 to 80 bars. Weitkamp et al.

[30] studied the regeneration of the catalyst with H_2 in the gas phase at 15 bars and up to 300 °C. The authors observed that after this treatment the carbon content was lower than 0.1 wt.%. Several cycles of alkylation and regeneration were successfully performed by the former authors with an identical product composition and butene conversion level in all of them.

1.4 References

1. Weitkamp J., Traa Y., *in* "Handbook of Heterogeneous Catalysis" (Ertl G., Knözinger H., Weitkamp J., Eds), Vol. 4, p.2039, VCH, Weinheim, 1997.
2. Von Ballmoos R., Harris D.H., Magee J.S., *in* "Handbook of Heterogeneous Catalysis" (Ertl G., Knözinger H., Weitkamp J., Eds).
3. Stell J., *Oil Gas J.* **99 (52)**, 75 (2001).
4. Albright L.F., Chemtech 40 (1998).
5. Feller A., Lercher J.A., Proceedings of the DGMK-conference, 2002-4.
6. Feller A., Zuazo I., Guzmán A., Barth J.O., Lercher J.A., *J. Catal* **216**, 313 (2003).
7. Schmerling L., *J.Am.Chem.Soc.* **67**, 1778 (1945).
8. Schmerling L., *J.Am.Chem.Soc.* **68**, 275 (1946).
9. Schmerling L., *Ind.Eng.Chem.*. **45**, 1447 (1953).
10. Guisnet M., Gnep N.S., *Appl. Catal. A* **146**, 33 (1996).
11. Corma A., Martínez A., *Catal. Rev.-Sci. Eng.* **35**, 483 (1993).
12. Cardona F., Gnep N.S., Guisnet M., Szabo G., Nascimento P., *Appl. Catal. A* **128**, 243 (1995).
13. Gorin M.H., Kuhn C.S., Miles C.B., *Ind. Eng. Chem.* **38**, 795 (1946).
14. Deno N.C., Peterson H.J:, Saines G.S., *Chem. Rev.* **60**, 7 (1960).
15. Hofmann J.E., Schriesheim A, Preprints, *Div. Petr. Chem., Am. Chem. Soc.* **6 (4)**, C57 (1961).
16. Simpson M.F., Wie J., Sundaresan S., *Ind. Eng. Chem. Res.* **35**, 3861 (1996).
17. Guisnet M., Magnoux P., *Catal. Today* **36**, 477 (1997).
18. Pater J., Cardona F., Canaff C., Gnep N.S., Szabo G., Guisnet M., *Ind. Eng. Chen. Res.* **38**, 3822 (1999).
19. Weitkamp J., Maixner S., *Zeolites* **7**, 6 (1987).
20. Flego C., Kiricsi I., Parker W.O. Jr., Clerici M.G., *Appl. Catal. A* **124**, 107 (1995).
21. Flego C., Galasso L., Kiricsi I., Clerici M.G., *Stud. Surf. Sci. Catal.* **88**, 585 (1994).

22. Feller A., Barth J.O., Zuazo I., Guzmán A., Lercher J.A., *J. Catal* **220**, 192 (2003).
23. Querini C.A., Roa E., *Appl. Catal. A* **163**, 199 (1997).
24. Sahebdelfar S., Kazemeini M., Khorasheh F., Badakhshan A., *Chem. Eng. Sci.* **57**, 3611 (2002).
25. Querini C.A., *Cat. Today* **62**, 135 (2000).
26. Ginosar D.M., Thompson D.N., Burch K.C., *Appl. Catal. A* (2004).
27. Nassionou G.A.D., Magnoux P., Guisnet M., *Microp. Mesop. Mater.* **22**, 389 (1998).
28. Rørvik T., Mostad H., Ellestad O.H., Stöcker M., *Appl. Catal A* **137**, 235 (1996).
29. He, Y., He Y., Xie W., Fu Q., U.S. Patent 6,492,571 B1 (2002).
30. Josl R., Klingmann R., Traa Y., Gläser R., Weitkamp J., *Catal. Commun.* **5**, 239 (2004).

Chapter 2

Detailed time-on-stream/deactivation study in zeolite catalyzed iso-butane/butene alkylation

Abstract

The product distribution and coke analysis with time-on-stream of rare-earth exchanged zeolite X in iso-butane/2-butene alkylation was studied. The produced alkylate, the deactivated catalysts and the isolated deposits were analyzed by a wide range of techniques. Although saturated compounds are usually considered to be the only alkylation product also small fractions of unsaturated products as alkenes or cyclic compounds were detected. The compounds found in the deactivated catalysts were mainly large alkanes following a $(CH_2)_3$ series. Minor amounts of alkenes and an almost absence of cyclic or aromatic compounds were found in the deposits. The catalyst is deactivated by two different mechanisms: acid site blocking by pore filling (and at some extent by acid site covering) and pore mouth plugging.

2.1 Introduction

Alkylate of iso-butane with C_3-C_5 olefins is an ideal blending component for reformulated gasoline, because alkylate has a high octane number with a low octane sensitivity (difference between RON and MON), and is mainly formed by multibranched paraffins [1]. The reaction is catalyzed by strong acids, of which only sulfuric and hydrofluoric acid, are commercially used [2]. The replacement of sulfuric and hydrofluoric acid is desirable due to their transport and handling hazards, their corrosiveness and the environmental problems associated with the disposal of spent acid.

Zeolites were the first solid acids tested as alternatives to sulfuric and hydrofluoric acid in iso-butane/alkene alkylation [3]. The main factor impeding the industrial use of zeolites as catalysts for iso-butane/butene alkylation has been their rapid deactivation. In order to achieve an economically feasible industrial process, the catalysts must, therefore, be frequently regenerated. The patent literature suggests that multiple regenerations (as many as several hundred) are needed for processes based on solid catalysts to be competitive with existing processes based on H_2SO_4 and HF [4]. A detailed knowledge of product distribution and coke built-up with time-on-stream (TOS) on the catalyst is mandatory to understand the deactivation route(s) of iso-butane/butene alkylation and to find solutions for improvement.

Many of studies reported over the last years on iso-butane/alkene alkylation used either a non-adequate reaction system or non-adequate reaction conditions, favoring rapid catalyst deactivation. Under these conditions, detailed studies on alkylation *vs.* time-on-stream can hardly be performed or the catalysts were investigated at a late stage of deactivation. A high product quality and slow catalyst deactivation, up to 12-16 hours lifetime, has been achieved for the present study by the use of a well-stirred tank reactor operated at very high conversion allowing a minimal olefin concentration, while maintaining high space velocities.

An optimized lanthanum exchanged zeolite of faujasite structure containing platinum was chosen for the study with the aim of better understanding the reasons for catalyst deactivation and the product/coke evolution with time-on-stream. Product distribution was analyzed *on-line* with time-on-stream by GC analysis. The produced alkylate and the recovered deposits from the catalysts were analyzed by several techniques such as ^{1}H-NMR [5-7], GC and GC-MS [5-8] or UV/VIS [6]. Surface coke species were analyzed by UV/VIS [8-12] and MALDI-TOF MS, which was already successfully applied to deactivated zeolites by Feller *et al.* [6].

TPO and BET measurements were applied to the deactivated catalyst to determine the amount of deposited coke and the fraction of free micropore volume with time-on-stream.

2.2 Experimental

2.2.1 Catalyst preparation

The parent material used for this series of experiments was a Na-X zeolite obtained from Chemische Werke Bad Köstritz (Si/Al = 1.2). The parent material was converted in its acidic form by multiple lanthanum ion exchanges and its posterior calcination. In the first step, the parent material was 1-3 times exchanged with a 0.2 M aqueous lanthanum nitrate solution (liquid-to-solid ratio approximately 10 ml/g) at 70ºC for two hours. The resulting material was washed with doubly distilled water to remove nitrate, and then calcined with a slow temperature increment up to 450 ºC maintaining this temperature for one hour. This was followed by a second ion-exchange step and then loading of platinum (ca. 0.3 wt.%) with a $[Pt(NH_3)_4](NO_3)_2$ solution. Samples were calcined and reduced afterwards.

2.2.2 Catalytic experiments

The zeolite based alkylation of iso-butane with 2-butene was carried out in a stirred tank reactor (50 ml Hastelloy C-276 autoclave from Autoclave Engineers Co.) operated in continuous mode at a stirring speed of 1600 rpm. The catalysts, in the form of pellets from 0.7 to 2 mm size, were used in a catalytic basket "Robinson-Mahoney micro stationary catalyst basket" type. In this configuration temperature gradients are avoided compared to the situation in which the catalyst is used as slurry. Liquefied cis-2-butene was received from Messer with 99.5% purity, trans-2-butene being the main impurity. Liquefied iso-butane was received from Messer with 99.95% purity.

For this series of experiments the catalyst sample (typically 2.6 g) was activated *in situ* within the alkylation reactor at 160-190˚C for 16 h in flowing hydrogen. After cooling down to reaction temperature (75˚C) and pressurization with hydrogen, the reactor was filled with liquid iso-butane at a pressure of 20 bars. The iso-butane butene mixture with a molar paraffin-to-olefin (PO) ratio of 10 was by-passed to decrease the delay time as much as possible (the PO ratio was checked by GC analysis before the start of the reaction). The reaction was started by admitting the mixture with a molar PO ratio of 10 and an olefin space

velocity (OSV) of 0.2 g_{butene} / ($g_{catalysts}$ h), conditions that are comparable to those industrially employed for severe operations with H_2SO_4.

Five reactions were performed up to a pre-set TOS. The first reaction was stopped at TOS close to the beginning of deactivation, when butene conversion was not complete anymore. The corresponding time-on-stream was named "lifetime". Four more reactions were done up to 20, 40, 60 and 80 % of the lifetime shown by the catalyst (2.5 h, 5.0 h, 7.5 h and 10.0 h, respectively)

To study the true alkylation performance of the catalysts, the butene conversion has to be complete (which also is the industrial mode of operation). When operating at low conversion levels, oligomerization predominates with mainly unsaturated products and rapid catalyst deactivation as consequence. Once a reaction was stopped, the coked sample was dried with N_2 at reaction temperature and stored for further analysis.

The products from the alkylation reaction were passed through a six-port-valve with a sample loop after the pressure was lowered to ambient pressure. The contents of the loop in the six-port-valve were injected automatically into an HP 6830 gas chromatograph equipped with a FID-detector and a 50 m DB-1 column. Downstream of the six-port-valve, the product stream was condensed into a cold trap cooled with a dry ice/iso-propanol mixture (at T = –80 ºC). The product was collected over the whole time-on-stream and was weighed and analyzed chromatographically to give the integral product composition. The results were compared with the mathematical integration of the differential data points gathered during the run, with the differences being less than 10%.

Note that the alkylation reactions were not performed at steady state in strict sense. When the reaction was started, the reactor only contained iso-butane. With the introduction of the iso-butane/butene mixture and the subsequent (near-) complete conversion of butene, the contents of the reactor steadily change their composition to an iso-butane/product mixture, with an increasing fraction of products with time-on-stream. Under typical conditions (catalyst mass = 2.6 g, P/O ratio = 10 and OSV = 0.2 hrs^{-1}), steady state is theoretically reached after approximately 20 hrs, with the exit stream consisting of a 20-25 wt.% products in iso-butane mixture. However, typical catalyst lifetimes were only in the range of 5 to 14 hours. With the knowledge of the theoretical butene build-up curve derived from the mass balance (and its experimental verification in a blank run without catalyst) conversions and

yields were calculated. At complete butene conversion the theoretical maximum yield is 2.04 $g_{product}/g_{butene}$, assuming a 1:1 stoichiometry of iso-butane alkylation with butene.

2.2.3 Catalyst characterization

The prepared material was analyzed by a broad range of different physicochemical methods. The amount of remaining sodium (Na^+) and the bulk Si/Al ratio were determined by AAS. The crystallite size and morphology was analyzed by SEM and the unit cell size by XRD. With nitrogen adsorption at 77K the pore volume was estimated. Two different adsorption / desorption methods were used for acidity measurements, i.e., pyridine TPD in a vacuum-setup with a mass spectrometric detector to estimate the total concentration of acid sites (at an adsorption temperature of 150 ºC and a slow ramp up to 800 ºC); sorption of pyridine monitored by IR spectroscopy to estimate the amount of Brønsted and Lewis acid sites as well as their strength.

2.2.4 Alkylate analysis

The alkylate produced was condensed in a trap cooled with a mixture of iso-propanol and dry ice at a temperature of ca. –80 ºC. After iso-butane evaporation, the liquid product (referred to as alkylate) was stored for further analysis. Next to the GC analysis the alkylate was analyzed by UV/VIS using a U-3000 Hitachi spectrophotometer from 190 to 500 nm. Hexane was used as a reference and also to further dilute the alkylate samples. By this technique relevant information on the olefinic and/or aromatic nature of alkylate samples was achieved. The alkylate was also analyzed by ^{1}H-NMR on a Bruker AM 360 spectrometer to obtain information on the abundance of the different functional groups present. $CHCl_3$ was used as an internal standard for calibrating the chemical shift (δ $CHCl_3$ = 7.24 ppm from TMS).

2.2.5 Characterization of used zeolites

Reactions were stopped after 2.5, 5, 7.5, 10 and 12.5 hours (20, 40, 60, 80 and 100% of the lifetime previously shown by the catalyst, respectively). The used catalysts were dried with a 100 ml/min flow of N_2 at reaction temperature and then stored for further analysis. UV/VIS spectra of the samples were recorded in a home-made cell using the fresh zeolite as standard in a wavelength range from 200 to 500 nm. Non-paraffinic compounds were seen in

all the measured samples. By TPO analysis, the fraction of carbon deposited and the maximum temperature required to completely burn it were determined. Matrix-assisted laser desorption/ionization time-of-flight mass spectroscopy (MALDI-TOF MS) was used to obtain the molecular weight distribution of the hydrocarbons deposited on the outer surface of the zeolite particle. A solution of 1% trifluoroacetic acid in acetonitrile was prepared. 10 mg of the deactivated catalyst were suspended in 100 µl of this solution. Another 100 µl of this solution were saturated with dihydroxybenzoic acid. The two parts were mixed and 0.5 µl of the resulting suspension were deposited on the sample holder. After air-drying the drop, the sample holder was introduced into the ion source of the mass spectrometer. MALDI-TOF mass spectra were recorded using a Bruker Biflex III MALDI-TOF mass spectrometer equipped with a N2 laser (ν = 337 nm) operating at a pulse rate of 3 Hz. The ions were accelerated with pulsed ion extraction after delay of 50 ns by a voltage of 28.5 kV. The analyzer was operated in reflecton mode, and the ions were detected using a microchannel-plated detector. The mass spectrometer was calibrated prior to measurement with a polystyrene standard of appropriate molecular mass. The same instrument was also used in laser desorption/ionization mass spectroscopy (LDI-MS). Here, the sample was suspended in water and put on the target without matrix. The experiments were conducted using the same settings as in the MALDI measurements. BET measurements were carried out to obtain the fraction of micropore volume still free at different times-on-stream

Deposits from the samples were made available by dissolution of the deactivated zeolite in 40% HF solution at room temperature. Unreacted HF was evaporated and the remainder was extracted with methylene chloride. The yellow/brown colored hydrocarbon phase contained the deposits and was used for further analysis. Coke formed from reaction at low temperatures was suggested to be 100% soluble in organic solvents [13] and to remain unaltered after the treatment with HF [14].

The deposits were characterized by UV/VIS spectroscopy upon dissolution with hexane in the wavelength region from 190 to 500 nm to obtain information on the olefinic and/or aromatic nature of the deposited compounds. They were also analyzed by ^{1}H-NMR spectroscopy on a Bruker AM 360 spectrometer. After evaporation of the methylene chloride solvent, the remaining tar-like polymer was re-dissolved in $CDCl_3$. Traces of $CHCl_3$ in the solvent were used as an internal standard for calibrating the chemical shift (δ $CHCl_3$ = 7.24 ppm from TMS). GC-MS was used to obtain information on the number and on the structure

of the individual compounds. MALDI mass spectra of the deposits were taken and compared with mass spectra of the deactivated zeolites.

2.3 Experimental results and interpretation

2.3.1 Physicochemical characterization

The fresh PtLaX sample was analyzed by a wide range of physicochemical techniques. The particle size determined by SEM ranged from 1 to 2 μm. A small fraction of particles with sizes smaller then 1μm was also observed. The SEM picture of this sample is shown in Figure 2.1.

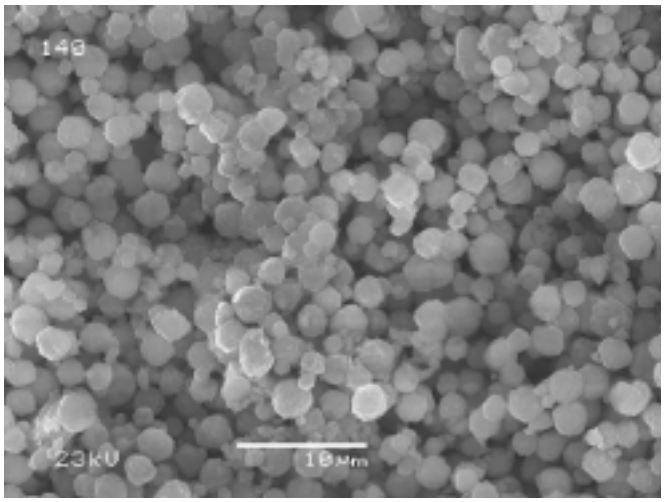

Figure 2.1: SEM of PtLaX sample.

The Na/Al molar ratio was 0.42 % and the bulk Si/Al was 1.11 as measured by AAS. The micropore volume measured by N_2 adsorption after activation at 120°C in vacuum for 10 hrs was 0.177 ml/g. The unit cell size was measured with X-ray diffraction for the parent material (Na-X) catalyst and for the exchanged/platinum-loaded catalyst. The unit cell size measured for the parent material was 24.98 Å (cubic lattice) and for the exchanged/platinum-loaded catalyst it was 25.01 Å. The main factors influencing the variation in the unit cell size are the ion exchange degree and the degree of dealumination. A higher exchange degree would be reflected in a higher unit cell size and a higher dealumination degree would produce a decrease in the unit cell size value. The total acid site concentration measured with TPD of

pyridine was 0.85 $mmol_{pyridine}/g_{catalyst}$. Sorption of pyridine monitored by IR spectroscopy was used to differentiate between Brønsted and Lewis acid sites and to obtain their relative strength and concentration. Three bands of adsorbed pyridine were analyzed, i.e., (i) the band at 1545 cm^{-1} indicative of pyridinium ions (sorption at Brønsted acid sites), (ii) the band at 1451 cm^{-1} indicative of pyridine bound at Al^{3+} Lewis acid sites and (iii) a band due to coordinatively bound pyridine between 1448 and 1435 cm^{-1} due to pyridine adsorbed on exchanged cations [15]. Ratios of extinction coefficients were taken from ref. [16]. The ratio of extinction coefficient for the band corresponding to pyridine-cation interactions remains unknown, and therefore no attempt to determine the total acidity by pyridine-IR was made. The acidity data of these materials are summarized in Table 2.1.

Table 2.1: Acid site characterization of the fresh catalyst.

Sample	Total acid site concentration[1]	BAS[2] 1545 cm^{-1} (150°C)	Strong BAS[2] (450°C)	LAS[2] 1451 cm^{-1} (150°C)	Strong LAS[2] (450°C)
	mmol/g	mmol/g	%	mmol/g	%
Pt-La-X	0.85	0.302	55	0.124	56

[1] Measured by adsorption of pyridine at 150°C measured by TPD analysis

[2] Measured by adsorption/desorption of pyridine monitored by IR

The IR spectra of adsorbed pyridine show that the concentration of strong BAS was 0.166 mmol/g and that the concentration of weak LAS was 0.124 mmol/g. In line with the criteria of Feller et al. [3] for suitable catalysts, the material used in the present study has a high concentration of strong Brønsted acid sites and a low concentration of weak Lewis acid sites. The authors found that suitable catalysts possessed a concentration of strong BAS between 0.1 and 0.15 $mmol/g_{catalyst}$ and a concentration of weak LAS between 0.1 and 0.12 $mmol/g_{catalyst}$.

2.3.2 Alkylation of iso-butane with n-butene

At 75°C, a P/O ratio of 10, and an OSV of 0.2 g butane/ ($g_{catalyst}$ h) the catalyst fully converted butene for 12.5 h (catalyst lifetime). Once the catalyst showed signs of slightly incomplete conversion of n-butene, it rapidly stopped producing alkylate. The deactivated

catalyst showed, however, low activity for the dimerization of n-butene for prolonged time on stream.

Figure 2.2 (a) compiles the product group selectivity for the three main groups of reaction products, *i.e.,* alkanes with 5 to 7 carbon atoms, octane isomers and alkanes with 9 and more carbon atoms (heavy fraction) as a function of time-on-stream. The selectivity to octanes remained constant during the first 5 hours and then decreased from 90 wt. % to approximately 75 wt.% at the beginning of deactivation. The light alkanes (C_5-C_7) generated by cracking and hydride transfer slightly increased in selectivity until the catalyst started to deactivate reaching a maximum value of approximately 14 wt.%. The selectivity to heavy fraction (C_{9+}) remained constant and low (around 8 wt.%) up to a time-on-stream close to the end of the catalyst lifetime.

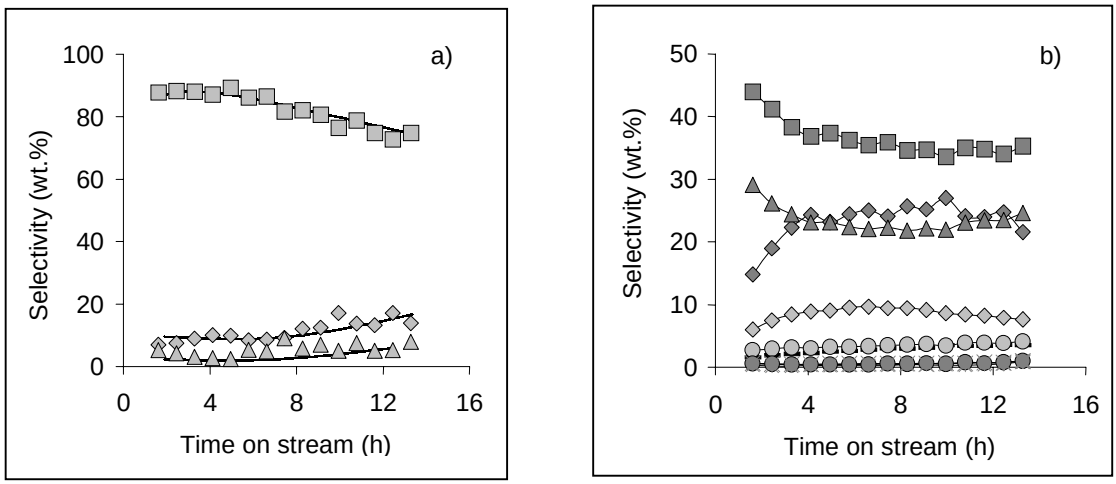

Figure 2.2: Alkylation performance of catalyst Pt-La-X_2. a) Product group selectivities with time-on-stream (◆ C_5-C_7 products, ■ C_8 products, △ C_{9+} products); b) selectivities in the C_8 fraction with time-on-stream (■ 2,3,3-TMP, ◆ 2,2,4-TMP, ▲ 2,3,4 TMP, ◇ 2,5-DMH/2,2,3-TMP, ○ 2,3-DMH, - 4-MHP/3,4-DMH, ● 2,4-DMH, × 3,4-DMH, ✳ Octenes). T = 75°C, OSV = 0.2 h^{-1}, P/O = 10.

The selectivity within the C_8 fraction is depicted in Figure 2.2 (b). Trimethylpentanes were the dominating isomers. It should be noted that trimethylpentanes are thermodynamically less favorable than dimethylhexanes indicating that isomerization

equilibrium with respect to the branching of the alkanes was not achieved. Within the trimethylpentanes, 2,3,3-TMP, 2,2,4-TMP and 2,3,4-TMP dominated and constituted together more than 80 wt.%. The 2,2,4-TMP selectivity increased during the first hours on stream, and it remained constant during the next hours. 2,2,3-TMP, which is the primary product of the alkylation of iso-butane with 2-butene (not separated from 2,5-DMH) passed through a maximum of selectivity at 10 wt.% following approximately the same trend as 2,2,4-TMP. High 2,2,4-TMP selectivity was accompanied by high 2,5-DMH/2,2,3-TMP selectivity. The rest of the compounds showed selectivities below 5 wt.% during the time of complete butene conversion. At the end of the lifetime, the selectivity to 3,4-DMH increased and octenes appeared in the product stream.

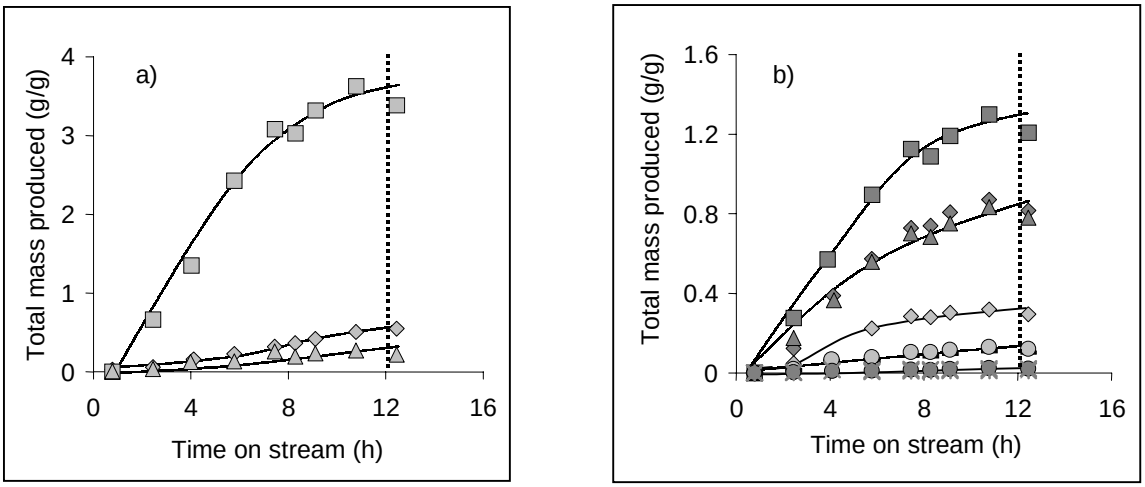

Figure 2.3: Alkylation performance of catalyst Pt-La-X. a) Total amount produced of the different product groups with time-on-stream (◇ C_5-C_7 products, ■ C_8 products, △ C_{9+} products); b) total amount produced of the individual C_8 products with time-on-stream (■ 2,3,3-TMP, ◆ 2,2,4-TMP, ▲ 2,3,4 TMP, ◇ 2,5-DMH/2,2,3-TMP, ○ 2,3-DMH, - 4-MHP/3,4-DMH, ● 2,4-DMH, × 3,4-DMH, ✳ Octenes).

In order to explore better the relation between the products, the integral amount of individual compounds produced with TOS was examined. In Figure 2.3 (a) the total amount of group products is depicted. The dashed line represents the approximate end of the complete butene conversion. The rate of formation of C_8 decreased after 8 hours on stream up to the end of the lifetime of the catalyst where octanes were not produced anymore. Feller et al. [3]

showed that the amount of C_8 formed during the deactivation time is mainly composed of octenes, being the formation of octanes stopped, at times close to the lifetime of the catalyst, as it can be seen in Figure 2.3 (b). The rate of formation of cracking products was constant along the catalyst lifetime and, on the other hand, heavy compounds started to be significant after 6 hours on stream.

2.3.3 Alkylate characterization

The alkylate samples collected during the individual experiments were analysed by UV/VIS spectroscopy. The results are compiled Figure 2.4. Due to the unknown concentrations and extinction coefficients of the individual compounds, the results are discussed only in qualitative terms. The range of measurement was from 190 to 500 nm. All spectra showed a complex absorbance from 200 - 300 nm. The main bands had maxima at 203nm, 223nm, 273nm and 283nm. Classically, molecules containing a conjugated double bond were considered to show a maximum absorption at higher values than 217 nm, molecules containing a homoannular conjugated double bond at higher values than 253 nm and molecules containing an heteroannular conjugated double bond at higher values than 214 nm. More recent studies showed that these values are only valid in case of molecules without strong steric effects. As an example, the authors expected a maximum absorption for 1,2-bis-(methylene)-cyclohexane of 273 nm while they experimentally found it at 220 nm [17]. This makes complicate a precise attribution of the bands experimentally measured for the alkylate. The band at 203 nm was predominant in all the alkylate samples. Bands at 223, 273 and 283 nm were almost absent for the alkylate corresponding to 2.5 hours on stream and their significance increased with time-on-stream. The spectrum from the sample at 100% lifetime showed a different pattern in which the abundance of compounds represented by peaks at 223, 273 and 283 nm decreased. This effect was seen once the butene conversion was lower than 100% and a higher amount of olefins were present in the product, which could provoke a shift in the relative intensity of the different bands. This effect can be attributed to a Diels-Alder reaction type of a conjugated double bond with an olefin to give a cyclic compound containing a non-conjugated double bond, which explains the disappearance of the high absorption wavelength bands.

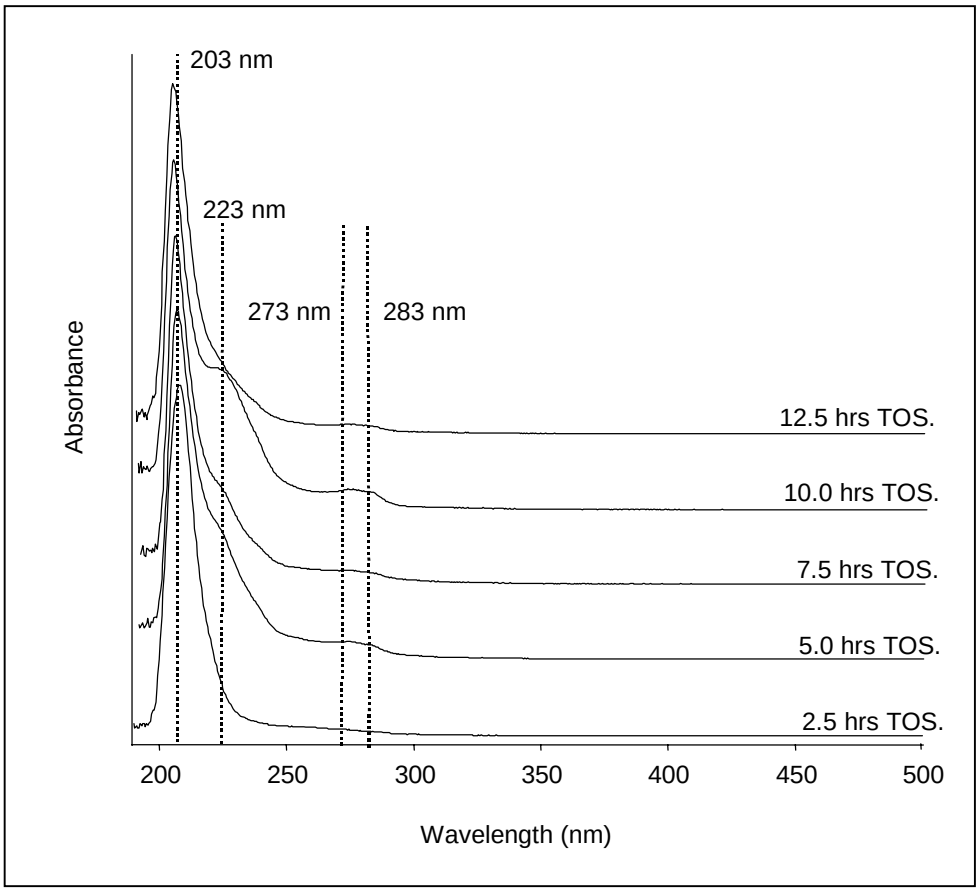

Figure 2.4: UV/VIS spectra of the alkylate collected during the different runs.

The alkylate collected at different times-on-stream was also analyzed by ^{1}H-NMR spectroscopy. The NMR spectra of alkylate are displayed in Figure 2.5. The chemical shift range from 3 ppm to 10 ppm was 2000 times magnified for all spectra in this figure. The fraction of protons in the individual positions obtained by the integration of the NMR spectra is shown in Figure 2.6. The signals between 0 and 1.1 ppm, which are the most abundant in all spectra, correspond to protons in CH_3 groups in α position to saturated C atoms with values between 86 and 87%. Signals between 1.1 and 1.4 ppm correspond to protons in CH_2 groups and signals between 1.4 and 1.7 correspond to protons in CH groups. No marked changes were seen in these groups with time-on-stream with values of ca. 6%. As an average, the CH_3, CH_2 and CH percentages would lead to an *i.e.* C_8 molecule containing five methyl groups in total. Signals between 1.7 and 3.5 ppm represent protons in CH_3, CH_2 and CH groups in α

position to unsaturated or aromatic carbon atoms. Due to the broad distribution of chemical shifts for these protons, a further classification within this range was not attempted. The fraction of protons within this chemical shift range increased steeply at the beginning of the reaction (0.008% at 2.5 h TOS to 0.016% at 5 h TOS). Then it remained constant up to 10 hours on stream, increasing again to a value of 0.022% at a time-on-stream close to the lifetime of the catalyst. Protons of olefinic groups appear between 4 and 6.6 ppm. Within this range a moderately intense peak was observed at 5.45 ppm. This is attributed to remaining traces of unreacted 2-butene. Up to 7.5 hours on stream, they amounted for ca. 0.025% increasing to ca. 0.07% in the next hours. Aromatic protons absorb in the range from 6.6 to 9 ppm. Two signals in this range (7.5 and 7.7 ppm) appeared after 10 hours on stream with a value of ca. 0.01 %. Those are tentatively attributed to protons of condensed aromatic molecules containing two rings. The lack of signals at higher chemical shifts than 8.1 ppm in the spectra suggests the absence of condensed aromatic molecules with three or more rings.

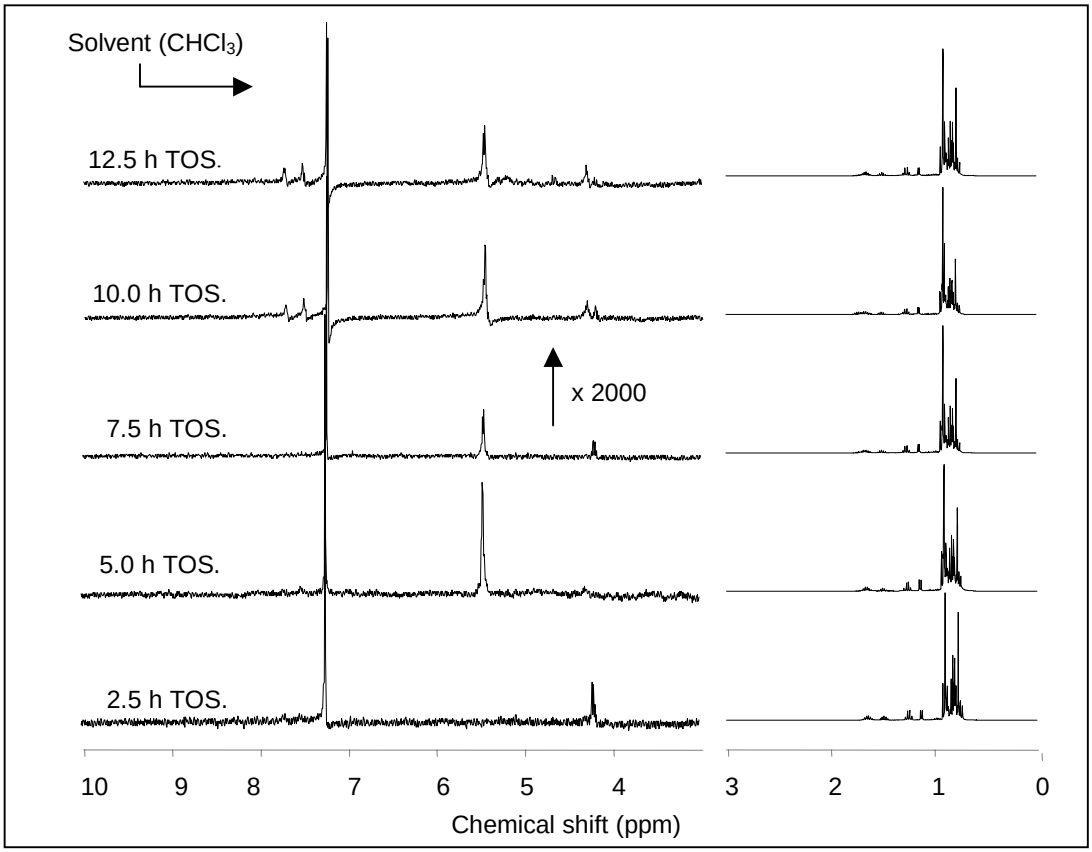

Figure 2.5: ^{1}H NMR spectra of alkylate collected during the different runs.

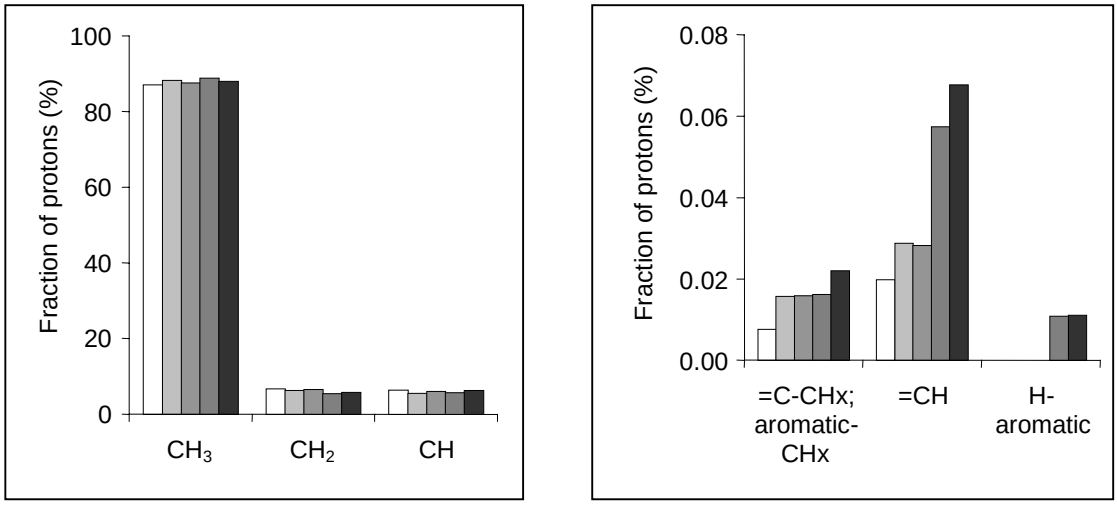

Figure 2.6: Fraction of protons in the individual positions obtained by the integration of the NMR-spectra in Figure 1.7. (□ 2.5 h TOS, ▫ 5 h TOS, ▫ 7.5 h TOS, ▫ 10 h TOS, ■ 12.5 h TOS).

2.3.4 Characterization of coked catalyst

UV/VIS spectroscopy

The coked catalyst was analyzed by UV/VIS spectroscopy. In Figure 2.7, spectra of the UV/VIS detectable compounds formed during the alkylation reaction at different times-on-streams are depicted. Four main bands were present for all the spectra in the following ranges: 280-340, 340-420, 440-500 and 500-600 nm. These bands are attributed to allyl-type carbenium ions [10]. Bands in the 280-340 nm wavelength range were attributed to mono-enyl carbenium ions, in the 340-420 nm wavelength range to dienyl carbenium ions, in the 440-500 wavelength range to trienyl carbenium ions and in the 500-600 nm wavelength range to tetraenyl carbenium ions [18]. Although these bands were attributed to allyl carbenium ions they could also be attributed to aryl carbenium ions (which appear at higher wavelength than 300 nm) or to benzenium cations (which appear at higher wavelength than 200 nm) [19].

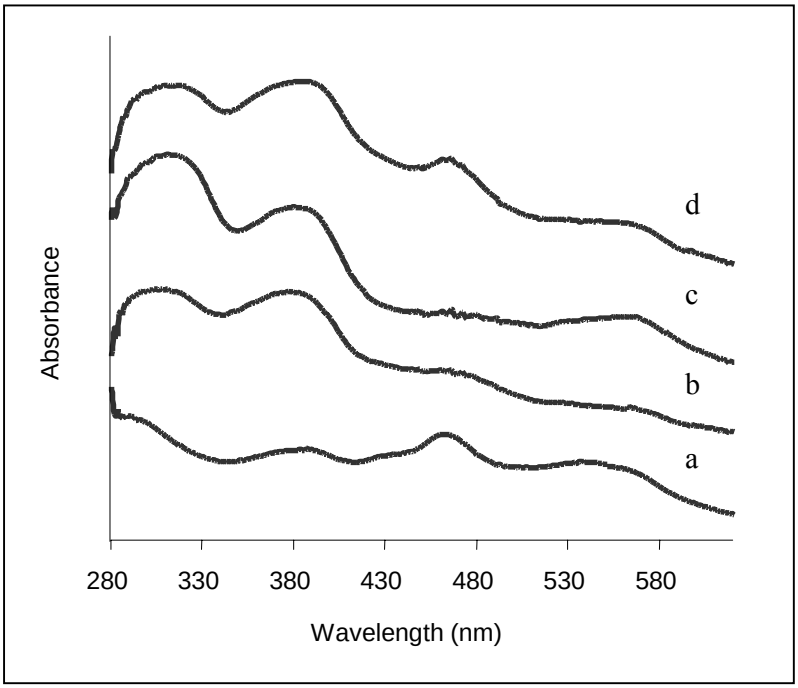

Figure 2.7: UV/VIS spectra of the coked zeolite different times-on-stream. (a) After 2.5 h TOS; (b) after 5 h TOS; (c) after 10h TOS; (d) after 12.5 h TOS.

Low intensity bands with maxima at 310 nm and 385 nm were present after 2.5 hours on stream corresponding to mono and dienyl carbenium ions. The catalyst also showed after 2.5 hours on stream a moderately intense peak with a maximum at ca. 465 nm corresponding to trienyl carbenium ions. The latter was almost absent for catalysts after 5 and 10 hours on stream although it was more intense again after 12.5 hours on stream. Spectra after 5, 10 and 12.5 hours on stream showed high intensity peaks with maxima at ca. 310 nm and 385 nm, respectively.

Temperature programmed oxidation (TPO)

The rate of CO_2 evolution of the coked catalysts during TPO are shown in Figure 2.8 (a). Two main peaks were present in the spectra for all coked zeolites: the low temperature peak below 300°C and a high temperature peak at temperatures ranging from 400 to 600°C. Samples at 10 and 12.5 hours on stream showed an additional peak overlapped to the low temperature peak with a maximum at ca. 30°C lower temperature than the former. The

maximum for the low temperature peak remained at values close to 250°C during the whole reaction. On the other hand, a 50°C shift to higher temperatures with time-on-stream (from ca. 480°C to 530°C) was seen for the high temperature peak when going from 2.5 to 12.5 hours on stream.

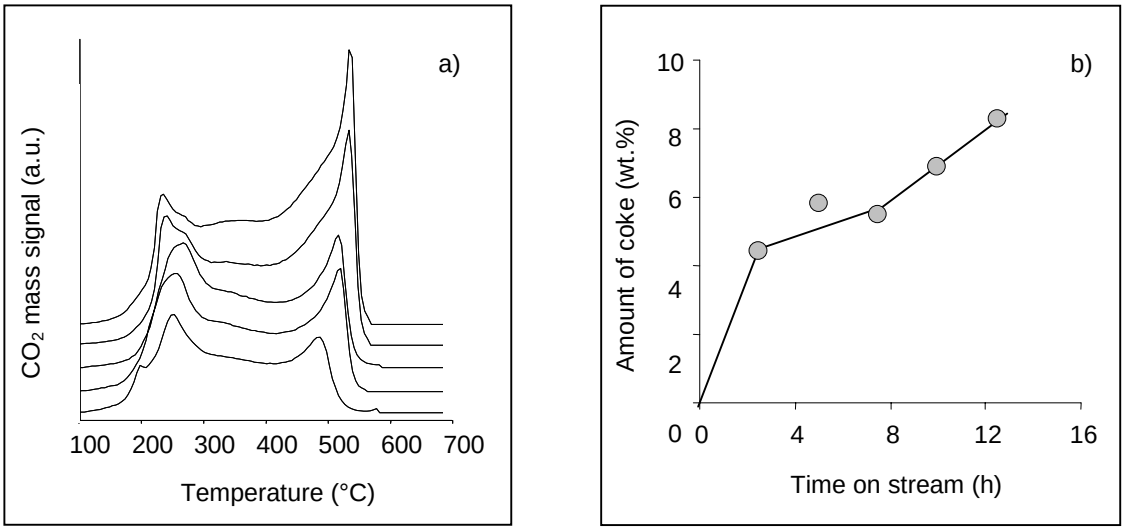

Figure 2.8: a) CO_2 mass signal for TPO analyses of the coked catalysts at different times-on-stream. (a) After 2.5 h TOS; (b) after 5 h TOS; (c) after 7.5h TOS; (d) after 10 h TOS; (e) after 12.5 h TOS. b) Amount of coke as a function of time-on-stream.

The area of the first peak (low temperature peak) hardly changed with time-on-stream while the area of the second peak (high temperature peak) steeply increased with time-on-stream. The amount of carbonaceous deposits after 2.5 hours on stream was already 4.4 wt.%, as shown in Figure 2.8 (b). It continued increasing with a much lower rate during the next hours, from 4.4 wt.% at 2.5 hours on stream to 5.6 wt.% at 7.5 hours on stream. Then, the accumulation rate increased and the amount of deposits increased from 5.6 wt.% at 7.5 hours on stream to 8.3 wt.% at 12.5 hours on stream. This shows that approximately 50% of the total amount of accumulated deposits was already deposited at the early stage of reaction.

N_2 adsorption isotherm

The deactivated catalysts were analyzed by nitrogen adsorption. The fresh and coked catalysts were activated at 120°C for 10 h in vacuum. The micropore volume and BET surface area for the fresh catalyst measured after outgassing at 120°C were 0.177 ml/g and 464 m^2/g

respectively, being those similar values to the ones reported in the literature for FAU zeolites [6, 21].

Figure 2.9 (a) shows the t-plot analysis of the fresh and reacted catalysts and Figure 2.9 (b) shows the occupied micropore volume with respect to the amount of deposits accumulated in the catalyst pores. In these Figures, three different periods of micropore volume occupancy are distinguished:

Period 1, in which in a short increment of time-on-stream, a large fraction of the micropore volume was occupied. In this period, 4.4 wt.% of accumulated deposits occupied approximately 0.07 ml/$g_{catalyst}$. Assuming the average density for the deposits to be 0.75 $g_{deposits}$/ml (typical for hydrocarbons), the volume occupied by 4.4 wt.% deposits would be ca. 0.06 ml. A slightly higher occupation of micropore volume was observed experimentally with respect to the theoretical value. This shows that not only the micropores are filled with deposits but also pore mouth plugging takes place at some extent.

Period 2 is considered from 2.5 hours on stream up to 7.5 hours on stream. Approximately 0.01 ml of micropore volume was occupied by 1.5 wt.% of accumulated deposits. The theoretical volume occupied by 1.5 wt.% deposits would be ca. 0.02 ml. A slightly higher occupation of micropore volume was observed experimentally with respect to the theoretical value. This shows that not only the micropores are filled with deposits but also pore mouth plugging takes place at some extent.

Period 3 is considered from 7.5 hours on stream up to the end of reaction. In this period, approximately 2.8 wt.% of accumulated deposits occupied 0.07 ml/$g_{catalyst}$. The theoretical volume occupied by 2.8 wt.% deposits would be ca. 0.04 ml. A more intense pore mouth plugging process takes place during period 3 compared to periods 1 and 2.

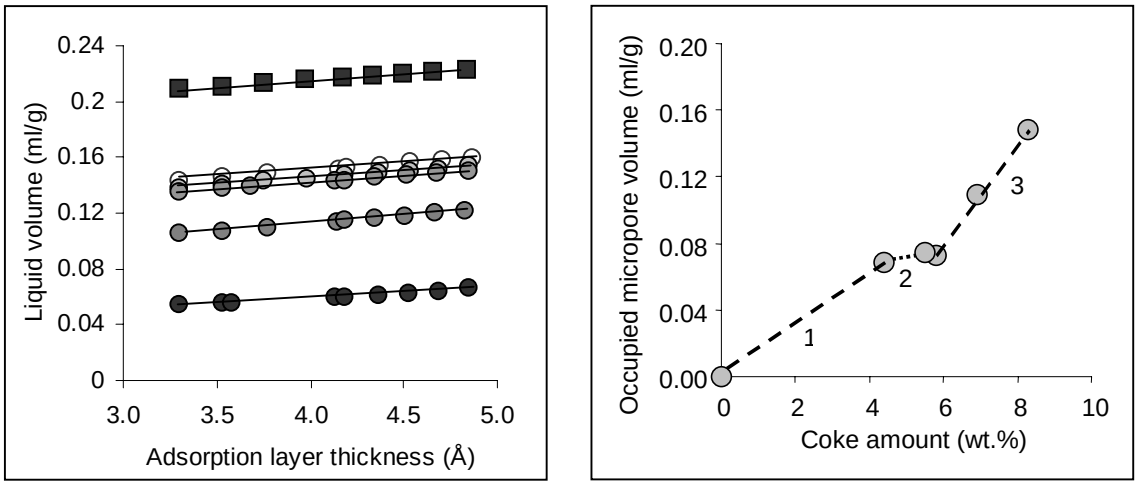

Figure 2.9: a) T-plot of the fresh catalyst (■) and deactivated catalyst (○ 2.5 h TOS, ○ 5 h TOS, ○ 7.5 h TOS, ○ 10 h TOS and ● 12.5 h TOS); b) Occupied micropore volume as a function of the amount of deposited coke.

Figure 2.10 (a) shows the decrease in the free micropore volume with respect to the time-on-stream and Figure 2.10 (a) with respect to the amount of accumulated deposits. Three different periods were clearly distinguished with respect to time-on-stream. In the first period the amount of free micropore volume decreased to approximately 60% of the initial micropore volume. In the second period it decreased very slightly. In the third period it decreased steeply again, being at the end of the reaction roughly 16% of the total micropore volume still free. The same trend was observed with respect to the amount of accumulated deposits but not so marked. As a result of a more intense pore mouth plugging process, the rate of decrease of free micropore volume was higher at the last stages of reaction than at the early stages of reaction.

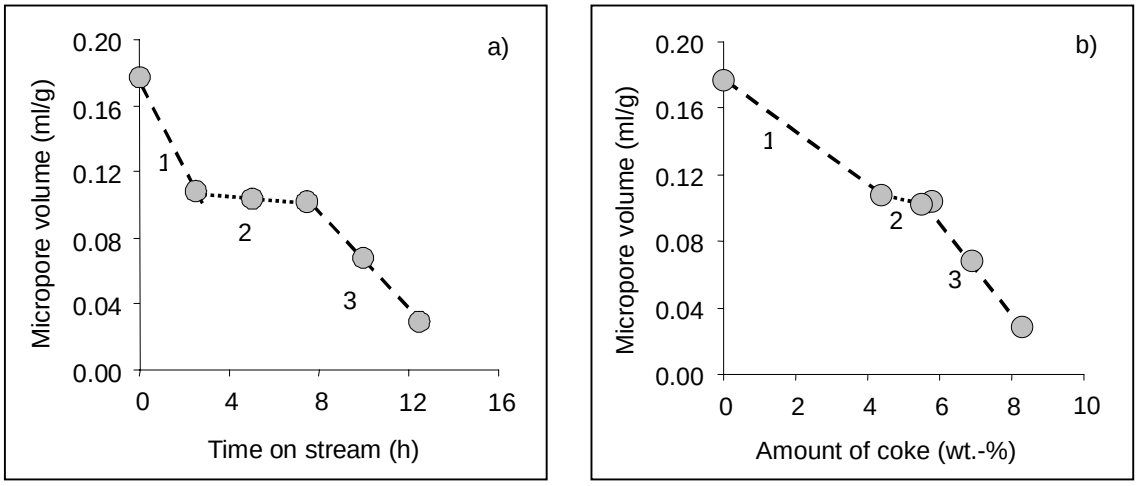

Figure 2.10: a) Micropore volume after outgassing at 120°C as a function of time-on-stream. b) Micropore volume after outgassing at 120°C as a function of percentage of coke.

Matrix-assisted Laser desorption/ionization time-of-flight mass spectroscopy

The deactivated catalysts were analysed by MALDI-TOF MS employing DHB as matrix. The mass spectra are displayed in Figure 2.11. All samples gave a Gaussian-curve distribution of masses with peaks in the mass range from approximately 150 to 360 m/z with a maximum from 220 to 262 m/z. Additional peaks to the Gaussian-curve distribution were observed for spectra after 2.5, 5 and 7.5 hours on stream with masses of 431 and 445. Assuming the detected ions to be of the typical $[M+H]^+$ nature (which leads to uneven masses for hydrocarbons), this series would correspond to molecules of a general C_nH_{2n-4}, C_nH_{2n-18} or even a C_nH_{2n-32} a formula. A common pattern was found for all samples following a 14 m/z addition series being the series based on 151 + 14*n*. In agreement with Feller *et al.* [6], every forth of the peaks exhibited a higher intensity than the Gaussian distribution, which would correspond to a $(CH_2)_4$ additions. The maximum in the Gaussian distribution of masses shifted slightly to higher masses with time-on-stream going from 220 m/z at 2.5 hours on stream to 262 at 12.5 hours on stream. Similar results were observed by Guisnet *et al.* [5] when doing the analysis of the deposited coke during the alkylation reaction. They observed masses from 164 to 388 with a 14 unit of mass difference between one molecule and the preceding one. The authors assigned these masses to compounds having a C_nH_{2n-4} formula (with *n* between 12 and 28).

Peaks at 155, 137 and 178 correspond to $[DHB + H]^+$, $[DHB\text{-}OH]^+$ and $[DHB + Na]^+$, respectively [20]. LDI-TOF spectra from the deactivated catalysts showed no presence of masses in the studied range. By LDI-TOF spectroscopy, only molecules with absorption in the region of the wavelength of the laser (λ = 337 nm) can be desorbed and ionised. The UV/VIS spectra (see Figure 2.7) of the deactivated catalysts did not show a significant absorption at 337 nm.

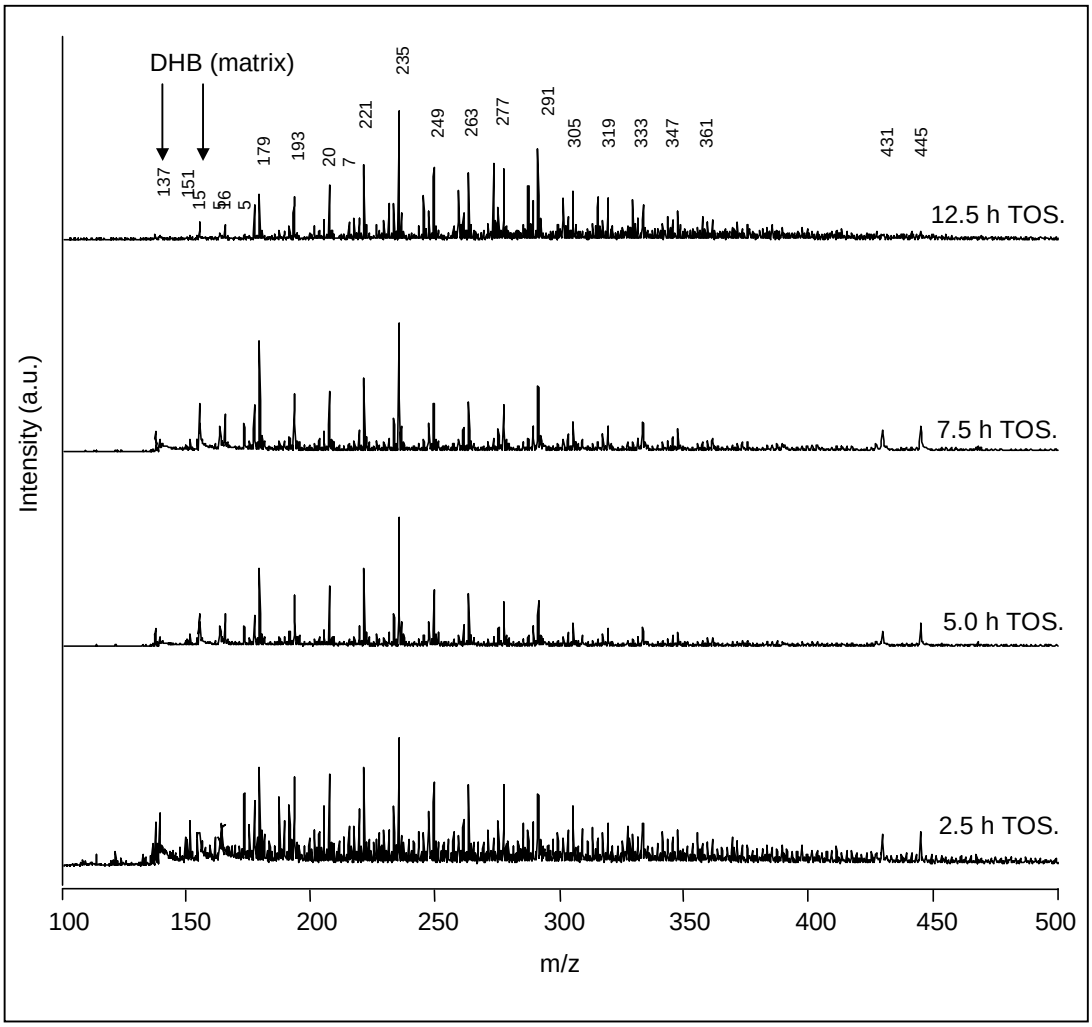

Figure 2.11: MALDI-TOF mass spectra of the deactivated catalysts after 2.5, 5, 7.5 and 12.5 hours on stream.

2.3.5 Recovered deposits analysis

GC/MS analysis

GC/MS analysis of the deposits shows a broad range of different hydrocarbon compounds ranging from C_9 to C_{42}. They are mainly paraffinic compounds following a series with a $(CH_2)_3$ difference from one alkane to the preceding one. A small fraction of C_{16} alkanes was also observed with a value close to 2 wt.%. Unsaturated compounds were also observed with an approximately constant selectivity of 4.5 wt.% during the whole reaction. Not well-resolved spectra of several peaks, which could correspond to aromatic compounds, appeared from the beginning of reaction with a constant selectivity close to 0.5 wt.%. Figure 2.12 shows the main groups in the deposits.

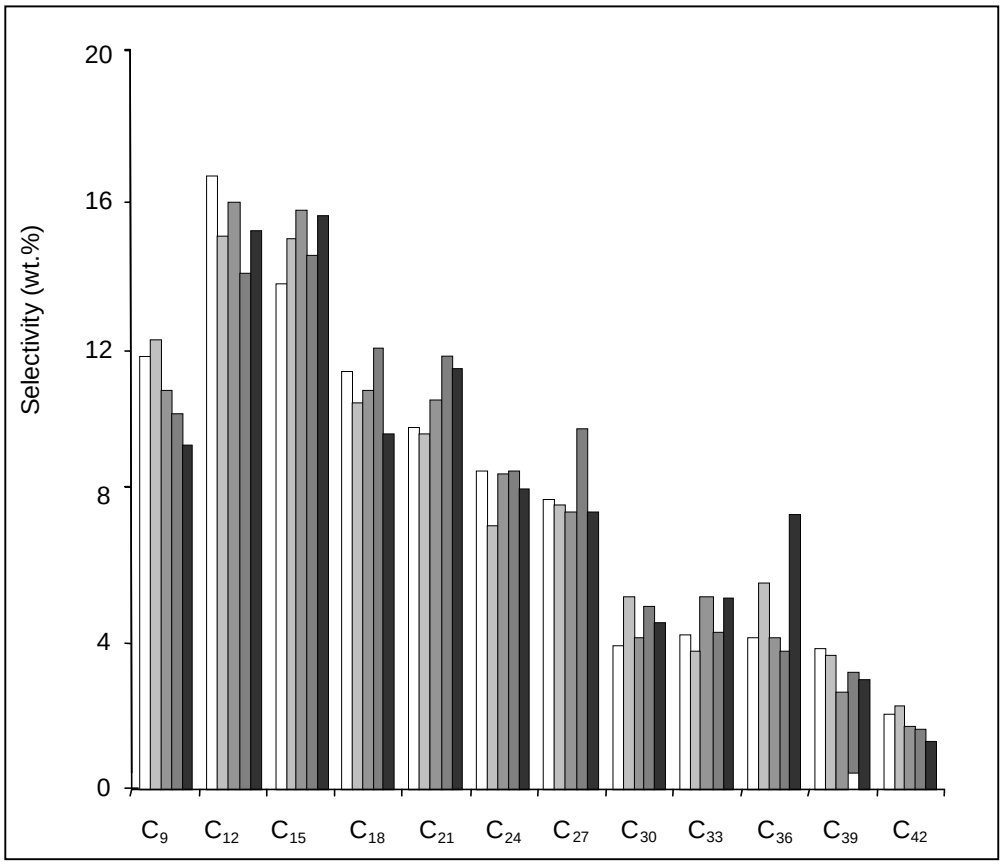

Figure 2.12: Selectivity to the main groups from the recovered deposits (□ 2.5 h TOS, ▫ 5 h TOS, ▫ 7.5 h TOS, ▫ 10 h TOS, ■ 12.5 h TOS).

MALDI-TOF mass spectra from the deposits were also taken. No ions were detected for any of the deposits. For this reason it is postulated that ions, which are ionizable by MALDI-TOF, are only present on the surface of the catalyst or they represent a minority fraction within the total amount of coke and thus, being their concentration in the deposits too low to be detected.

UV/VIS spectroscopy

The recovered deposits at different times-on-stream were analyzed with UV/VIS spectroscopy, as shown in Figure 2.13. Every spectrum represents the deposits retained in the catalyst from the beginning of reaction until a defined time-on-stream. Due to the unknown concentration and extinction coefficients of the individual compounds, the results are discussed only in qualitative terms. For the spectra after 2.5, 5 and 7.5 hours on stream a main band at 203 nm was seen whereas for spectra at 10 and 12.5 hours on stream a broad band ranging from 250 to 350 nm was observed. Shown as an inset in Figure 2.13 is the UV/VIS spectrum of the alkylate at 10 hours on stream (dashed line) compared to the recovered deposits at the same time-on-stream. The spectrum of the deposits showed broader bands than the alkylate suggesting a bigger number of different compounds and absorption at higher wavelength occurred than for the alkylate. UV/VIS spectra from the recovered deposits revealed the presence of unsaturated and/or aromatics species. No absorption was detected for higher wavelengths than 400 nm.

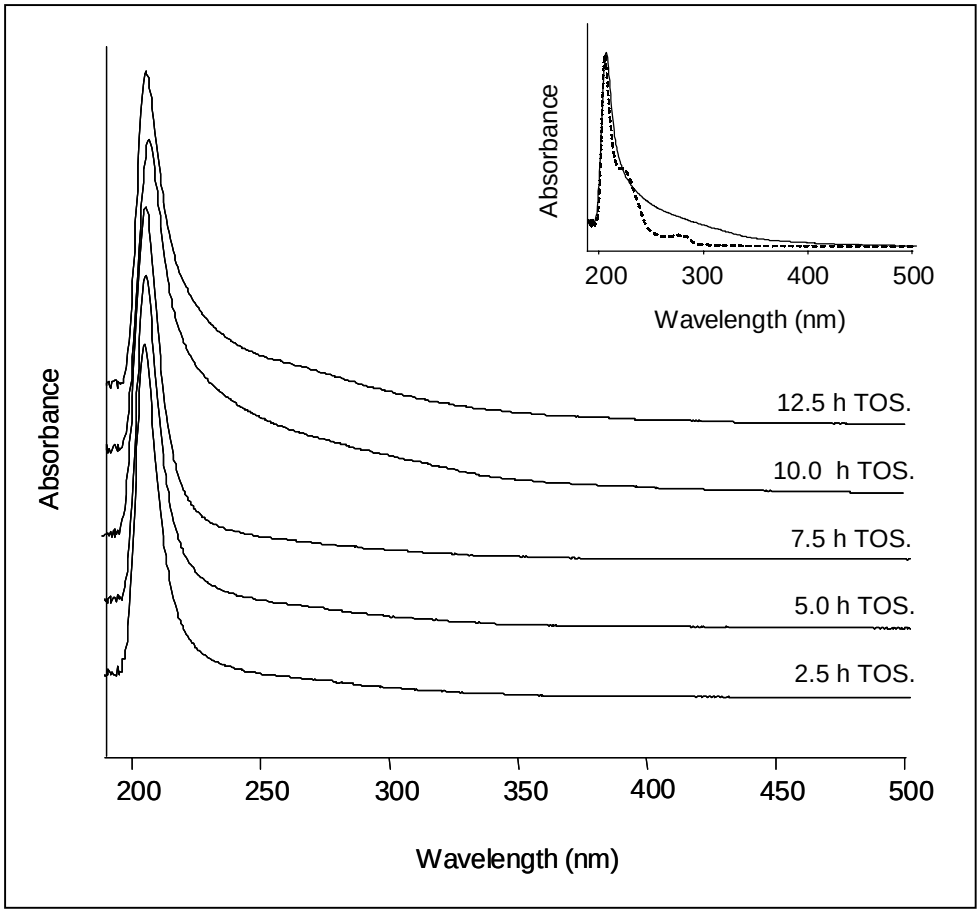

Figure 2.13: UV/VIS spectra of the recovered deposits extracted with methylene chloride after HF treatment from alkylation runs at different times-on-stream.

NMR spectra of the deposits

The recovered deposits were also analyzed by ^{1}H-NMR. The NMR spectra of the recovered deposits are displayed in Figure 2.14. A higher degree of overlapping of the peaks is seen for the deposits than for the alkylate which makes the quantitative analysis more uncertain.

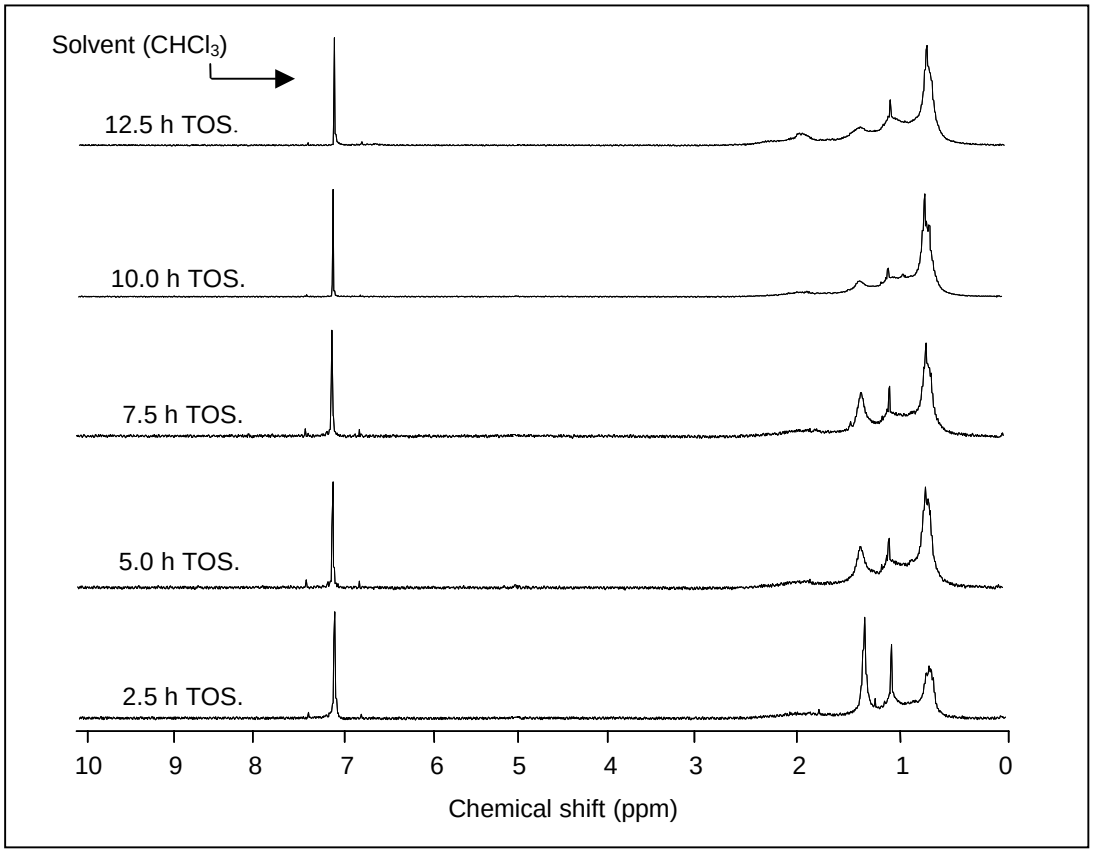

Figure 2.14: ^{1}H NMR spectra of the recovered deposits after 2.5, 5, 7.5, 10 and 12.5 h time-on-stream.

The results from the quantitative analysis are displayed in Figure 2.15. The fraction of protons in CH_3 groups in α position to saturated C atoms increased with time-on-stream from ca. 43% at 2.5 hours on stream to 55% at 12.5 hours on stream, values which are lower than for the alkylate indicating a lower degree of branching in the deposits compared to the alkylate. The fraction of protons in CH_2 groups also increased with time-on-stream from ca. 21% to 29% which is roughly 4 times the percentage found for protons in CH_2 groups in the alkylate. On the other hand, protons in CH groups steeply decreased with time-on-stream from ca. 31% to 10%. The fraction of protons in this position after 2.5 hours on stream was ca. 5 times higher than in the alkylate, but it was practically the same at the end of the reaction. As an average, the CH_3, CH_2 and CH percentages would lead to a C_9 molecule with four methyl groups in total (*i.e.* 2,4-dimethyl heptane). Protons in CH_3, CH_2 and CH groups in

α position to unsaturated or aromatic carbon atoms remained relatively constant with time-on-stream with values ranging from 3.5% to 5%. This indicates that approximately 6 wt.% of the retained deposits would present an olefinic nature. The fraction of unsaturated compounds obtained by ^{1}H-NMR analysis basically agrees with the amount obtained by GC/MS. No protons of olefinic groups appeared in any of the samples, which would indicate that the carbon atoms containing the double bond are completely substituted, i.e. 2,3-dimethyl-2-heptene. A similar result was obtained by Guisnet et al. [5] while doing alkylation of iso-butane with 2-butene over a USHY zeolite at 50°C.The fraction of aromatic protons remained constant over the whole reaction with a value close to 0.3%. The fraction of protons in CH_3, CH_2 and CH groups in α position to unsaturated or aromatic carbon atoms, of protons of olefinic groups and of aromatic protons found in the alkylate was much lower than in the deposits.

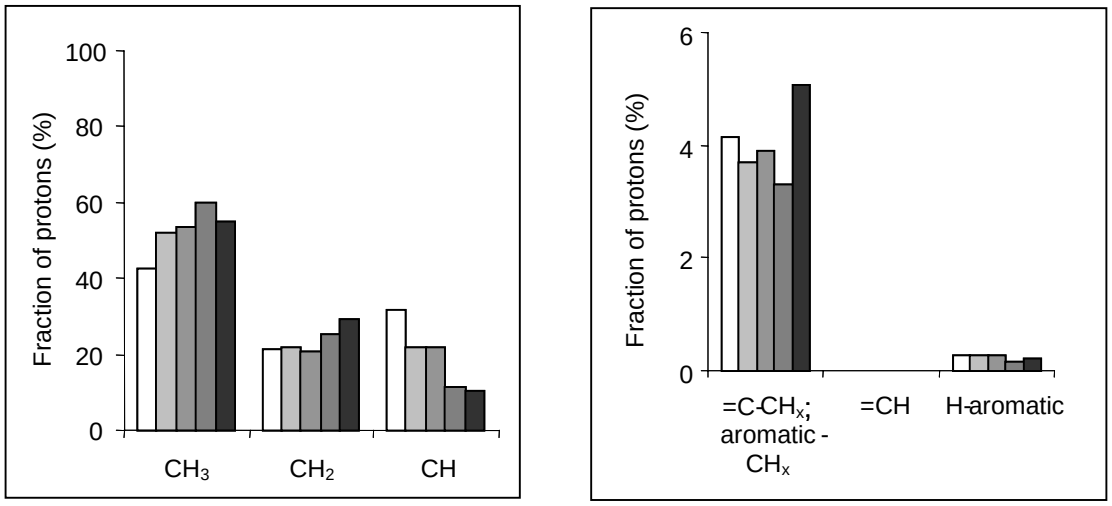

Figure 2.15: Fraction of protons in the individual positions obtained by the integration of the NMR-spectra in Figure 1.7. (□ 2.5 h TOS, ▫ 5 h TOS, ▫ 7.5 h TOS, ▫ 10 h TOS, ■ 12.5 h TOS).

2.4 Discussion

2.4.1 Main alkylation mechanism and product selectivity overview

As shown in Figure 2.2, the product from alkylation is a mixture of methyl-branched

alkanes with a high content of isooctanes. The main fraction of the alkylate consists of different octane molecules and, in particular, trimethylpentanes, dimethylhexanes and methylheptanes. Besides, a considerable amount of isopentane, isohexanes, isoheptanes and hydrocarbons with nine or more carbon atoms is present. This suggests that many individual reactions contribute to the product distribution as observed here. No simple and straightforward single-step mechanism is operative but the reaction involves a set of parallel and consecutive reaction steps. The majority of molecules produced during the alkylation reaction are C_8 molecules and, in particular, trimethylpentanes (TMPs) and dimethylhexanes (DMHs). The widely accepted basic catalytic cycle for iso-butane-butene alkylation as adapted from Schmerling [22, 23] is shown in Figure 2.16. As seen from the figure, the three main individual steps that take part in the basic alkylation cycle are: alkene addition, isomerization and hydride transfer.

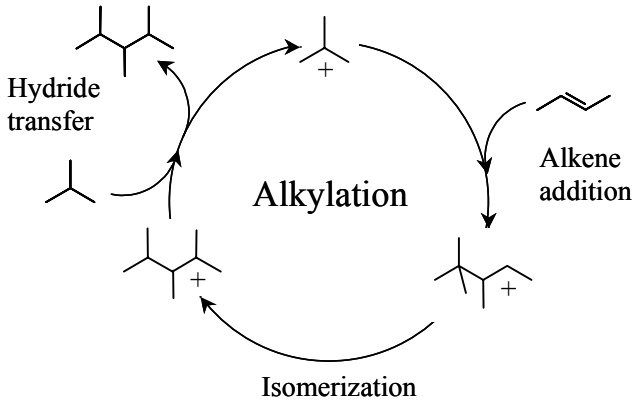

Figure 2.16: Alkylation of iso-butane with n-butene catalytic cycle.

2,2,3-TMP is the primary product of the alkylation reaction with 2-butene as feed alkene, although it was experimentally seen only in small amounts (its measured selectivity was less than 10 wt.%). Speculatively, this is attributed to the steric difficulties to achieve hydride transfer, as the carbenium ion is protected by an iso-butyl and an ethyl group, while all other TMP isomers have one methyl group adjacent to the carbon that forms the alkoxy bond to the catalyst. The main components of the TMP fraction during the alkylation reaction are 2,3,3-, 2,3,4- and 2,2,4-TMP, which constituted together more than 80 wt.% within the C_8 fraction. Therefore, a fast isomerization of the primary TMP cation has to occur through hydride- and

methyl- shifts. Although the equilibrium composition is not reached, long residence times favor these rearrangements [24]. 2,2,4-TMP is also a product from the self-alkylation of iso-butane. The self-alkylation mechanism starts with the decomposition of the butoxy group into a free Brønsted acid site and iso-butene (proton transfer from the tert-butyl carbenium ion to the catalyst). Iso-butene will react with another tert-butyl ion to form an isooctyl ion. At the same time, a feed alkene repeats the initiation step to form a sec-alkyl ion, which after receiving a hydride gives the tert-butyl ion and an n-alkane. DMHs were also observed during the alkylation reaction and, in particular, 2,5-, 2,4-, and 3,4-DMH as the majority species, which partially stem from a rapid isomerization of the feed. Weitkamp *et al.* [4] found as the only reasonable way to account for the occurrence of light and heavy products, i.e., products with odd carbon numbers, the formation of C_8, C_{12}, C_{16} and perhaps even higher molecular weight intermediates from the C_4 feed hydrocarbons followed by cracking steps. Cracking would lead to a carbenium ion (alkoxy group) and one corresponding olefin that will be added to another carbenium ion. Both can desorb *via* hydride transfer from iso-butane as alkanes. Cracking most likely accounts for some of the produced octanes.

The same authors [4] established type A type β-scission as preferential if not exclusive in which a tertiary carbenium ion cracks to give another tertiary carbenium ion and an olefin as seen in figure 2.17. Type A β-scission can only be considered for compounds with at least 8 carbon atoms.

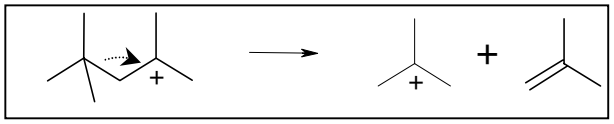

Figure 2.17: Type A β-scission for octyl carbenium ion.

As shown in section 2.3.5 the deposits recovered from alkylation runs followed a series with a $(CH_2)_3$ difference from one hydrocarbon to the preceding one, instead of the expected to be predominant, $(CH_2)_4$ series. Therefore, it is proposed that the accumulated deposits are mainly formed by propene oligomerization, in which type B β-scission is involved.

Correlations between the acidity and the alkylation performance revealed that the acid strength required to perform the different reactions occurring during alkylation decreases in the order: cracking > alkylation (addition of butene to a tertiary butyl) > dimerization

(addition of a butene to a secondary butyl) [25]. Thus, catalysts with a higher concentration of weak Brønsted acid sites would enhance the oligomerization to cracking ratio and would lead to a more rapid deactivation. On the other hand and, although Lewis acid sites do not catalyze the alkylation reaction, their presence influences the alkylation performance. Besides the ability to increase the formation of unsaturated compounds [26], Lewis acid sites have been claimed to increase the local olefin concentration producing an acceleration of the oligomerization and thus, they enhance the deactivation rate [27].

2.4.2 Alkylate quality evolution with time-on-stream

UV/VIS analyses from the alkylate give qualitative information on the structure of the unsaturated compounds in the product. All alkylate samples showed conjugated and non-conjugated double bonds. Homo and hetero-conjugated double bonds steeply increased their relevance at the last stages of the reaction. ^{1}H-NMR gave further information on the structure of the alkylate molecules and their relevance. Similar degree of branching was seen for all alkylate samples as shown by the constant fraction of protons in CH_3 groups in α position to saturated C atoms. This method revealed an increase in the concentration of unsaturated with time-on-stream but, on the other hand, it was always very low with a maximum fraction of protons at these positions close to 0.1%. Aromatic compounds were only seen at late times-on-stream. As shown by UV/VIS and ^{1}H-NMR results, during the time of (near-) complete conversion a mixture of saturated iso-alkanes is almost exclusively produced, with a majority of C_8 iso-alkanes. At times-on-stream close to deactivation, and although in very low amounts, the selectivity to unsaturated compounds increased and some aromatics appeared in the alkylate. The production of unsaturated compounds starts to be relevant at times-on-stream close to deactivation, as sites strong enough to catalyze hydride transfer deactivate first, and oligomerization / dimerization already happens on weak acid sites.

2.4.3 *Chemical nature of the deposits*

The formation of deposits at low reaction temperatures during the transformation of organic compounds over acid catalysts is usually considered to mainly involve condensation and rearrangement steps, thus, being the deposits not polyaromatic and therefore, on microporous catalysts, the retention of deposit molecules would be mainly due to steric blockage within the micropores [28]. Thus, the deposits in alkylation have been usually

related to saturated species that result from multiple alkylation and oligomerization of butenes and other alkenes [29, 30]. The results presented here demonstrate that the carbonaceous deposits retained in the zeolite pores during the iso-butane/butene alkylation reaction are mainly resulting from oligomerization of propene. Propene is claimed to be formed as a result of 2-butene isomerization through a bimolecular mechanism and the formation of an octyl-carbenium ion. Therefore, products from butene isomerization would be responsible for the formation some of the octanes produced during the alkylation reaction by simple hydride transfer to the octyl-carbenium ion formed. A posterior B type β-scission step would produce a propene molecule and an isopentane molecule through hydride transfer, as shown in Figure 2.18. Propene would rapidly oligomerize and it would be converted to alkanes through hydride transfer from iso-butane. The products from propene oligomerization would either crack again to give smaller compounds, leave the catalyst through hydride transfer as alkanes or be accumulated in the pores. As shown with GC/MS analysis, a rapid cracking/oligomerization equilibrium is achieved within the pores of the catalysts leading to a non-variable nature of the deposits with time-on-stream.

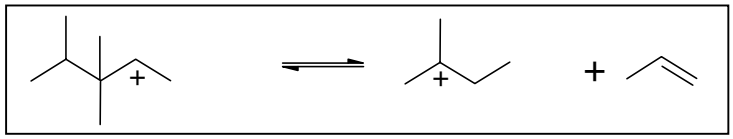

Figure 2.18: Type B β-scission for an octyl carbenium ion.

Deactivation takes place due to a two front mechanism. The first front leading to deactivation is the obstruction of the active sites by pore blocking or pore filling as proposed by Querini *et al*. [21] and Sahebdelfar *et al.* [31]. Some of the active sites would be directly obstructed by strongly absorbed compounds as alkenes or aromatics on them, as already shown by Pater *et al.* [5] and Loenders *et al.* [32]. The second front leading to deactivation implies pore mouth plugging by highly unsaturated compounds. Pore mouth plugging was already considered of relevance in solid acid catalyzed alkylation by some authors in the past [21,31].

Solid UV/VIS and MALDI-TOF MS from the coked zeolites showed the presence of unsaturated compounds on the surface of the catalyst already after 2.5 hours on stream. However, none of these methods can detect the presence of saturated hydrocarbons, and,

therefore, these have to be considered only as qualitative measurements. Absorption bands between 300 and 400 nm in the UV/VIS spectra of deactivated catalysts were attributed to alkenyl cations by Flego *et al.* [9]. Also aryl and benzenium cations exhibit absorption maxima between 300 and 400 nm [19]. As seen by MALDI-TOF, the main compounds detected on the surface from the catalyst are based on the series 150 + 14*n*. As previously shown in section 1.3.4, this would correspond to a C_nH_{2n-4}, C_nH_{2n-18} or C_nH_{2n-32} chemical formula. A shift to 50 m/z units in the maximum of the Gaussian distribution to higher masses was observed with time-on-stream. When considering a C_nH_{2n-4} compound as the start from the series, this can be attributed to a cyclopentadiene containing some methyl ramifications. This type of compound can be formed *via* cyclization (1,5-cyclization) and subsequent hydride transfer and methyl shifts as shown in Figure 2.19. In a first step a large cation probably produced *via* oligomerization has to crack to form a large and branched alkene, which might transfer a hydride to another carbenium ion and, thus, form an alkenyl carbenium ion, which can desorb *via* proton transfer as a diene. Further hydride transfer from the diene would give a dienylic cation that easily rearranges into an alkyl-substituted ring *via i.e.* 1,5-cyclization and subsequent hydride and methyl shifts. The formed cyclopentenyl cations are very stable [31, 32] and have been observed as free cations in zeolites [35, 36]. The same sequence is seen when absorbing alkenes in concentrated sulphuric acid. The alkenes disproportionate on the one hand into a layer of saturated hydrocarbons and, on the other hand into highly unsaturated cyclic compounds dissolved in the acid phase, which turns a dark red colour [37, 38].

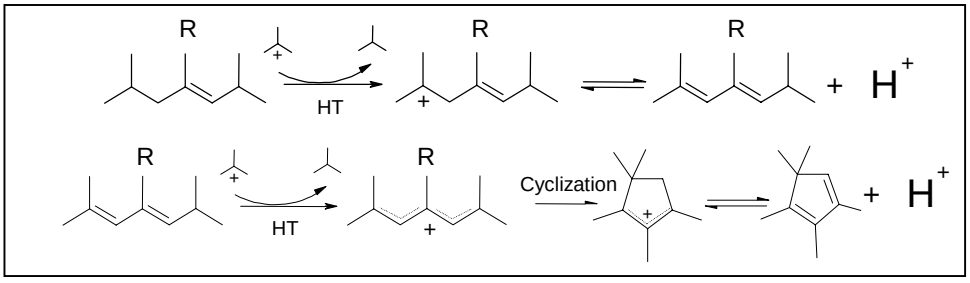

Figure 2.19: Formation of cyclopentadienes *via* a 1,5-cyclization (R = methyl, ethyl, propyl…).

Moreover, cyclic dienes and particularly cyclopentadienes were claimed to be intermediates in the formation of benzenic compounds from alkanes, alkenes and naphthenes. The cyclic dienes were observed to be produced in several processes *i.e.* the transformation of olefinic and saturated naphthenes over zeolites and over FCC catalysts [39,40] and also form naphthenes over bifunctional reforming catalysts [41]. Besides this observation for dienes, it is remarkable that cyclopentadienes were found to be rapidly transformed into polyaromatic species (coke) over acid catalysts such as chlorinated alumina [41], over zeolites [39] and over the bifunctional reforming catalysts [41,42]. Anderson *et al.* reviewed the different modes of transformation of cyclopentadienes into polyaromatic compounds [39,43].

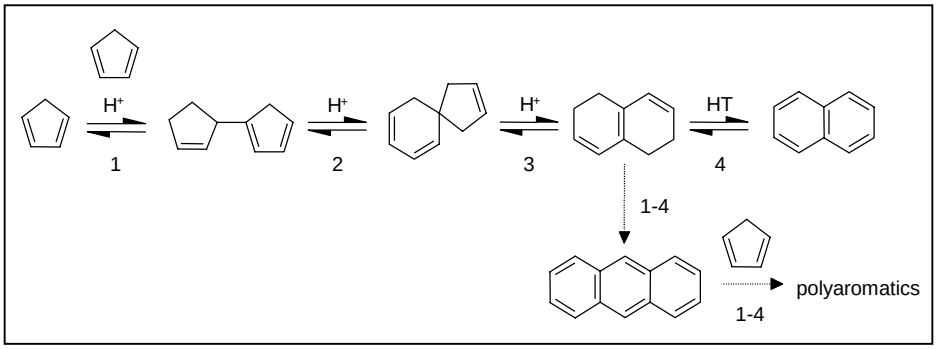

Figure 2.20: Transformation of cyclopentadiene into polyaromatics over acidic catalysts. Adapted from Guisnet *et al.* [14].

As a general mechanism Guisnet *et al.* [14] proposed the simplified scheme depicted in Figure 2.20, involving alkylation (1), isomerization through protonated cyclopropane intermediates (2 and 3), and hydrogen transfer (4). Through this mechanism mass 179 is attributed to anthracene (C_nH_{2n-18}) and thus, the corresponding following masses partially to CH_2 group additions to it. Within the polyaromatic molecules formed, o-phenylenepyrene (with a chemical formula $C_{22}H_{12}$) would correspond to mass 276 in the MALDI-TOF spectra. Therefore, the higher the time-on-stream, the more relevant the more unsaturated products ($C_nH_{2n-32} > C_nH_{2n-18} > C_nH_{2n-4}$) are.

Masses detected by MALDI-TOF spectroscopy showed a 50 m/z units shift in the maximum of the Gaussian distribution to higher masses with time-on-stream. By assuming C_nH_{2n-4} compounds (*i.e.* cyclopentadiene) responsible for the lower masses and C_nH_{2n-18} (*i.e.* anthracene) and C_nH_{2n-32} (*i.e.* o-phenylenepyrene) compounds responsible for the higher

masses detected by MALDI-TOF, a higher unsaturation degree with respect to time-on-stream was observed for the molecules retained on the surface.

No masses were detected by MALDI-TOF MS after dissolution of the catalyst and posterior measurement. Therefore, it is postulated that the concentration of MALDI-TOF detectable species is low within the total amount of coke. These types of molecules are responsible for pore mouth plugging when they accumulate on the surface of the catalyst.

The mass distribution and nature of the deposits in the catalyst pores remained approximately invariable with time-on-stream as shown by GC-MS analysis. GC-MS showed deposits to be mainly formed by compounds following a $(CH_2)_3$ series with molecules from C_9H_{20} to $C_{42}H_{86}$ with a maximum at $C_{15}H_{32}$. A small fraction of C_{16} alkanes was also observed with values close to 2 wt.% for catalyst A and between 3 and 4 wt.% for catalysts B and C. A fraction of the detected C_{12} isomers and the detected C_{16} isomers are a result of iso-butane/butene multiple alkylation. No bigger hydrocarbons than $C_{16}H_{34}$ as a result of multiple alkylation were observed. A high cracking rate has to occur to give C_3H_6 as the terminal end. A fast equilibrium for the accumulated deposits was observed, as their nature did not vary with time-on-stream. GC-MS, ^{1}H-NMR and UV-VIS analyses from the deposits confirmed the presence of unsaturated compounds. The significance of the unsaturated compounds in the coke can be estimated from ^{1}H-NMR and GC-MS. These methods revealed an approximately constant concentration (5-6 wt.%) of unsaturated compounds with time-on-stream. The predominant paraffinic nature from the deposits was also confirmed by these two methods. This is in agreement with what was found by Weitkamp *et al.* [30] studying the nature of the coke formed in the iso-butane/butene reaction by means of CP/MAS ^{13}C NMR spectroscopy. No olefinic protons were found by ^{1}H-NMR from the deposits. A higher amount of non-paraffinic compounds was found for the accumulated deposits than for the produced alkylate.

Three main rates of deposit accumulation and free micropore volume decrease were observed with TPO and N_2 adsorption analysis. In period 1 a large increment in the amount of accumulated deposits caused a large increment in the amount of occupied micropore volume. Along this period the deposits are thought to be mainly formed in the micropores as a result of propene oligomerization. In period 2 a small fraction of deposits are accumulated in the pores and cycled/aromatic molecules start to plug some entrances of the pores. In accordance, a slow rate of micropore volume occupation was observed along this period. In period 3, the amount of accumulated deposits increased steeply as shown with TPO analysis and bigger

molecules were formed on the surface of the catalyst, as shown with MALDI-TOF analysis, which plug the pore entrances. A subsequent decrease in free micropore volume was determined by N_2 adsorption isotherms. The total amount of deposited coke on the spent catalyst is consistent with the results reported in the literature [5, 21, 30].

Two main peaks (low and high temperature) were observed by burning the carbonaceous deposits off during TPO analysis. A shift to higher temperatures and an increase in the high temperature peak to low temperature peak ratio was found with time-on-stream, which would be a result of the difficulty to diffuse out higher amounts of coke at the end of the reaction and of the different mass distribution of compounds retained on the surface of the catalyst with time-on-stream. Based on the TPO results, it is postulated that a more severe regeneration procedure would be required, to bring the catalyst back to its initial state, with time-on-stream.

As shown by BET measurements, the fraction of free micropore decreased rapidly at the beginning and end of reaction, whereas it hardly decreased at intermediate times-on-stream. It followed a similar trend as the amount of deposited coke. Possibly, the decrease in the micropore volume at early stages of reaction is more related to accumulation of deposits in the catalyst pores and at the end stages of the reaction is more related to pore mouth plugging. Assuming the average density for the deposits to be 0.75 $g_{deposits}$/ml (typical for hydrocarbons), the volume occupied by 8.3 wt.% would be ca. 0.11 ml/$g_{catalyst}$. Taking into account an initial micropore volume of 0.18 ml/$g_{catalyst}$, roughly 13 wt.% of deposits would fit in the pores of the catalyst. Therefore, the pores of the catalyst are not full of deposits at times-on-stream close to deactivation. On the other hand, the micropore volume measurements showed that, in the same case, approximately 0.15 ml/ $g_{catalyst}$ were occupied at the end of reaction. Therefore, pore mouth plugging has to occur during the iso-butane/butene alkylation reaction.

2.5 Conclusions

During the solid catalyzed iso-butane/butene alkylation reaction a high quality alkylate is produced that is practically free of unsaturated compounds and aromatics, even at times close

to deactivation. Trimethylpentanes amount for approximately 80 wt.% of the produced alkylate what provides a high RON number.

Coke deposited in the pores of the catalyst is mainly formed by highly branched paraffinic compounds following a $(CH_2)_3$ series and with molecular weights from 128 g/mol to 548 g/mol. Small amounts of $C_{12}H_{26}$ and $C_{16}H_{34}$ from multiple alkylation were also detected in the deposits. Low amounts of olefins and aromatics are also found in the deposits. Cyclic compounds and aromatics are formed on the surface of the catalyst as observed by MALDI-TOF. These types of compounds were responsible of pore mouth plugging during the reaction and, at a great extent, of the deactivation of the catalyst.

Catalyst deactivation is believed follow two main mechanisms: pore filling (and at some extent acid site covering) and pore mouth plugging.

2.6 References

1. Corma A., Martínez A., Arroyo P.A., Monteiro J.L.F., Sousa-Aguiar E.F., *Appl. Catal. A* **142**, 139 (1996).
2. Stell J., *Oil Gas J.* **99(52)**, 75 (2001).
3. Feller A., Zuazo I., Guzmán A., Barth J.O., Lercher J.A., *J. Catal.* **216**, 313 (2003).
4. Weitkamp J., Traa Y., *in* "Handbook of Heterogeneous Catalysis" (Ertl G., Knözinger H., Weitkamp J., Eds), Vol. 4, p.2039, VCH, Weinheim, 1997.
5. Pater J., Cardona F., Canaff C., Gnep N.S., Szabo G., Guisnet M., *Ind. Eng. Chem. Res.* **38**, 3822 (1999).
6. Feller A., Barth J.O., Guzmán A., Zuazo I., Lercher J.A., *J. Catal* **220**, 192 (2003).
7. He Y., He Y., *Catal. Today* **74**, 45 (2002).
8. Yoo K., Burckle E.C., Smirniotis P.G., *Catal. Lett*. **74**, 85 (2001).
9. Flego C., Kiricsi I., Parker Jr. W.O., Clerici M.G., *Appl. Catal. A* **124**, 107 (1995).
10. Förster H., Kiricsi I., *Zeol*. **7**, 508 (1987), and references cited therein.
11. Kiricsi I., Flego C., Bellusi G., *Appl. Catal.* **126**, 401 (1995).
12. Kiricsi I., Pálinkó I., Kollár T., *J. Molec. Struct.* **651-653**, 331 (2003).
13. Guisnet M., *J. Molec. Catal. A: Chem.* **182**, 367 (2002).
14. Guisnet M., Magnoux P., *Appl. Catal. A* **212**, 83 (2001).
15. J.A. Lercher, C.H. Gründling and G.Eder-Mirth, Catal. Today, 27, 353 (1996).
16. Emeis C.A., J. Catal. 141, 347 (1993).

17. Hesse M., Meier H., Zeeh B., in "Spektroskopische methoden in der organischen chemie" (Hesse M., Meier H., Zeeh B., Eds), Edition. 4, p.13, Georg Thieme Verlag Stuttgart-New York, 1997.
18. Sorensen, T.S. in Carbonium Ions, Vol. II, (Eds. G.A.Olah and R.P.Schleyer), Wiley-Interscience, New York, 1970, p.807.
19. Olah, G.A., Pittman C.U.Jr., Symons M.C., in *Carbonium Ions*, Vol. I, (Ed. G.A.Olah and R.P.Schleyer), Wiley-Interscience, New York, 1968, p.153.
20. Pruns J.K., Vietzke J.-P., Strassner M., Rapp C., Hintze U., König W.A., *Rapid Commun. Mass Spectrom*. **16**, 208 (2002).
21. Querini C.A., Roa E., *Appl. Catal. A* **163**, 199 (1997).
22. Schmerling L., J.Am.Chem.Soc. **67**, 1778 (1945).
23. Schmerling L., J.Am.Chem.Soc. **68**, 275 (1946).
24. Gorin M.H., Kuhn C.S., Miles C.B., *Ind. Eng. Chem.* **38**, 795 (1946).
25. Corma A., Martínez A., Martínez C., *J. Catal. A* **146**, 185 (1994).
26. Diaz-Mendoza, F.A., Pernett-Bolano L., Cardona-Martinez N., *Thermochim. Acta* **312**, 47 (1998).
27. Nivarthy G.S., Seshan K., Lercher J.A., *Microp. & Mesop. Mater.* **22**, 379 (1998).
28. Guisnet M., Magnoux., *Appl. Catal. A* **212**, 83 (2001).
29. Stöcker M., Mostad H., Rørvik T., *Catal. Lett.* **28**, 203 (1994).
30. Weitkamp J,. Maixner S., *Zeolites* **7**, 6 (1987).
31. Sahebdelfar S., Kazemeini M., Khorasheh F., Badakhshan A., *Chem. Eng. Sci.* **57**, 3611 (2002).
32. Loenders R., Jacons P.A., Martens J.A., *J. Catal.* **176**, 545 (1998).
33. Deno N.C., in *Carbonium Ions*, Vol. II, (Eds. G.A.Olah and R.P.Schleyer), Wiley-Interscience, New York, 1970, p.783.
34. Sorensen T.S., in *Carbonium Ions*, Vol. II, (Eds. G.A.Olah and R.P.Schleyer), Wiley-Interscience, New York, 1970, p.807.
35. Nicholas J.B., Haw J.F., *J.Am.Chem.Soc.* **120**, 11804 (1998).
36. Yang S., Kondo J.N., Domen K., *Catal. Today* **73**, 113 (2002).
37. Deno N,C., Boyd D.B., Hodge J.D., Pittman C.U., Turner J.O., *J. Am.Chem.Soc.* **86**, 1745 (1964).

38. Olah G.A., Olah J.A., in *Carbonium Ions*, Vol. II, (Eds. G.A.Olah and R.P.Schleyer), Wiley-Interscience, New York, 1970, p.715.
39. Anderson J.R., Chang Y.F., Western R.J., *J. Catal.* **118**, 466 (1989).
40. Mercier des Rochettes B., Marcilly C., Gueguen C., Bousquet J., *Stud. Surf. Sci. Catal.* **34**, 589 (1987).
41. Barbier J., Elassal L., Gnep N.S., Guisnet M., Molina W., Zhang Y.R., Bournonvillle J.P., Franck J.P., *Bull. Soc. Chim. France* **245**, 250 (1984).
42. Parera J.-M., Cerderone R.J., Querini C.A., *Stud. Surf. Sci. Catal.* **68**, 133 (1987).
43. Anderson J.R., Chang Y.F:, Western R.J., *Stud. Surf. Sci. Catal.* **127**, 113 (1991).

Chapter 3

Impact on the alkylate produced and accumulated deposits for different performing catalysts in iso-butane/butene alkylation

Abstract

A detailed study on iso-butane/2-butene alkylation for three rare-earth exchanged zeolites X (high, middle and low performance) was done. To better understand why zeolites with a similar structure perform differently, a "double-front" study was carried out: on the one hand, a complete physicochemical characterization of the three catalysts was performed; on the other hand, the alkylate and the coked zeolites were investigated at different stages of deactivation.

3.1 Introduction

Iso-butane alkylation with olefins is an important refinery process producing branched paraffins of high octane number. This process is commercially catalyzed by hydrofluoric or sulphuric acids, which can cause serious equipment corrosion and environmental pollution [1]. Alkylate is the cleanest gasoline blending stream produced in a refinery and it is considered to be an essential requirement for producing environmentally sound reformulated gasoline [2]. Zeolites were the first solid acids tested as alternatives to sulphuric and hydrofluoric acids in iso-butane/alkene alkylation [3], the main drawback being their rapid deactivation, which, up to date, has prevented their industrial application. Therefore, in order to achieve an economically feasible industrial process, the catalysts must be frequently regenerated. The patent literature suggests that multiple regenerations (as many as several hundred) are needed for processes based on solid catalysts to be competitive with existing processes based on H_2SO_4 and HF [4].

Since the 1940's, a large number of authors [5-15] have studied the product distribution and the mechanism of acid catalysed alkylation reactions. Louis Schmerling [5, 6] was one of the pioneers in studying the mechanism of the alkylation of paraffins, his conclusions being still valid nowadays. Different types of solid catalysts were investigated, especially zeolites as EMT, Beta or FAU.

Deactivation in iso-butane/butene alkylation was also intensively investigated by a large number of authors [16-24] during the past years. A Plug Flow Reactor (PFR) system was chosen for the majority of these studies, showing that the lifetimes of the catalysts were too short (in the order of minutes) to allow a detailed time-on-stream (TOS) study for the alkylation reaction.

In this work three different performing catalysts were tested in the iso-butane/butene alkylation reaction. For the sake of simplicity, high, middle and low performance catalysts (will be onwards named "A", "B" and "C", respectively). The scope of this study was, on the one hand, to understand how the quality of a catalyst is reflected in the alkylate produced and in the carbonaceous deposits retained in it and, on the other hand, to understand why zeolites, which in principle are similar, perform so differently with lifetimes ranging from 5 to 12.5 hours on stream.

The type of reactor chosen was a continuous stirred tank reactor (CSTR) in which, lifetimes of several hours at (near-) industrial conditions were achieved. Product distribution

was analysed *on-line* by GC analysis. The alkylate produced and the carbonaceous deposits were analysed using several techniques as ^{1}H NMR [16, 17, 23], GC and GC-MS [16, 17, 23, 25] or UV/VIS [16]. Coked catalysts were analysed by TPO and MALDI-TOF / LDI-TOF, which was already successfully applied to coked zeolites by Feller *et al.* [16].

3.2 Experimental

3.2.1 *Catalyst preparation*

The parent material used for this series of experiments was a Na-X zeolite obtained from Chemische Bad Köstritz (Si/Al = 1.2). This zeolite was first converted to its acidic form by multiple lanthanum ion exchanges and its posterior calcination. The parent material was 1-3 times exchanged with a 0.2 M aqueous lanthanum nitrate solution (liquid-to-solid ratio approximately 10 ml/g) at 70ºC for two hours. After nitrate removal by washing with doubly distilled water, the zeolite was calcined under air with a slow temperature increment up to 450ºC maintaining this temperature for one hour. This was followed by a second ion-exchange step with the 0.2 M aqueous lanthanum nitrate solution and then loading of platinum (ca. 0.3 wt.%) with a [Pt $(NH_3)_4$] $(NO_3)_2$ solution by ion-exchange. Samples were finally calcined under air with a slow temperature increment up to 450ºC maintaining this temperature for one hour and reduced afterwards.

3.2.2 *Catalytic experiments*

The alkylation of iso-butane with 2-butene was carried out in a stirred tank reactor (50 ml Hastelloy C-276 autoclave from Autoclave Engineers Co.) operated in continuous mode at a stirring speed of 1600 rpm. Liquefied cis-2-butene was received from Messer with 99.5% purity, being trans-2-butene the main impurity. Liquefied iso-butane was received from Messer with 99.95% purity. The catalyst (typically 2.6 g, in form of pellets from 0.7 to 2.0 mm in size) was used in a catalytic basket (Robinson-Mahoney micro stationary catalyst basket). With this configuration temperature gradients are avoided as compared to experiments in which reactions are carried out as slurry. The catalyst was activated *in situ* in the alkylation reactor at 160-190˚C for 16 h under flowing hydrogen. After cooling down to reaction temperature (75˚C) and pressurization with hydrogen (at 20 bar), the reactor was

filled with liquid iso-butane at a pressure of 20 bars. The iso-butane/butene mixture was by-passed to decrease the delay time, in order to achieve the desired molar paraffin-to-olefin ratio at the entrance of the reactor as much as possible (it was always checked by GC analysis before reaction start). The reaction was then started by admitting the mixture with a molar paraffin-to-olefin (P/O) ratio of 10 and an olefin space velocity (OSV) of 0.2 g_{butene} / ($g_{catalysts}$ h), conditions that are comparable to industrially employed parameters.

Five different reactions were carried out for each zeolite. The first reaction of each series was stopped just at the beginning of deactivation, *i.e.* when butene conversion was not complete anymore. That time-on-stream was called "lifetime". To study the true alkylation performance of the catalysts, the butene conversion has to be complete (as in the usual industrial operation mode). In fact, at not complete conversion, oligomerization predominates and rapid catalyst deactivation occurs. Four more reactions were carried out for every catalyst up to 20, 40, 60 and 80% of their lifetimes. Once a reaction was finished, the coked sample was dried with N_2 at reaction temperature and stored for further analysis.

After expansion to atmospheric pressure, the product passed through a six-port-valve with a sample loop, and automatically injected into an HP 6830 gas chromatograph equipped with a FID-detector and a 50 m DB-1 column. Downstream of the six-port-valve, the product stream was condensed into a cold trap (at -80ºC) over the whole time on stream. The integral product composition was determined by chromatographic analysis. Note that the alkylation reaction is not performed in steady state. When the reaction is started, the reactor contains only iso-butane. With the introduction of the iso-butane/2-butene mixture and the subsequent (near-) complete conversion of butene, the reactor content steadily changes its composition to an iso-butane/products mixture, with an increasing fraction of products. Under typical conditions (catalyst mass = 2.6 g, P/O ratio = 10 and OSV = 0.2 h^{-1}), steady state is theoretically reached after approx. 20 h, with the exit stream consisting of a 20-25 wt.% products in iso-butane mixture. However, typical catalyst lifetimes were in the range of 5 to 14 h. Hence, steady state conditions were not reached. With the knowledge of the theoretical butene build-up curve derived from the mass balance (and its experimental verification in a blank run without catalyst), conversions and yields were calculated. At complete butene conversion the theoretical maximum yield is 2.04 $g_{product}/g_{butene}$, assuming a 1:1 stoichiometry of iso-butane alkylation with butene.

3.2.3 *Catalyst characterization*

The prepared materials were analysed using a broad range of different techniques. The amount of remaining sodium (Na^+) and the bulk Si/Al ratio were determined by AAS. The crystallite size and morphology were analysed by SEM and the unit cell size by XRD. The free pore volume was estimated with nitrogen adsorption at 77K. Two different adsorption / desorption methods were used for acidity measurements: Pyridine TPD in a vacuum-setup with a mass spectrometer detector to estimate the total number of acid sites (adsorption temperature of 150ºC and a slow ramp up to 800ºC); Sorption of pyridine monitored by IR spectroscopy to estimate the amount of Brønsted and Lewis acid sites as well as their strength. The catalyst was pressed into a self-supporting wafer, which was placed into the sorption cell, where it was activated in vacuum for 1 h at 450°C. Then, the catalyst was cooled down to 150°C and pyridine at a partial pressure of 10^{-2} mbar was introduced into the system. After saturation of all acid sites, the sample was outgassed for 1 h at 150°C followed by a linear increase of 10 K/min to 450 °C and maintaining that temperature for 1 h. Subsequently, the cell was cooled down again to 150 °C. Spectra of the sample were taken before adsorption of pyridine at 150 °C, after outgassing at 150 °C and 450 °C.

3.2.4 *Alkylate analysis*

The produced alkylate was condensed in a trap cooled with a mixture of iso-propanol and dry ice at a temperature of ca. –80ºC. After iso-butane evaporation, the liquid product was stored for further analysis. The liquid alkylate was analysed by UV/VIS using a U-3000 Hitachi Spectrophotometer in the wavelength region from 190 to 500 nm. Hexane was used as a reference and also to further dilute the alkylate samples. By means of this technique relevant information on the olefinic and/or aromatic nature of alkylate was achieved. Liquid alkylate was also analysed by ^{1}H-NMR on a Bruker AM 360 spectrometer to obtain information on the abundance of the different functional groups present. $CDCl_3$ was used as an internal standard for calibrating the chemical shift (δ $CDCl_3$ = 7.24 ppm from TMS). GC-MS was used to obtain information on the structure of the individual compounds.

3.2.5 *Coked zeolite characterization*

Coked zeolites were dried with 100 ml/min of N_2 at reaction temperature and then stored for further analysis. The amount of carbonaceous deposits was determined by TPO; the burning-off profile gave us an idea of how difficult it would be to remove the accumulated species deposited in the catalyst. Matrix-assisted laser desorption/ionisation time-of-flight mass spectroscopy (MALDI-TOF-MS) was applied to the deactivated catalysts to obtain the molecular weight distribution of the hydrocarbon deposits on the zeolite (near-) surface.

Deposits from every sample were prepared by complete dissolution of the deactivated zeolite in a 40% hydrofluoric acid solution at room temperature. Unreacted HF was evaporated and the remainder was recovered with methylene chloride. The brown coloured hydrocarbon phase containing the deposits was used for further analysis. The amount and structure of the individual compounds was determined by GC-MS. MALDI mass spectra of the deposits were compared with mass spectra of the deactivated zeolites.

3.3 Experimental results and interpretation

3.3.1 *Physicochemical characterization*

The fresh PtLaX samples were analysed using a wide range of techniques. The particle size measured by SEM ranged from 1 to 2 μm for all samples. No differences in shape or particle size were seen when comparing the different catalysts by this technique. SEM pictures from sample A and B are shown in Figure 3.1.

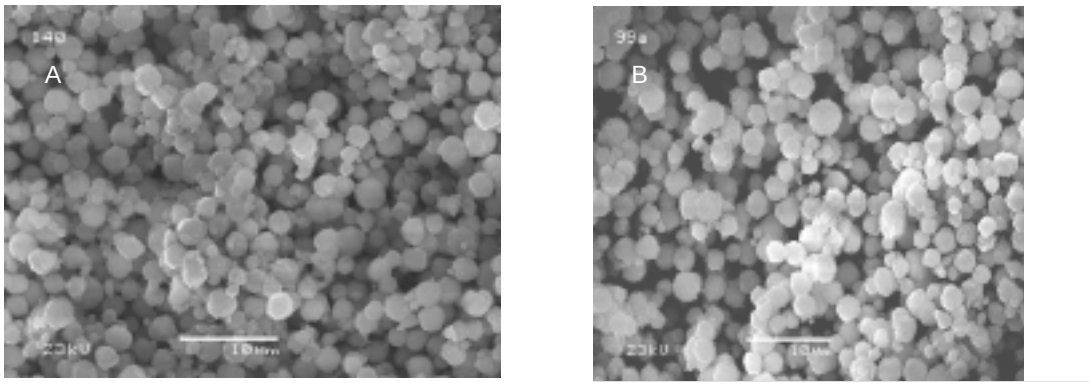

Figure 3.1: SEM pictures of samples A and B.

The total acid site concentration measured by TPD was ca. 0.8 $mmol_{pyridine}$ / $g_{catalyst}$ for all catalysts. No direct correlation was found when comparing the total concentration of acid sites with the lifetime of the different samples. Sorption of pyridine monitored by IR spectroscopy was used to differentiate between Brønsted and Lewis acid sites and to obtain their relative strength and concentration. Three bands of adsorbed pyridine were analysed, *i.e.* (i) the band at 1545 cm^{-1} indicative of pyridinium ions (sorption at Brønsted acid sites), (ii) the band at 1451 cm^{-1} indicative of pyridine bound at Al^{3+} Lewis acid sites and (iii) a band due to coordinatively bound pyridine between 1448 and 1435 cm^{-1} due to pyridine adsorbed on exchanged cations [30]. Ratios of extinction coefficients were taken from ref. [30]. The ratio of extinction coefficient for the band corresponding to pyridine-cation interactions remains unknown, and therefore no attempt to determine the total acidity by pyridine-IR was made. Acidity data are summarized in Table 3.1.

Table 3.1: Acid site characterization data of the fresh catalysts.

Sample	Total acid site concentration[1]	Total BAS 1545 cm^{-1} (150°C)[2]	Strong BAS (450°C)[2]	Total LAS 1451 cm^{-1} (150°C)[2]	Strong LAS (450°C)[2]
	mmol/g	mmol/g	mmol/g	mmol/g	mmol/g
A	0.85	0.30	0.165	0.12	0.069
B	0.73	0.32	0.167	0.13	0.088
C	0.80	0.34	0.109	0.19	0.087

[1] Measured by adsorption of pyridine at 100°C measured by TPD analysis

[2] Measured by adsorption/desorption of pyridine monitored by IR

The concentration of strong Brønsted acid sites was similar for catalysts A and B. Sample C showed the lowest concentration of strong Brønsted acid sites. Catalyst A showed a concentration of strong Lewis acid sites lower than catalysts B and C. Therefore, catalyst A, which was our best alkylation catalyst, had the highest concentration of strong Brønsted acid sites (and similar to catalyst B) and the lowest concentration of strong Lewis acid sites. On the other hand, catalyst C, which was the worst catalyst for the alkylation reaction, had the lowest concentration of strong Brønsted acid sites and the highest concentration of Lewis acid sites.

Similar molar Si/Al ratios and amounts of platinum loading were observed for the three catalysts with values close to 1.1 mol/mol and 0.23 wt.%, respectively. A higher ion exchange degree was obtained for catalysts A and B as compared to catalyst C (due to a higher number of Lanthanum exchange steps), with Na/Al ratio values lower than 1 mol/mol for catalysts A and B, and with a Na/Al ratio of approximately 5 mol/mol for sample C.

Micropore volume and surface area were measured by N_2 adsorption after activation at 120°C in vacuum for 10 h. No significant differences were seen among the different samples. Data are summarized in Table 3.2.

Table 3.2: Physical properties of the fresh catalyst.

Sample	Micropore volume	BET surface area
	ml/g	m^2/g
A	0.177	464
B	0.163	502
C	0.164	467

The unit cell size measured for the parent material (NaX) by X-Ray diffraction was 24.983 Å. Samples A and B showed similar unit cell size with values close to 25.010 Å whereas the unit cell size for sample C was slightly smaller (24.993 Å). The main factors influencing the unit cell size of the prepared catalysts are the ion exchange degree and the degree of dealumination. A higher ion exchange degree would be reflected in a higher unit cell size and a higher dealumination degree would produce a decrease in the unit cell size.

3.3.2 *Alkylation experiments*

A wide range of catalysts, all based on PtLaX, were initally screened in alkylation reaction in order to select three catalysts with high (A), middle (B) and a low (C) performance. Using a reaction temperature of 75°C, a P/O ratio of 10 and an OSV of 0.2 g_{butene} / ($g_{catalyst}$ h), the time of (near-) complete butene conversion (named catalyst lifetime) was 12.5, 10 and 5 h for catalysts A, B and C, respectively. The butene conversion profile with respect to time-on-stream for these catalysts is shown in Figure 3.2. The shaded areas show the difference in the

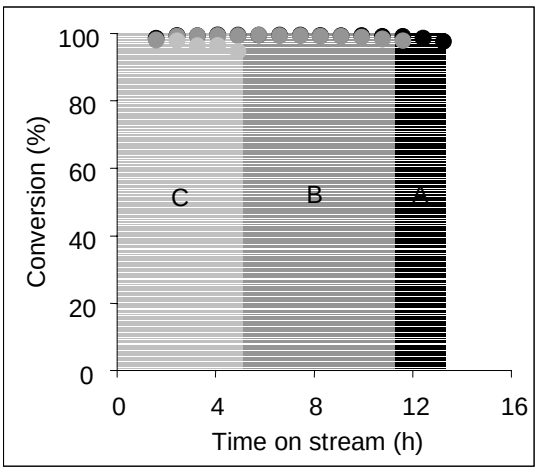

Figure 3.2: 2-butene conversion with time on stream for catalysts A, B and C.

useful lifetime. Figures 3.3 (a), 3.4 (a) and 3.5 (a) compile the selectivity for the three main groups of reaction products, *i.e.* alkanes with 5 to 7 carbon atoms, octane isomers and alkanes with 9 and more carbon atoms (heavy fraction), as a function of time-on-stream. The selectivity within the C_8 fraction is depicted in Figures 3.3 (b), 3.4 (b) and 3.5 (b).

The selectivity to octanes for catalyst A remained constant during the first 5 hours and then decreased from 90 wt. % to approximately 75 wt.% at the end of the lifetime of the catalyst (12.5 h). The selectivity to light alkanes (C_5-C_7) generated by cracking and hydride transfer slightly increased reaching a maximum value of approximately 14 wt.% after 12.5 h. The selectivity to heavy fraction (C_{9+}) remained constant and low (around 8 wt.%) during all the catalyst lifetime.

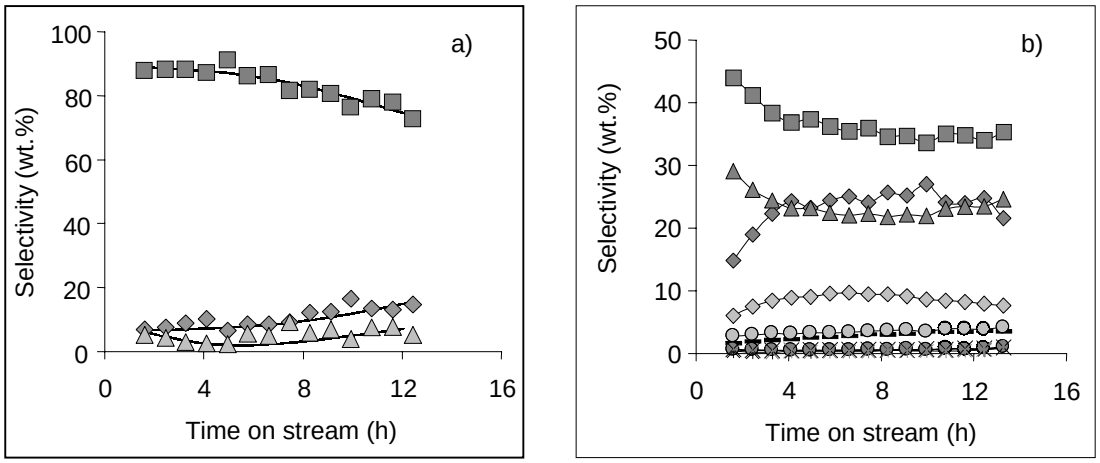

Figure 3.3: Alkylation performance of catalyst A. a) Product group selectivities with time on stream (◇ C_5-C_7 products, ■ C_8 products, △ C_{9+} products); b) selectivities in the C_8 fraction with time on stream (▫ 2,3,3-TMP, ◆ 2,2,4-TMP, ▲ 2,3,4 TMP, ◇ 2,5-DMH/2,2,3-TMP, ○ 2,3-DMH, ● 4-MHP/3,4-DMH, - 2,4-DMH, × 3,4-DMH, ✳ Octenes). T = 75°C, OSV = 0.2 h^{-1}, P/O = 10.

Trimethylpentanes were the dominating isomers within the C_8 fraction. It should be that trimethylpentanes are thermodynamically less favorable than dimethylhexanes, which indicates that isomerization equilibrium was not achieved. Among the trimethylpentanes, 2,3,3-TMP, 2,2,4-TMP and 2,3,4-TMP were predominant and constituted together more than 80 wt.%. The 2,2,4-TMP selectivity increased from 15 to 25 wt.% during the first 3 hours and then remained constant. 2,2,3-TMP, which is the primary product of the alkylation of iso-butane with 2-butene, was not separated from 2,5-DMH. Its selectivity passed through a maximum of approximately 10 wt.% after 6 h on stream. Other compounds showed selectivities below 5 wt.% during the entire course of the reaction. At the end of the lifetime, the selectivity to 3,4-DMH started to increase and octenes appeared in the product stream, although the selectivities to both compounds remained very low (<1.0 wt.%).

Compared to catalyst A, catalyst B showed smaller variations of the selectivity for the three main fractions of products and within the C_8 fraction. The C_8 fraction selectivity decreased continuously from the beginning of reaction. The selectivity to cracking products was higher for the catalyst B (up to 20 wt.%) than for catalyst A. The selectivity for the heavy fraction (C_{9+}) was similar for catalysts A and B.

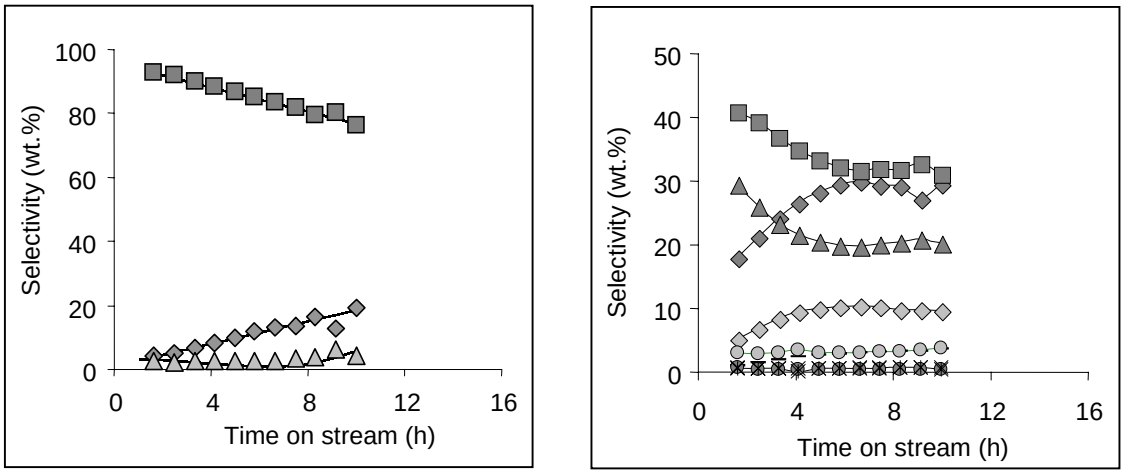

Figure 3.4: Alkylation performance of catalyst B. a) Product group selectivities with time on stream (◇ C_5-C_7 products, ■ C_8 products, △ C_{9+} products); b) selectivities in the C_8 fraction with time on stream (■ 2,3,3-TMP, ◆ 2,2,4-TMP, ▲ 2,3,4 TMP, ◇ 2,5-DMH/2,2,3-TMP, ○ 2,3-DMH, ● 4-MHP/3,4-DMH, - 2,4-DMH, × 3,4-DMH, ✳ Octenes). T = 75°C, OSV = 0.2 h^{-1}, P/O = 10.

Trimethylpentanes were the dominating isomers within the C_8 fraction. Among the trimethylpentanes, 2,3,3-TMP, 2,2,4-TMP and 2,3,4-TMP were predominant and constituted together more than 80 wt.%. The 2,2,4-TMP selectivity reached a maximum in selectivity of ca. 30 wt.% after 7 hours on stream. 2,2,3-TMP, which is the primary product of the alkylation of iso-butane with 2-butene, was not separated from 2,5-DMH. Its selectivity passed through a maximum of 10 wt.%, following approximately the same trend as 2,2,4-TMP. The other compounds showed selectivities below 5 wt.%. At the end of the lifetime, the selectivity to 3,4 DMH started to increase and octenes appeared in the product stream but, as with catalyst A, the selectivities to both remained very low (<1.0 wt.%).

The selectivity to the C_8 fraction was lower for catalyst C than for catalysts A and B, as shown in Figure 3.5 (a). While the C_8 fraction selectivity was between 90 and 75 wt.% for catalysts A and B, it remained close to 70 wt.% for catalyst C. The selectivity to the cracking fraction was close to 20 wt.% during the complete time on stream and the selectivity to the heavy fraction (C_{9+}) was approximately 14 wt.%.

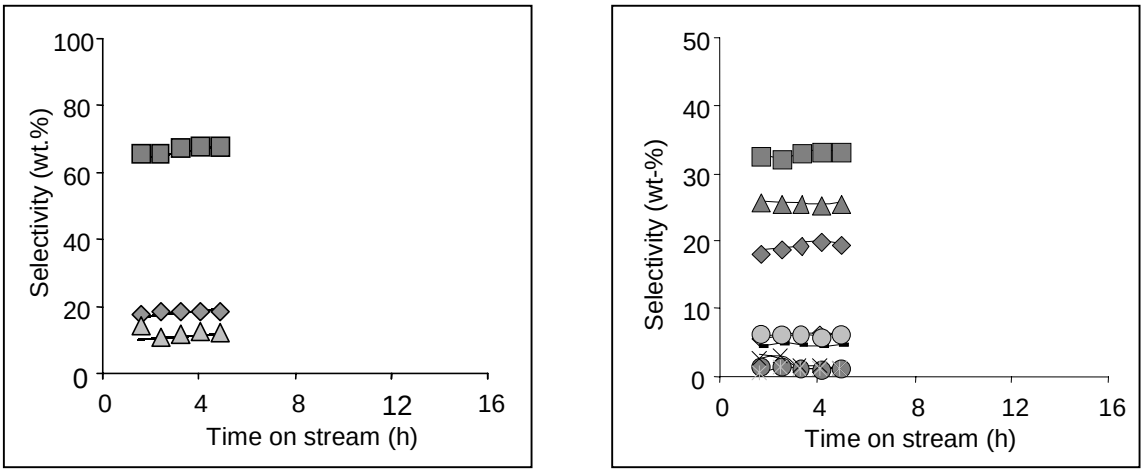

Figure 3.5: Alkylation performance of catalyst C. a) Product group selectivity with time on stream (◆ C_5-C_7 products, ■ C_8 products, △ C_{9+} products); b) selectivity in the C_8 fraction with time on stream (■ 2,3,3-TMP, ◆ 2,2,4-TMP, ▲ 2,3,4 TMP, ◇ 2,5-DMH/2,2,3-TMP, ○ 2,3-DMH, ● 4-MHP/3,4-DMH, - 2,4-DMH, × 3,4-DMH, * Octenes). T = 75°C, OSV = 0.2 h^{-1}, P/O = 10.

Trimethylpentanes were the dominating isomers within the C_8 fraction. Among the trimethylpentanes, 2,3,3-TMP, 2,2,4-TMP and 2,3,4-TMP were predominant and constituted together ca. 75 wt.%. The 2,2,4-TMP selectivity reached a maximum in selectivity of ca. 20 wt.% after 4 hours on stream. 2,2,3-TMP, which is the primary product of the alkylation of iso-butane with 2-butene, was not separated from 2,5-DMH. Its selectivity was constant with a value of approximately 6 wt.%, following approximately the same trend as 2,2,4-TMP. The rest of compounds showed selectivities below 5 wt.% during the time of complete butene conversion. At the end of the lifetime, the selectivity to 3,4 DMH started to increase and octenes appeared in the product stream but, as observed for catalysts A and B, the selectivities to both remained very low (<1.5 wt.%).

In order to better understand the relation between the products, the integral amount of each compound produced during the lifetime of the catalyst was determined (Table 2.3). The products compared are virtually free of olefins and represent the yield along the usable lifetime.

Table 3.3: Lifetime and integral group product selectivity for the different samples.

Sample	Lifetime	Group product selectivity		
		C_5-C_7	C_8	C_{9+}
	h	wt.%		
A	12.5	13.2	81.4	5.3
B	10	15.2	80.8	4.0
C	5	18.4	69.3	12.4

The integral group selectivity for the different fractions is similar for catalysts A and B. The selectivity to the light alkanes was slightly higher for catalyst B as compared to catalyst A, and the selectivity to heavy compounds slightly lower. Catalyst C showed lower integral selectivity to the C_8 fraction and a higher selectivity to the cracking and the heavy compounds as compared to catalysts A and B. Catalyst C produced an alkylate of lower quality.

3.3.3 Alkylate characterization

The analysis of the alkylate produced with the three catalysts A, B and C at different times-on-stream was performed by UV/VIS spectroscopy. Figure 3.6 shows the evolution for catalyst A. Similar patterns were also observed for the other two catalysts (B and C). Every spectrum represents the alkylate that was collected from the beginning of the reaction up to a defined time-on-stream. Due to the unknown concentration and extinction coefficients of the individual compounds, the results are discussed only in qualitative terms. All spectra showed a complex absorbance from 200 to approximately 300 nm. The main components appeared at 203, 223, 273 and 283 nm. The peak at 203 nm represents non-conjugated and conjugated double bonds while the peaks from 217 nm onwards represent only conjugated double bonds. Hetero-conjugated double bonds usually appear at the low-end region approximately from 217 to 230 nm (*e.g.* C_5H_8 appears at 222 nm) and homo-conjugated at the high-end region (*e.g.* C_8H_{12} appears at 273 nm and $C_{17}H_{26}$ appears at 283 nm). The significance of the bands at 223, 273 and 283 nm increased with time on stream. The spectrum from the sample at 100% lifetime showed a different pattern in which the abundance of compounds represented by peaks at 223, 273 and 283 nm decreased. This effect was observed for all the three catalysts once the butene conversion was lower than 100%, and a higher amount of olefins were present in the product, which could cause a shift in the relative intensity of the different bands. This effect can be attributed to a Diels-Alder reaction type of a conjugated double bond with an olefin to give a cyclic compound containing a non-conjugated double bond, which explains the disappearance of the high absorption wavelength bands.

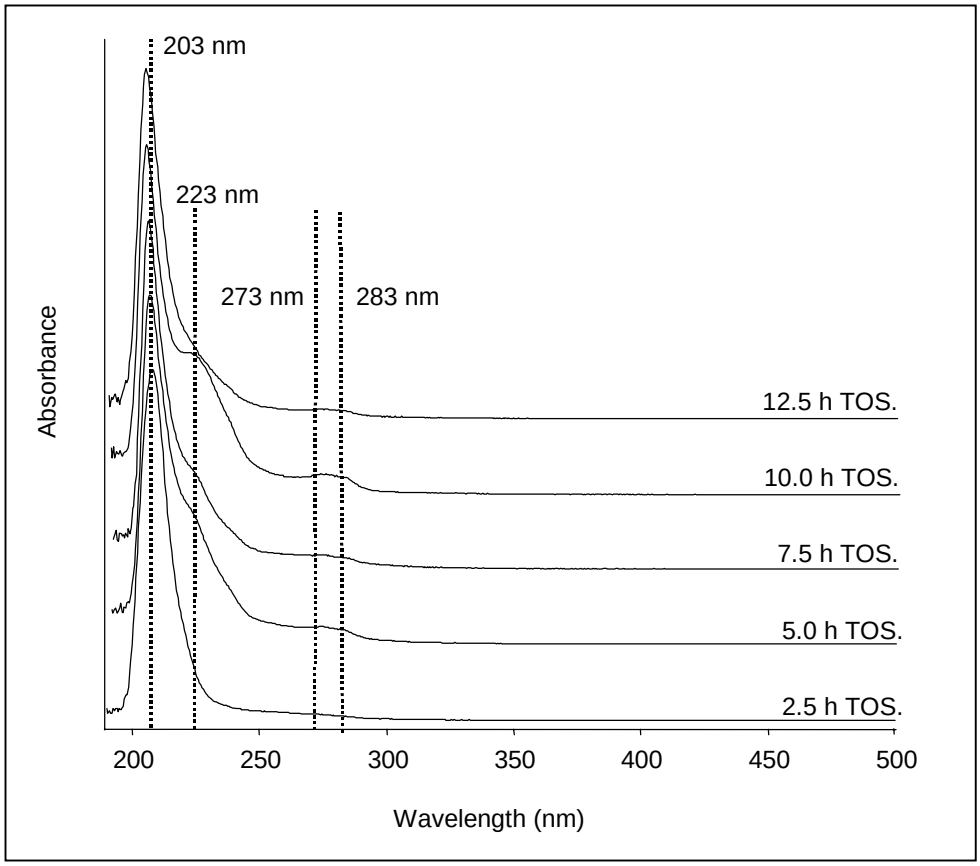

Figure 3.6: UV/VIS spectrum of the alkylate produced by catalyst A.

Some representative comparisons of the alkylate produced by the three catalysts are depicted in Figure 3.7 in order to observe the differences among the samples.

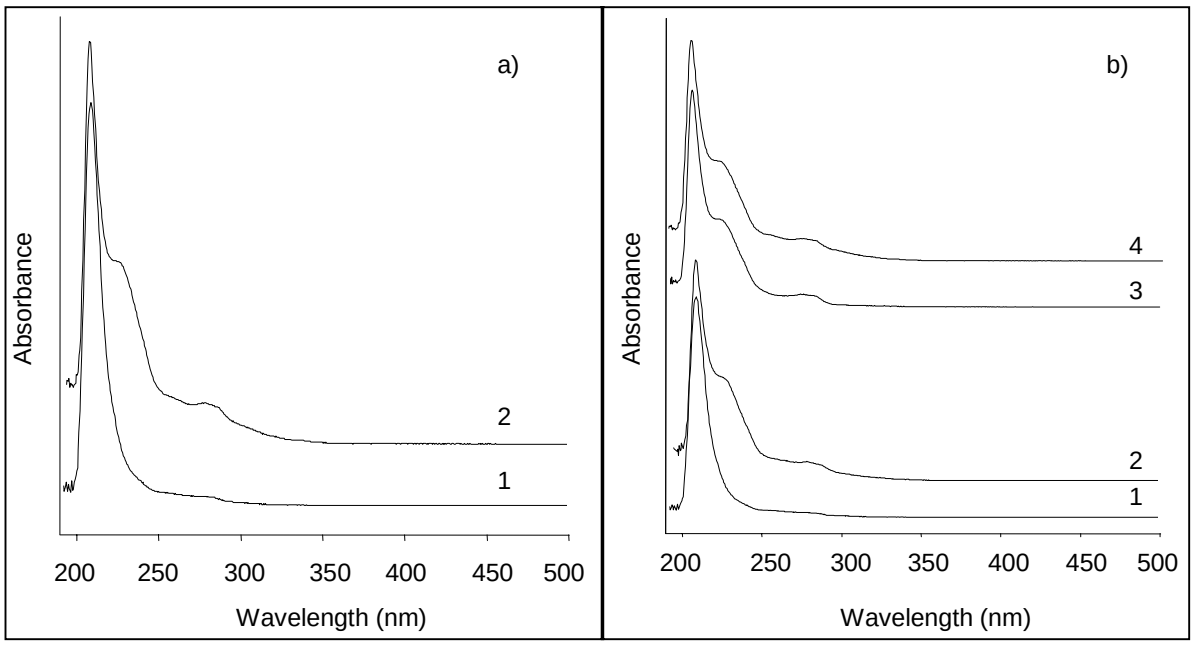

Figure 3.7: UV/VIS spectra of heavy-end fraction alkylate: a) 1 - catalyst B and 2 – catalyst C after 4 h TOS; b) 1 - catalyst B after 20% lifetime (2 h TOS), 2 - catalyst C after 20% lifetime (1 h TOS), 3 - catalyst A after 80% lifetime (10 h TOS), 4 - catalyst C after 80% lifetime (4 h TOS).

Figure 3.7 (a) shows the UV/VIS spectra from the alkylate produced by catalysts B (curve 1) and C (curve 2) after 4 hours on stream. Bands at 223, 273 and 283 nm were already abundant for catalyst C after 4 hours on stream whereas they were practically absent for catalyst B. In figure 3.7 (B) are shown two examples of comparison between the alkylate produced at similar percentages of lifetime: spectra 1 and 2 refer to samples B and C after 20% lifetime respectively; spectra 3 and 4 refer to samples A and C after 80% lifetime respectively. At 20% lifetime bands at 223, 273 and 283 nm were not present for sample B whereas sample C showed already the three bands. At 80% lifetime these bands were present for both catalysts A and C with similar absorbace intensities. Therefore, compounds containing conjugated double bonds appeared before, with respect to both time-on-stream and percentage of lifetime, for the worst catalyst (C) as compared to the other two (A and B).

The alkylate collected at different times-on-stream for the three catalysts was also analysed by ^{1}H NMR spectroscopy. The evolution of the alkylate produced by catalyst A is shown in Figure 3.8 as a representative example.

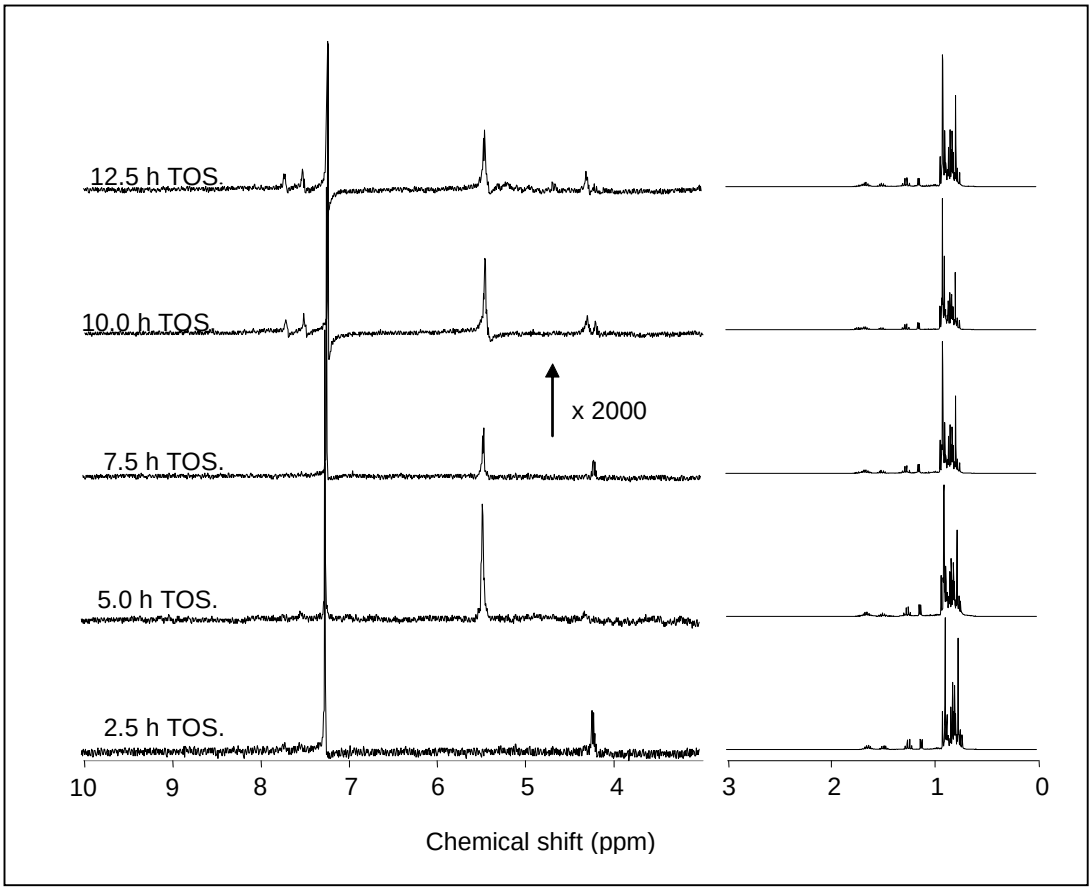

Figure 3.8: ^{1}H NMR spectra of the alkylate collected during the defined TOS.

In this figure the signals in the interval between 3 and 10 ppm are magnified 2000 times. The peaks in each spectrum can be grouped to distinguish protons in different positions. The signal between 0 and 1.1 ppm corresponds to protons in CH_3 groups in α position to saturated C atoms. Signals between 1.1 and 1.4 ppm correspond to protons in CH_2 groups and signals between 1.4 and 1.7 correspond to protons in CH groups. Signals between 1.7 and 3.5 ppm represent protons in CH_3, CH_2 and CH groups in α position to unsaturated or aromatic carbon atoms. Due to the broad distribution of chemical shifts for these protons, a further classification within this range was not attempted. Protons of olefinic groups appear between

4 and 6.6 ppm. Within this range a moderately intense peak was observed at 5.45 ppm. This is attributed to remaining traces of unreacted 2-butene. Aromatic protons absorb in the range from 6.6 to 9 ppm. The lack of signals at chemical shifts higher than 8.1 ppm in the spectra suggests the absence of condensed aromatic molecules with three or more rings.

The contributions of each type of protons for the three samples are shown in Figures 3.9, 3.10 and 3.11.

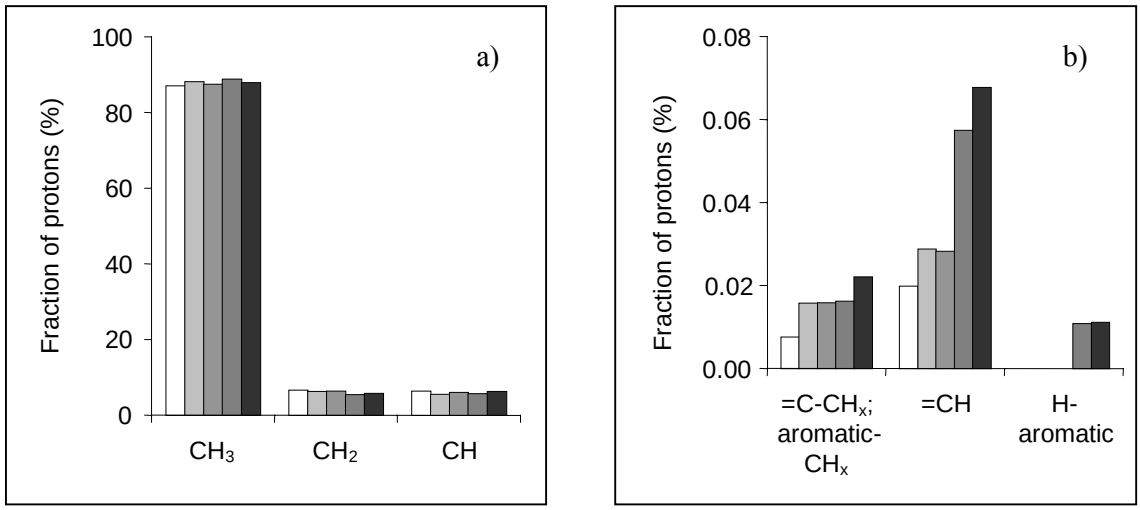

Figure 3.9: Fraction of protons in the individual positions obtained by the integration of the NMR-spectra for Sample A (□ 2.5 h TOS, ▫ 5 h TOS, ▫ 7.5 h TOS, ▪ 10 h TOS, ▪ 12.5 h TOS).

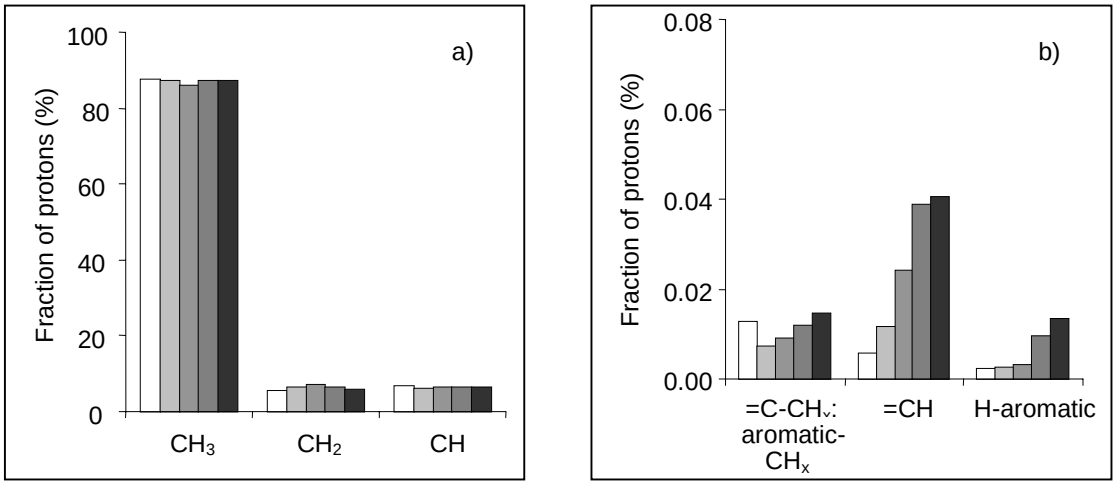

Figure 3.10: Fraction of protons in the individual positions obtained by the integration of the NMR-spectra for Sample B (□ 2 h TOS, ▫ 4 h TOS, ▪ 6 h TOS, ▪ 8 h TOS, ■ 10 h TOS).

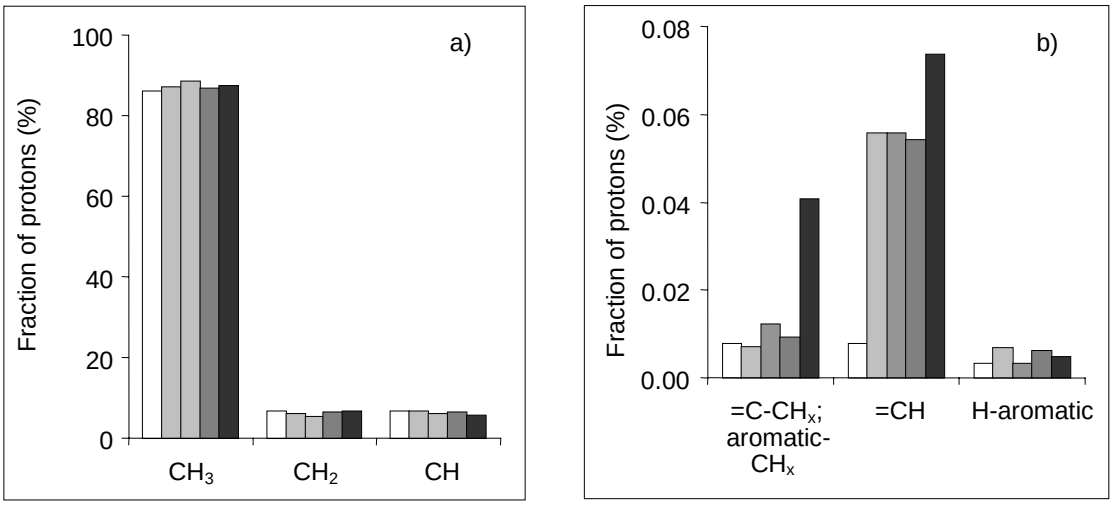

Figure 3.11: Fraction of protons in the individual positions obtained by the integration of the NMR-spectra for Sample C (□ 1 h TOS, ▫ 2 h TOS, ▪ 3 h TOS, ▪ 4 h TOS, ■ 5 hrs TOS).

As shown in Figures 3.9 (a), 3.10 (a) and 3.11 (a), the fraction of protons corresponding to CH_3 groups in α position to saturated C atoms remained stable with time-on-stream and showed practically no differences among the catalysts with values close to 86%. The fraction of protons in CH_2 and CH positions was also constant with time-on-stream and within the different catalysts with values of ca. 7% and 6%, respectively. The fraction of protons in CH_3, CH_2 and CH groups in α position to unsaturated or aromatic carbon atoms increased with time-on-stream for all samples. For catalysts A and B it reached a maximum of approximately 0.02% while for catalyst C it reached a maximum of approximately 0.04%. The fraction of protons of olefinic groups increased with time-on-stream for all samples reaching a maximum of approximately 0.07% for catalyst A and C and a maximum of approximately 0.04% for catalyst B. After 2 hours on stream its value for catalyst C reached already 0.06% while it was lower than 0.02% for catalysts A and B, which agrees with the results obtained with UV/VIS spectroscopy. Aromatic protons appeared after 10 hours on stream for catalyst A whereas they were present from the beginning of reaction for catalysts B and C with values of

approximately 0.01%. The fraction of aromatic protons was lower than 0.02% in all cases. Although CH groups in α position to unsaturated or aromatic carbon atoms, protons of olefinic groups and aromatic protons appeared for all samples, their sum never exceeded 0.13% for a defined time-on-stream, thus being minority species.

3.3.4 Characterization of the coked catalysts

Temperature programmed oxidation (TPO)

Figure 3.12 (a) shows the TPO profile of CO_2 release from the coked catalysts A. Similar trends were observed for the other catalysts. Two main peaks were present in all spectra: the first at temperatures lower than 300°C ("low temperature peak") and the second at temperatures ranging from 400 to 600°C ("high temperature peak"). The maximum for the low temperature peak remained at values close to 250°C during the whole reaction for the three catalysts. On the other hand, for all catalysts the maximum of the high temperature peak shifted approximately from 480 to 530 °C when going from early stages of reaction to the end of the usable lifetime. The area of the low temperature peak hardly changed with time-on-stream while the area of the second peak (high temperature peak) increased steeply with time-on-stream.

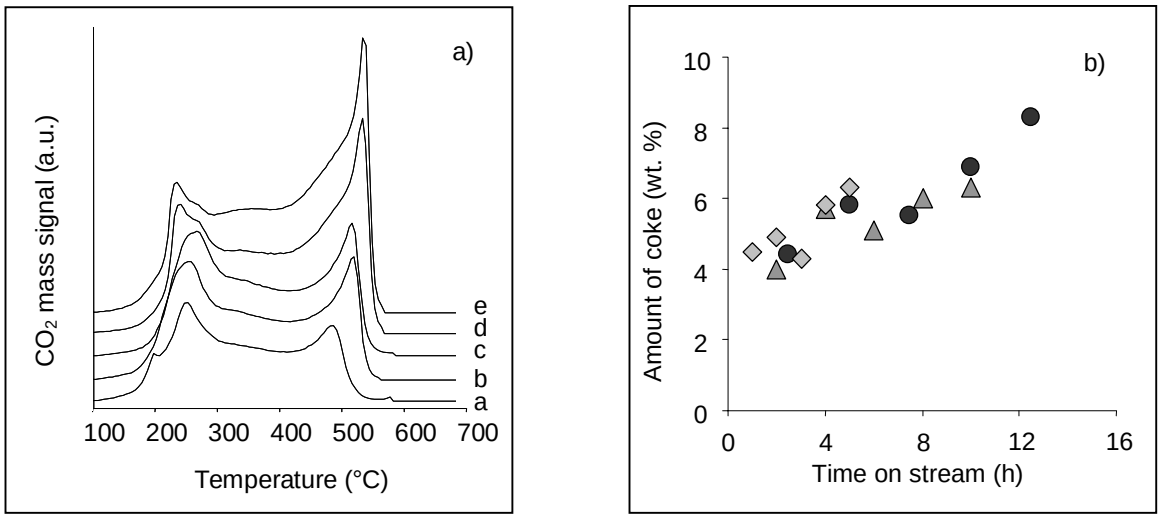

Figure 3.12: a) High temperature CO_2 mass signal for TPO analyses of the coked catalysts A at different times on stream. (a) After 2.5 h TOS; (b) after 5 h TOS; (c) after 7.5 h TOS; (d)

after 10 h TOS; (e) after 12.5 h TOS. b) Amount of deposited coke *vs* TOS for samples A (●), B (▲) and C (◇).

The amount of deposits accumulated for catalysts A, B and C is shown in Figure 3.12 (b). At 20% of the lifetime (corresponding to 2.5, 2 and 1 h on stream for catalysts A, B and C, respectively), the amount of accumulated deposits was found to be approximately the same for all catalysts (ca. 4.4 wt.%).. Thus, at the early stages of reaction the rate of accumulation of deposits with respect to time-on-stream was for catalyst C > catalyst B ~ catalyst A. The same trend was also observed during entire course of the reaction. Thus, whereas after 5 hours on stream approximately 6.3 wt.% of deposits was accumulated in catalyst C, 10 hours on stream were necessary to accumulate such amount of deposits in catalysts A and B. Deposits were accumulated at a similar rate for catalysts A and B, but approximately a 2 wt.% higher percentage of deposits was necessary to deactivate catalyst A as compared to catalyst B.

N_2 adsorption isotherm

The fresh and deactivated catalysts were activated at 120°C for 10 h in vacuum and analysed by nitrogen adsorption. The micropore volume and BET surface area measured were 0.177 ml/g and 464 m^2/g for catalyst A, 0.163 ml/g and 502 m^2/g for catalyst B and 0.164 ml/g and 467 m^2/g for catalyst C. Figure 3.13 (a) shows that the free micropore decreased rapidly for the three catalysts at early stages of the reaction, then it stayed approximately constant for the next hours and finally dropped again. The rate of decrease of free micropore volume followed the order: C > B > A. This results in good agreement with the sequence of rate observed in the accumulation of deposits. The free micropore volume with respect to the percentage of lifetime is shown in Figure 3.13 (b). Three different periods of micropore volume occupation were distinguished:

- Period 1, in which in a short percentage of lifetime a large fraction of the micropore volume was occupied. All samples contained approximately 4.4 wt.% of accumulated deposits after 20% of their lifetime (2.5, 2 and 1 h for catalysts A, B and C, respectively), independently on the performance in the alkylation reaction. Therefore, deposits accumulated more rapidly for catalyst C than for catalysts A and B, and more for catalyst B than for catalyst A. Approximately 39% of the initial micropore volume was occupied after 20% lifetime for catalyst A and 45% of the initial micropore volume for catalysts B and C.

- Period 2 was considered from 20% to 60-80% of catalyst lifetime. A low decrease of free micropore volume was observed, which agrees with the low amount of accumulated deposits in this period for all catalysts.

- Period 3 was considered from 60-80% to 100% of catalyst lifetime. The free micropore volume decreased steeply during the third period although the decrease was more moderate than during period 1. The final free micropore volume for catalysts A, B and C was 0.029, 0.035 and 0.040 ml/g, which represents 16%, 21% and 24% of the initial micropore volume, respectively.

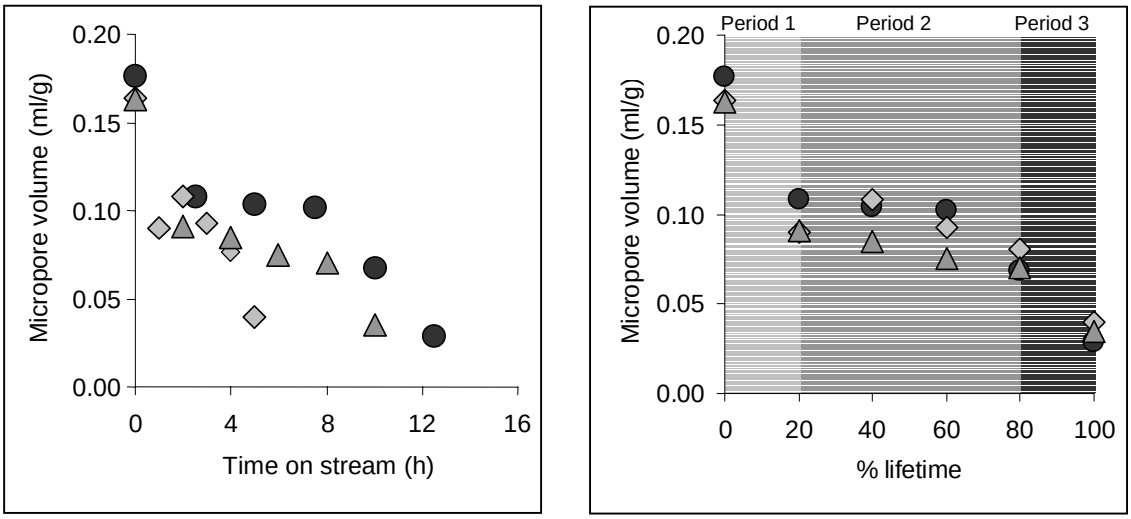

Figure 3.13: a) Micropore volume after outgassing at 120°C as a function of time-on-stream. b) Micropore volume after outgassing at 120°C as a function of percentage of coke. Samples A (●), B (▲) and C (◇) are depicted.

The amount of micropore volume occupied during the reactions with respect to amount of accumulated deposits is shown in Figure 3.14. Periods 1, 2 and 3 (and 3´ that refers to period 3 for catalysts B and C, which showed a faster occupation than catalyst A) are represented with colored areas in the figure.

During period 1, a similar amount of micropore volume was occupied for all catalysts with respect to the amount of accumulated deposits. Approximately 0.07 ml of micropore volume was occupied by 4.4 wt.% of accumulated deposits. Assuming the average density for the deposits to be 0.75 $g_{deposits}$/ml (typical for hydrocarbons), the volume occupied by 4.4

wt.% deposits would be ca. 0.06 ml. A slightly higher occupation of micropore volume was observed experimentally with respect to the theoretical value. This shows that not only the micropores are filled with deposits but also that pore mouth plugging takes place at some extent.

During period 2 a small amount of deposits were accumulated and the occupied micropore volume slightly increased. Approximately 0.01 ml of micropore volume was occupied by 1.5 wt.% of accumulated deposits for all catalysts. The theoretical volume occupied by 1.5 wt.% deposits would be ca. 0.02 ml. A slightly lower occupation of micropore volume was observed experimentally with respect to the theoretical value.

During period 3 the occupation of micropore volume was slower for catalyst A than for catalysts B and C with respect to the amount of accumulated deposits. For all catalysts the reduction of micropore volume was more rapid in period 3 than in periods 1 or 2. Approximately 0.04 ml of micropore volume was occupied by 0.5 wt.% of accumulated deposits for catalysts B and C. The theoretical volume occupied by 0.5 wt.% deposits would be ca. 0.007 ml. The much higher occupation of micropore volume with respect to the theoretical value can be explained by pore mouth plugging with cyclic/aromatic species. Approximately 0.07 ml of micropore volume was occupied by 2.8 wt.% of accumulated deposits for catalysts A. The theoretical volume occupied by 2.8 wt.% deposits would be ca. 0.04 ml. Pore mouth plugging also takes place in the case of catalyst A but at a lower rate as in the case of catalysts B and C.

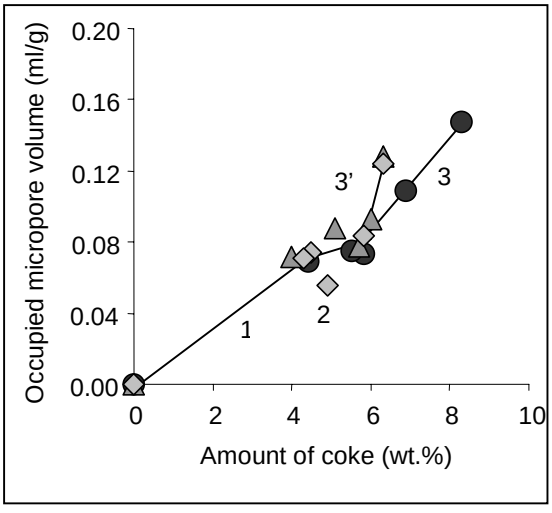

Figure 3.14: Occupied micropore volume after outgassing at 120°C as a function of the percentage of coke. Samples A (●), B (▲) and C (◈) are depicted (1- period 1, 2- period 2, 3 & 3´- period 3).

Matrix-assisted Laser desorption/ionization time-of-flight mass spectroscopy

The deactivated catalysts were analysed by MALDI-TOF MS employing DHB as matrix. All samples gave a Gaussian-curve distribution of masses with peaks in the mass range from approximately 150 to 360 with a maximum from 192 to 262 m/z. Additional peaks (corresponding to masses 431 and 445 m/z) were observed for some arbitrary spectra. Assuming the detected ions to be of the typical $[M+H]^+$ nature (which leads to uneven masses for hydrocarbons), this series would correspond to molecules of a general C_nH_{2n-4} or C_nH_{2n-18} formula. A common pattern was found for all samples following a 14 m/z addition series, the main peaks being based on the series 151 + 14*n*. In agreement with Feller *et al.* [16], every fourth of the peaks exhibited a higher intensity than the Gaussian distribution, which would correspond to a $(CH_2)_4$ addition. The maximum in the Gaussian distribution of masses shifted slightly to higher masses with time-on-stream from 220 m/z at the beginning of the reactions to 262 at times-on-stream close to the lifetime. Peaks at 155, 137 and 178 correspond to $[DHB + H]^+$, $[DHB\text{-}OH]^+$ and $[DHB + Na]^+$, respectively [31]. MALDI-TOF spectra for the three catalysts at 100% lifetime are shown in Figure 3.15 (a). All samples showed a Gaussian distribution of masses with values between 150 and 360 m/z. The maximum on the Gaussian distribution was shifted to higher masses for sample A as compared to the maximum for samples B and C, when all of them were measured at 100% lifetime. Moreover, more intense peaks in the high-end region of masses were observed in the following order: catalyst A > catalyst B > catalyst C. Spectra of samples A and C are shown in Figure 3.15 (b) after 5 hours on stream. Both catalysts showed similar MALDI-TOF spectra after 5 hours on stream with the same maximum in the Gaussian distribution of 220 m/z.

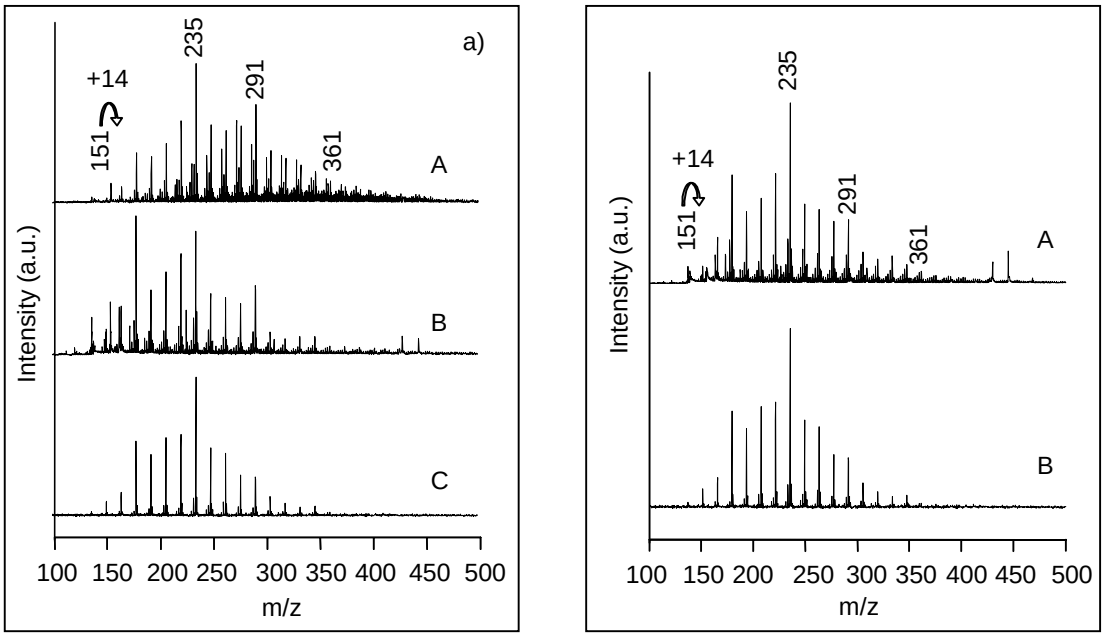

Figure 3.15: a) MALDI-TOF mass spectra of the deactivated catalysts A, B and C at 100% lifetime (12.5, 10 and 5 h, respectively); b) MALDI-TOF mass spectra of the deactivated catalysts A and C after 5 h TOS.

3.3.5 *Analysis of recovered deposits*

The deposits from the three catalysts were analysed by GC/MS. No significant variation in the distribution of masses with respect to the time-on-stream was observed for any of the catalysts. As a representative example, the main groups in the deposits for catalysts A, B and C are depicted in Figure 3.16 at 60% of their lifetime (7.5, 6 and 3 hours on stream, respectively). The deposits showed a broad range of different hydrocarbon compounds ranging from C_9 to C_{42} for catalyst A and from C_{18} to C_{45} for catalysts B and C. The maximum in the group distribution was C_{12}-C_{15} for catalyst A and C_{24}-C_{27} for catalysts B and C. The deposits are mainly paraffinic compounds that followed a series with a $(CH_2)_3$ difference from one alkane to the preceding one. A small fraction of C_{16} alkanes was also observed with values close to 2 wt.% for catalyst A and close to 3 wt.% for catalysts B and C. Similar results were found by He *et al.* [23] when doing alkylation on heteropoly acids. The authors found a majority of saturated species in the accumulated deposits with odd numbers and following a

$(CH_2)_3$ series. A fraction of the detected C_{12} isomers and the detected C_{16} isomers are a result of iso-butane/butene multiple alkylation. No hydrocarbons heavier than $C_{16}H_{34}$ as result of multiple alkylation were observed. A high cracking rate has to occur to give C_3H_6 as the terminal end. A fast equilibrium for the accumulated deposits was observed, as their nature did not vary with time-on-stream. A similar amount of unsaturated compounds was detected for catalysts A, B and C with a value close to 4.5 wt.%. Not well-resolved spectra of several peaks, which could correspond to aromatic compounds, appeared from the beginning of reaction with a constant selectivity close to 0.5 wt.% for the three catalysts.

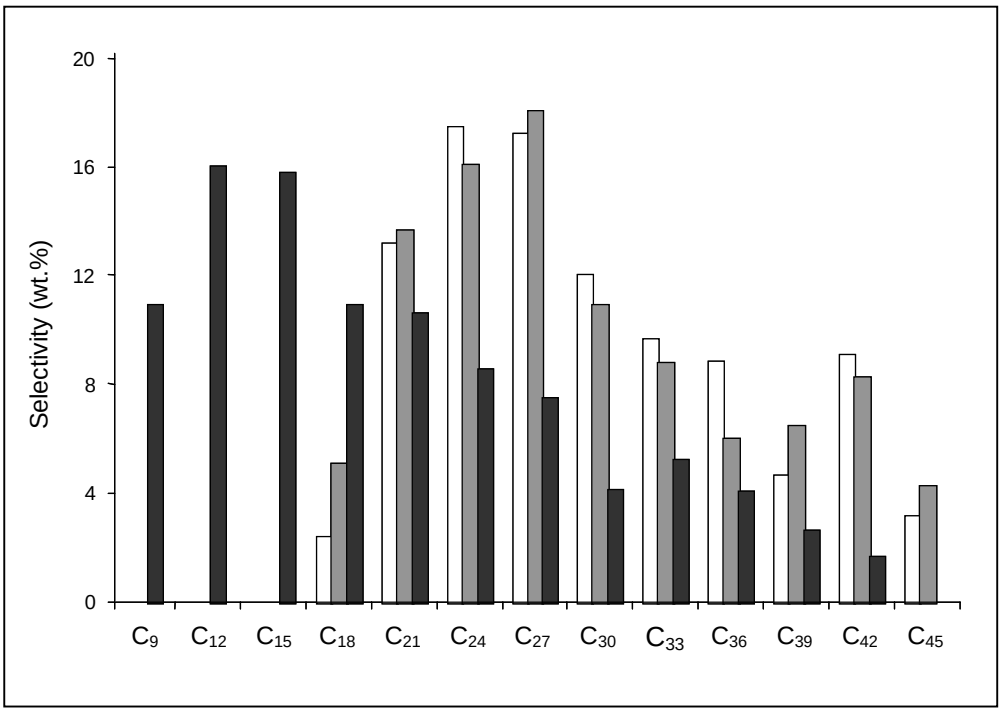

Figure 3.16: Selectivity to the main groups from the recovered deposits (■ catalyst A, ■ catalyst B and □ catalyst C).

MALDI-TOF mass spectra from the deposits were also taken. No ions were detected for any of the deposits. For this reason it is postulated that ions, which are ionizable by MALDI-TOF, are only present at the surface or they represent a minority fraction within the total amount of coke, so that their concentration in the deposits is too low to be detected.

3.4 Discussion

3.4.1 *Physicochemical properties influencing the performance of a catalyst for the iso-butane / 2-butene alkylation reaction and their impact on the quality of the alkylate produced*

The iso-butane / 2-butene reaction was studied in detail for three catalysts, obtained from the same Na-X zeolite and having different lifetime. The goal of this study was to identify which characteristics of the catalyst can lead to a different performance and to investigate the impact of different performances on the quality of the alkylate produced.

The three catalysts presented similar particle size and micropore volume. Therefore, these two parameters did not influence the catalytic performance.

The ion exchange degree achieved was higher for catalysts A (lifetime of 12.5 h) and B (lifetime of 10 h) than for catalyst C (lifetime of 5 h). As shown by Feller *et al.* [3], the amount of residual Na^+ is one of the main parameters influencing the strength of the Brønsted acid sites. Residual Na^+ seems to weaken neighboring Brønsted acid sites. A linear correlation was found by Feller *et al*. between the catalyst lifetime and the fraction of strong Brønsted acid sites; catalysts with longer lifetimes present also a higher fraction of strong Brønsted acid sites. According to these results, our best catalyst (A) showed a high concentration of strong Brønsted acid sites and a low concentration of strong Lewis acid sites.

The unit cell size measured was smaller for catalyst C than for catalysts A and B, which can be a result of the lower exchange degree or can also be due to a higher dealumination degree. Dealumination of the catalyst would lead to the transformation of Brønsted into Lewis acid sites, which increases the concentration of olefins near the Brønsted acid sites accelerating the deactivation. The catalyst that had a lower lanthanum ion exchange degree and higher Lewis acid site concentration showed the lower unit cell size among the three catalysts studied.

The inferior catalyst (C) led to more cracking and to more heavy products, which is in agreement with the former results from Feller *et al.* [3]. Heavy compounds (C_{9+}) are responsible for a more rapid deactivation. An alkylate of lower quality was produced by the inferior catalyst due to the lower selectivity to C_8 and to the lower TMP/DMH ratio. A lower selectivity to 2,2,4- and 2,2,3-TMP was observed for the inferior catalyst. In agreement with

our results, Li *et al.* [33], found higher 2,2,4- and 2,2,3-TMP when increasing the strength of the acid.

The presence of unsaturated compounds in the alkylate was confirmed by UV/VIS and ^{1}H-NMR. Olefinic compounds appeared only after 10 hours on stream for the best catalyst (A) whereas they appeared from the beginning of the reaction for the other catalysts (B and C). The concentration of unsaturated and olefinic compounds increased with time-on-stream although it remained very low during the usable lifetime for all catalysts. The higher concentration and more rapid appearance of unsaturated compounds for the inferior catalyst is a result of a higher olefin addition to hydride transfer rate for this catalyst. Weak Brønsted acid sites were found to catalyze dimerization [33]. Therefore, a high concentration of weak Brønsted acid sites promotes the formation of unsaturated compounds that adsorb or react with alkoxy groups and enhance the rate of deactivation. The lower the concentration of weak Brønsted acid sites, the higher the hydride transfer rate will be and the longer the catalyst will be active.

3.4.2 *Chemical nature of the deposits*

As shown with GC/MS analysis, the nature of the carbonaceous deposits was unchanged with respect to the time on stream. This technique revealed a mainly paraffinic nature of the deposits following a $(CH_2)_3$ series for all catalysts. The best catalyst accumulated deposits in the C_9H_{20} to $C_{42}H_{86}$ range with a maximum at $C_{12}H_{26}$-$C_{15}H_{32}$. The other catalysts accumulated deposits in the $C_{15}H_{32}$ to $C_{45}H_{92}$ range with a maximum at $C_{24}H_{50}$-$C_{27}H_{56}$. Therefore, a higher hydride transfer to oligomerization rate is expected for superior catalysts. A fraction of the detected C_{12} isomers and the detected C_{16} isomers are a result of iso-butane/butene multiple alkylation. No hydrocarbons higher than $C_{16}H_{34}$ were observed as a result of multiple alkylation.

The results presented here demonstrate that the carbonaceous deposits retained in the zeolite pores during the iso-butane / 2-butene alkylation reaction result mainly from oligomerization of propene and posterior hydride transfer. Propene is claimed to be formed by cracking of an octyl-carbenium ion formed during the isomerization of 2-butene through a bimolecular mechanism. Different products can be formed by β-scission of an octyl-carbenium ion. A first route would produce propene and an isopentyl carbenium ion, as shown in Figure 2.17. The isopentyl carbenium ion would be transformed to the corresponding

alkane through hydride transfer. A second route would produce butene and a butyl carbenium ion, products that would not be distinguished from the feed. A third route would produce pentene and a propyl carbenium ion, being this route highly unfavourable, as it would require the formation of a secondary carbenium ion. Propene was found to rapidly oligomerize to give alkane molecules up to $C_{45}H_{92}$. The products from propene oligomerization would either crack again to give smaller compounds, leave the catalyst through hydride transfer as alkanes or be accumulated in the pores.

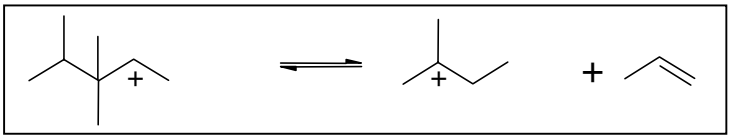

Figure 3.17: Type B β-scission for an octyl carbenium ion.

Isomers of C_{12} and C_{16} compounds were also present in the deposits. These are typical compounds from multiple alkylation. Alkylation compounds heavier than $C_{16,}$,as a result of multiple alkylation, were not observed.

MALDI-TOF MS from the coked zeolites proved the presence of unsaturated compounds on the surface of the catalyst for all the catalysts studied. This method cannot detect the presence of saturated hydrocarbons and therefore it has to be considered only as a qualitative measurement. The main compounds detected on the surface from the catalyst are based on a series 150 + 14*n*. This type of compounds would correspond to a C_nH_{2n-4} or C_nH_{2n-18} chemical formula (*i.e.* n-methyl cyclopentadiene and anthracene, see chapter 1). A similar maximum in the Gaussian distribution was determined for the different samples at the same time-on-stream. A shift of 50 m/z units in the maximum of the Gaussian distribution towards higher masses was observed from the beginning to the end of the reaction. No differences were observed in the nature of the MALDI detectable compounds accumulated on the surface for the three catalysts.

3.4.3 *Impact of the formation of deposits*

The coked catalysts were analyzed using a wide range of techniques. As measured by TPO, a similar coke oxidation pattern was observed for the three catalysts with two main peaks, the first maximum close to 250°C and the second maximum between 500 and 550°C.

For all catalysts the high temperature peak increased with time-on-stream whereas the low temperature peak hardly increased. The increase in the ratio between the high temperature peak and the low temperature peak can be attributed to a higher amount of deposits in the catalyst, which are difficult to release. Moreover, the temperature to completely burn off the coke increased with the time on stream

The accumulation of deposits was more rapid for the worst catalyst, which enhances the deactivation. Deposits were more rapidly accumulated at the beginning of reaction for all catalysts as compared to the following stages of reaction. The same effect was observed by Pater *et al.* [17] when doing the iso-butane/butene alkylation reaction on USHY. At the initial stages of reaction the strongest acid sites are still not deactivated, being the catalyst more active and leading to higher isomerization and cracking rates and, consequently, to higher oligomerization rates of cracked products. After the initial stages of the reaction (approx. 20% lifetime) a subsequent period took place in which the amount of deposits slightly increased. This period lasted from 20% to 60-80% lifetime for all catalysts. Subsequently, a further increase in the amount of accumulated deposits occurred for all catalysts with a total amount of deposits of ca. 8.3 wt.% for the best catalyst and approximately 6.3 wt.% for the others two. The total amount of deposits accumulated on the spent catalysts is consistent with the results reported in the literature [17, 18, 21]. While studying the deactivation of solid acid catalysts during iso-butane alkylation with C_4 olefins, Querini *et al.* [21] found that catalysts, which showed higher stability produced more deposits during the alkylation reaction. This fact was related to both the acidity and pore structure of the catalyst.

Three main periods of micropore volume occupation were observed for all catalysts, corresponding to the different rates of accumulation of deposits observed. In period 1 a large increment in the amount of accumulated deposits caused a strong decrease of the micropore volume. Along this period the deposits are thought to be formed mainly in the micropore pores as a result of propene oligomerization. Pore mouth plugging happened at a small rate during period 1. In period 2 a small fraction of deposits were accumulated in the pores and pore mouth plugging started to be of major importance. In period 3, the amount of accumulated deposits slightly increased for the inferior catalysts but a rapid increase in the amount of occupied micropore volume was observed. Bigger molecules were formed on the surface of the catalyst, as shown with MALDI-TOF analysis, and plugged the micropore entrances. The best catalyst accumulated more deposits during this period and it showed a

more moderate increase in the amount of occupied micropore volume with respect to the amount of deposits accumulated. Therefore, a more moderate pore mouth plugging happened for catalyst A.

Assuming the average density for the deposits to be 0.75 $g_{deposits}$/ml (typical for hydrocarbons), the volume occupied by 8.3 wt.% (highest amount of accumulated deposits determined in the studied cases) would be ca. 0.11 ml/$g_{catalyst}$. Taking into account an initial micropore volume of 0.18 ml/$g_{catalyst}$, roughly 13 wt.% of deposits would fit in the pores of the catalyst. Therefore, the pores of the catalyst are not full of deposits at times-on-stream close to deactivation. On the other hand, the micropore volume measurements showed that, in the same case, approximately 0.15 ml/ $g_{catalyst}$ were occupied at the end of reaction. Therefore, pore mouth plugging has to occur during the iso-butane/butene alkylation reaction.

3.5 Conclusions

The avoidance of structural damage occurring during the modification procedure is the key factor for suitable alkylation catalyst. A high Na^+ exchange and a low dealumination degree are of major importance to ensure a catalyst with high performance. A high concentration of strong Brønsted acid sites is mandatory to favor the alkylation reaction and achieve a high hydride transfer rate. High concentration of weak Brønsted acid sites catalyzes dimerization. Na^+ cations weaken neighboring Brønsted acid sites. Dealumination of the catalyst leads to the transformation of Brønsted into Lewis acid sites, which increases the concentration of olefins near the Brønsted acid sites, accelerating the deactivation. A successful catalyst for alkylation has to possess a high concentration of strong Brønsted acid sites and a low concentration of Lewis acid sites.

A higher quality alkylate is produced by superior catalysts. Unsaturated compounds and aromatics appeared in higher concentration and at shorter times-on-stream in the alkylate produced by the inferior catalyst, although their concentration was very low in all cases.

Accumulated deposits in the pores of the catalyst are mainly formed by highly branched paraffinic compounds following a $(CH_2)_3$ series and with molecular weights from 128 g/mol to 548 g/mol. The deposits formed inside the pores of the catalyst are claimed to be a result of propene oligomerization. Superior catalysts showed lower masses in the deposits with a maximum at C_{12}-C_{15} while inferior catalysts showed a maximum at C_{24}-C_{27}. Low amounts of

olefins and aromatics were also found in the deposits. Small amounts of $C_{12}H_{26}$ and $C_{16}H_{34}$ from multiple alkylation were also detected in the deposits.

Cyclic compounds and aromatics are formed on the surface of the catalysts as observed by MALDI-TOF. These types of compounds were not detected when the zeolite was dissolved in HF and the coke molecules extracted with methylene chloride. Therefore their concentration was low within the total concentration of deposits. These types of molecules are responsible for pore mouth plugging on the surface of the catalyst. The size of the molecules detected by MALDI-TOF increased with time-on-stream for all catalysts. They were of a C_nH_{2n-4} and C_nH_{2n-18} nature with molecular masses ranging from 150 to 360.

3.6 References

1. Zhuang Y., Ng F.T.T., *Appl. Catal. A* **190**, 137 (2000).
2. Ginosar D.M., Thompson D.N., Coates K., Zalewski D.J., *Ind. Eng. Chem. Res*. **41**, 2864 (2002).
3. Feller A., Zuazo I., Guzmán A., Barth J.O., Lercher J.A., *J. Catal* **216**, 313 (2003).
4. Weitkamp J., Traa Y., *in* "Handbook of Heterogeneous Catalysis" (Ertl G., Knözinger H., Weitkamp J., Eds), Vol. 4, p.2039, VCH, Weinheim, 1997.
5. Schmerling L., *J.Am.Chem.Soc.* **67**, 1778 (1945).
6. Schmerling L., *J.Am.Chem.Soc.* **68**, 275 (1946).
7. Fan L., Nakamura I., Ishida S., Fujimoto K., *Ind. Eng. Chem. Res.* **36**, 1458 (1997).
8. Chu Y.F., Chester W., *Zeolites* **6**, 195 (1986).
9. Simpson M.F., Wei J., Sundaresan S., *Ind. Eng. Chem. Res*. **35**, 3861 (1996).
10. Nivarthy G.S., He Y., Seshan K., Lercher J.A., *J. Catal.* **176**, 192 (1998).
11. Nivarthy G.S., Feller A., Seshan K., Lercher J.A., *Microp. Mesop. Mater.* **35-36**, 75 (2000).
12. Mostad H.B., Stöcker M., Karlsson A., Rørvik T., *App. Catal. A* **144**, 305 (1996).
13. Stöcker M., Mostad H., Rørvik T., *Catal. Lett.* **28**, 203 (1994).
14. De Jong K.P., Mesters C.M.A.M., Peferoen D.G.R., van Brugge P.T.M., de Groot C., *Chem. Eng. Sci.* **51**, 2053 (1996).
15. Cardona F., Gnep N.S., Guisnet M., Szabo G., Nascimento P., *App. Catal. A* **128**, 243 (1995).

16. Feller A., Barth J.O., Guzmán A., Zuazo I., Lercher J.A., *J. Catal.* **220**, 192 (2003).
17. Pater J., Cardona F., Canaff C., Gnep N.S., Szabo G., Guisnet M., *Ind. Eng. Chem. Res.* **38**, 3822 (1999).
18. Weitkamp J., Maixner S., *Zeol.* **7**, 6 (1987).
19. Flego C., Kiricsi I., Parker Jr. W.O., Clerici M.G., *App. Catal. A* **124**, 107 (1995).
20. Sahebdelfar S., Kazemeine M., Khorasheh F., Badakhshan A., *Chem. Eng. Sci.* **57**, 3611 (2002).
21. Querini C.A., Roa E., *App. Catal A* **163**, 199 (1997).
22. Yoo K., Smirniotis P.G., *App. Catal A* **246**, 243 (2003).
23. He Y., He Y., *Catal. Today* **74**, 45 (2002).
24. Díaz-Mendoza, F.A., Pernett-Bolano L., Cardona-Martínez N., *Thermo. Acta* **312**, 47 (1998).
25. Yoo K., Burckle E.C., Smirniotis P.G., *Catal. Lett.* **74**,85 (2001).
26. Förster H., Kiricsi I., *Zeol*. **7**,508 (1987).
27. Kiricis I., Flego C., Bellusi G., *Appl. Catal.* **126**, 401 (1995).
28. Kiricis T., Pálinkó I., Kollár T., *J. Molec. Struct.* **651-653**, 331 (2003).
29. J.A. Lercher, C.H. Gründling and G.Eder-Mirth, Catal. Today, 27, 353 (1996).
30. Emeis C.A., J. Catal. 141, 347 (1993).
31. Pruns J.K., Vietzke J.-P., Strassner M., Rapp C., Hintze U., König W.A., *Rapid Commun. Mass Spectrom*. **16**, 208 (2002).
32. Li K.W., Eckert R.E., Albright L.F., *Ind. Eng. Chem. Process Des. Develop.* **9**, 441 (1970).
33. Mostad H.B., Stöcker M., Karlsson A., Rørvik T., *Appl. Catal. A* **144**, 305 (1996).

Chapter 4

Product characteristics during a stable solid acid catalyzed iso-butane/2-butene reaction

Abstract

The main drawback in the use of zeolites for iso-butane/butene alkylation is their rapid deactivation, which up to date has prevented their industrial application. Therefore, in order to achieve an economically feasible industrial process, the catalysts must be frequently regenerated.

A suitable method for the regeneration of catalysts used for iso-butane/butene alkylation has been developed. The method is based on cycles containing reaction, low temperature regeneration by washing with H_2 dissolved in iso-butane in the liquid phase and regeneration at elevated temperatures with H_2 in the gas phase.

Several sets of reaction/low temperature regeneration can be performed before high temperature regeneration is necessary. By high temperature regeneration the activity of the catalyst was driven back to its (near-) initial state. A stable catalyst performance with a high quality alkylate was achieved by this method along several cycles.

4.1 Introduction

Iso-butane/butene alkylation is widely used in the petroleum-chemical industry as a process for feedstock upgrading. The reaction is catalysed by strong acids, of which only sulphuric and hydrofluoric acid are commercially used [1]. The restriction in the use of sulphuric and hydrofluoric acid is desirable due to their transport and handling hazards, their corrosiveness and the environmental responsibility associated with the disposal of spent acid. Numerous efforts have been aimed at developing solid acid alkylation process to replace sulphuric acid or hydrofluoric acid processes [2] and zeolites were the first solid acids tested as alternative catalysts for that purpose [3]. The main drawback in the use of zeolites for iso-butane/butene alkylation is their rapid deactivation, which up to date has prevented their industrial application. Therefore, in order to achieve an economically feasible industrial process, the catalysts must be frequently regenerated. The patent literature suggests that multiple regenerations (as many as several hundred) are needed for processes based on solid catalysts to be competitive with existing processes [4].

Several authors have focused their studies on the regeneration procedure over the past few years. Querini [5] studied the regeneration of the catalyst by several methods, *i.e.,* in air, ozone, hydrogen, hydrogen peroxide and by using combined treatments. The author found hydrogen peroxide to be active for coke oxidation already at 90°C and a successful regeneration was achieved when the ozone treatment was followed by a hydrogen treatment. Ginosar *et al.* [6] studied the regeneration of the catalyst by using supercritical fluids, *i.e.* n-butane, iso-butane, n-pentane and iso-pentane. They found supercritical fluids to be more effective than near-critical fluids for the regeneration of the catalyst. Besides that, they found iso-butane to be the most effective among them with the added advantage that iso-butane is an alkylation reactant. Guisnet *et al.* [7, 8] and Stöcker *et al.* [9] investigated the regeneration by oxidative treatments. They found that temperatures as high as 600°C are needed to completely oxidize the deposited coke during the alkylation reaction. He *et al.* [2] investigated a regeneration process in which regeneration with dissolved H_2 in iso-butane, as well as regeneration with H_2 in the gas phase, was carried out with time length from 0.2 to 24 h, regeneration temperature from 25 to 300°C and pressure from 1 to 80 bars.

In a general context, Weitkamp *et al.* [4] describe three main modes of catalyst regeneration in the alkylation of iso-butane with butenes. As first mode, the authors suggested the treatment of the catalyst with a liquid, which does not contain alkenes under mild conditions. For the sake of simplicity the liquid chosen could be iso-butane, if possible under mild conditions. By means of this treatment a partial recovery of activity would be achieved. As second mode, the combustion of the retained coke in air, in air diluted with nitrogen or in oxygen is suggested. Provided the catalyst survives the high temperature conditions of the combustion, the activity would be completely recovered. As third mode, hydrogen treatment of the retained coke is suggested. A hydrogenation component such as platinum or palladium needs to be incorporated to the catalyst, as suggested by Yang [10], the hydrogen treatment being then considered as a bifunctional hydrocracking of long chain alkanes.

In this chapter, a reaction/regeneration cycle process is explored based on two different steps modes alternate reaction and low temperature regenerations and regeneration at elevated temperatures. The low temperature regeneration (lt-regeneration) was performed in the liquid phase, with dissolved H_2 in iso-butane, after 20% of the usable lifetime of the catalyst. The set reaction/lt-regeneration was usually 10 times repeated. The high temperature regeneration (ht-regeneration) was performed in the presence of gaseous H_2 at a pressure of 20 bar.

4.2 Experimental

Catalysts and reactants

The catalyst used for the iso-butane/butene reaction was a metal containing rare-earth exchanged FAU zeolite. The parent material used for this series of experiments was a Na-FAU zeolite obtained from Chemische Bad Köstritz. The parent material was converted in its acidic form by multiple lanthanum ion exchanges and its posterior calcination. In the first step, the parent material was 1-3 times exchanged with a 0.2 M aqueous lanthanum nitrate solution (liquid-to-solid ratio approximately 10 ml/g) at 70ºC for two hours. The resulting material was washed with doubly distilled water to remove nitrate, and then calcined with a slow temperature increment up to 450 ºC maintaining this temperature for one hour. This was followed by a second ion-exchange step and then loading of metal (ca. 0.3 wt.%) with a metal nitrate solution. Samples were calcined and reduced afterwards.

The liquefied gases were received from Messer with a purity of 99.95% (iso-butane) and 99.5% (2-butene).

Mode of operation

The alkylation of iso-butane with 2-butene was performed in a fixed bed reactor operated in continuous mode. The reactor used was a stainless steel tube with ½ inch outer diameter. Iso-butane and butene were fed using ISCO high-pressure syringe pumps. Hydrogen was added *via* a mass flow controller. After the reactor the product was expanded *via* an electronic backpressure regulator and passed through a six-port-valve with a sample loop. The content of that loop was injected automatically into an HP 6830 gas chromatograph equipped with a FID-detector and a 50 m HP-1 column. The amount of catalyst used for the long-term experiment was 0.4 g. HP VEE was used to program the automatic adjustment of the reaction and regeneration conditions.

A typical alkylation cycle is composed of two main steps: reaction/lt-regeneration (liquid phase) and ht-regeneration (gas phase). The sum of n-reactions/lt-regenerations and one time ht-regeneration is considered as one reaction cycle. The catalyst used for the iso-butane/butene reaction was a metal containing rare-earth exchanged FAU zeolite. The catalyst was used in form of pellets with sizes ranging from 200 to 315 μm and mixed with SiC. It was activated for 8 hours at 170°C under a 50 ml/min flow rate of H_2. The activation was done *in situ* within the alkylation reactor. After cooling down to reaction temperature (75°C) the reactor was filled with liquid iso-butane at a pressure of 20 bars. The alkylation reaction was started by admitting an iso-butane/butene mixture at a P/O ratio of 300 and with an OSV of 0.2 g_{olefin} / ($g_{catalyst}$ h). The reaction was performed up to 2.25 hours (approximately 20% of the usable lifetime previously determined for this catalyst) and then the butene flow was stopped. After 10 minutes of washing with iso-butane, a 10 ml/min flow of H_2 at 20 bars was added. The catalyst was lt-regenerated by the H_2 dissolved iso-butane for a similar time-span as the one used for the reaction. Usually, 10 sets of reaction/lt-regeneration were done before ht-regeneration was applied. The iso-butane flow was stopped and 50 ml/min flow of H_2 was passed over the catalyst for the ht-regeneration. The temperature was kept at 75°C for the first two hours and subsequently, it was increased by using a slow ramp up to temperatures ranging from 350 to 440°C, with a dwell time of 7 hours at the end temperature.

The products from the alkylation reaction, lt- and ht-regenerations were expanded and passed through a six-port-valve with a sample loop, the contents of which were injected

automatically into an HP 6830 gas chromatograph equipped with a FID-detector and a 50 m DB-1 column. Downstream of the six-port-valve, the product stream can be condensed into a cold trap cooled with a dry ice/isopropanol mixture (at –80ºC).

4.3 Results and interpretation

4.3.1 *Single reaction and reaction steps during the long-term alkylation experiment*

A single reaction was carried out in order to obtain the usable lifetime of the catalyst as well as to be able to compare product quality between a single reaction and a cycled reaction operation. The single alkylation reaction was performed employing a reaction temperature of 75°C, an olefin space velocity of 0.2 g_{olefin} / ($g_{catalyst}$ h) and a P/O ratio of 300. The lifetime achieved by the catalyst, defined as the time of (near-) complete butene conversion, was approximately 11 h as shown in Figure 4.1. Then, the conversion sharply dropped to values close to 50% and it continued dropping down to values close to 20 wt.% in the next 4 hours.

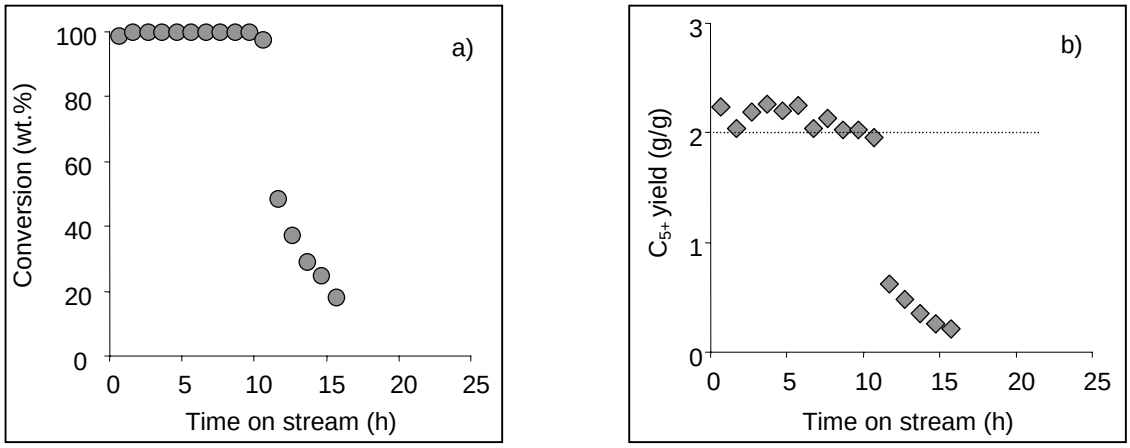

Figure 4.1: Alkylation performance during a single reaction. a) Butene conversion as a function of time-on-stream; b) C_{5+} product yield as a function of time-on-stream.

The yield was close to the theoretical maximum, 2.04 g/g (olefin), right from the earlier stages on stream as shown in Figure 4.1 (b). When the butene conversion was incomplete, the yield rapidly dropped to values lower than 1g/g (olefin).

Figure 4.2 (a) compiles the product group selectivity for the three main groups of reaction products, *i.e.*, alkanes with 5 to 7 carbon atoms, octane isomers and alkanes with 9 and more

carbon atoms (heavy fraction) as a function of time-on-stream. The selectivity to octanes decreased continuously from ca. 83 wt.% at the beginning of reaction to values close to 70 wt.% at times close to the end of its lifetime. Then, it dropped further to a value of approximately 65 wt.% after 4 hours. The light alkanes (C_5-C_7) generated by cracking and hydride transfer slightly increased in selectivity until the catalyst started to deactivate, reaching a maximum value of approximately 13 wt.%. As the butene conversion was not complete anymore, the selectivity to the light alkanes rapidly decreased to approximately 9 wt.% with a value close to 5 wt.% after 4 hours more on stream. The selectivity to heavy fraction (C_{9+}) increased until the catalyst started to deactivate, reaching a maximum value of approximately 14 wt.%. After the deactivation started to be apparent, the selectivity to heavy fraction increased steeply to a value close to 23 wt.% with a value close to 27 wt.% after 4 more hours on stream. The selectivity to n-butane decreased continuously from ca. 3 wt.% at the beginning of reaction to approximately 2 wt.% at times close to lifetime (when deactivation is apparent).

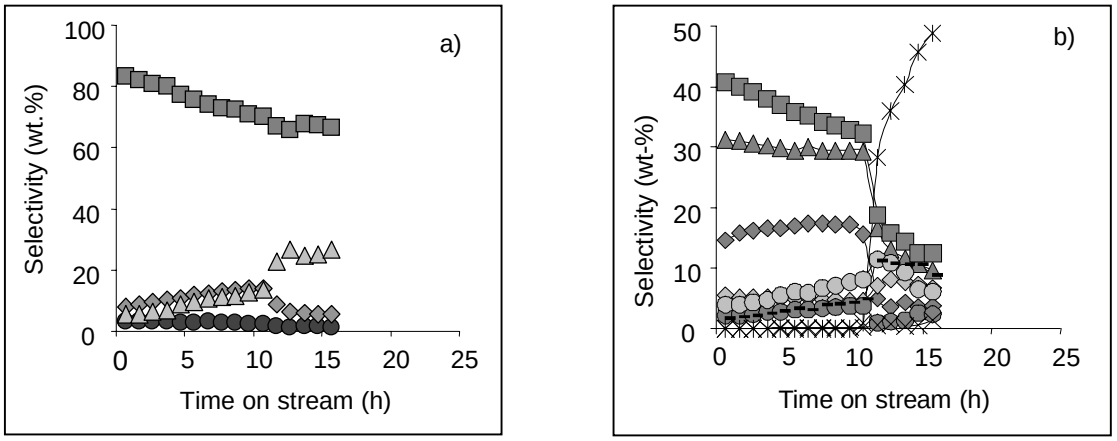

Figure 4.2: Alkylation performance of catalyst M-Re-FAU. a) Product group selectivities with time-on-stream (● n-C_4, ◇ C_5-C_7 products, ■ C_8 products, △ C_{9+} products); b) selectivities in the C_8 fraction with time-on-stream (■2,3,3-TMP,◆2,2,4-TMP, ▲2,3,4 TMP, ◇ 2,5-DMH/2,2,3-TMP,○ 2,3-DMH, - 4-MHP/3,4-DMH, ● 2,4-DMH, × 3,4-DMH, ✳ Octenes).

The selectivity within the C_8 fraction is depicted in Figure 4.2 (b). Trimethylpentanes were the dominating isomers. It should be noted that trimethylpentanes are

thermodynamically less favorable than dimethylhexanes, which indicates that isomerization equilibrium with respect to the branching of the alkanes was not achieved. Among the trimethylpentanes, 2,3,3-TMP, 2,2,4-TMP and 2,3,4-TMP dominated and constituted together approximately 80 wt.% of the C_8 fraction. The selectivity to 2,2,4-TMP passed through a maximum with a value close to 17 wt.% with values close to 15 wt.% at the beginning and end of the time of complete butene conversion and then, it steeply decreased to a value close to 5 wt.%. 2,2,3-TMP, which is the primary product of the alkylation of iso-butane with 2-butene (not separated from 2,5-DMH) slightly decreased during the time of complete butene conversion with values always close to 5 wt.%. Then, it rapidly increased to approximately 8 wt.%, decreasing again to 7 wt.% after the next 4 hours on stream. The selectivity to 2,3,3-TMP continuously decreased from values close to 41 wt.% at the beginning of reaction to values of ca. 32 wt.% at the end of it. The selectivity to 2,3,4-TMP was constant during the reaction, with values always close to 30 wt.%. The other octanes detected, 2,3-DMH, 2,4-DMH, 3,4-DMH and 4-MHP showed individual selectivities lower than 8 wt.% during the whole time-on-stream. Octenes were not detected up to times-on-stream close to deactivation. Once the butene conversion was not complete anymore, the selectivity to the main saturated compounds decreased dramatically. The selectivity to octenes increased up to values close to 50 wt.% in the next 4 hours on stream.

A reaction/lt-regeneration set of experiments was carried out in order to enlarge the useful lifetime of the catalyst. The reaction/lt-regeneration set was repeated 10 times typically before ht-regeneration was applied. By means of this procedure, the time-on-stream achieved in a reaction/lt-regeneration set was roughly 2 times the lifetime shown by the catalyst in a single reaction. The butene conversion and yield achieved for pure reaction time (time at which iso-butane/butene mixture is converted) during a representative case of a reaction/lt-regeneration set is shown in Figure 4.3 (a). Each point represents the respective measurement (conversion, yield, selectivities…) of every reaction.

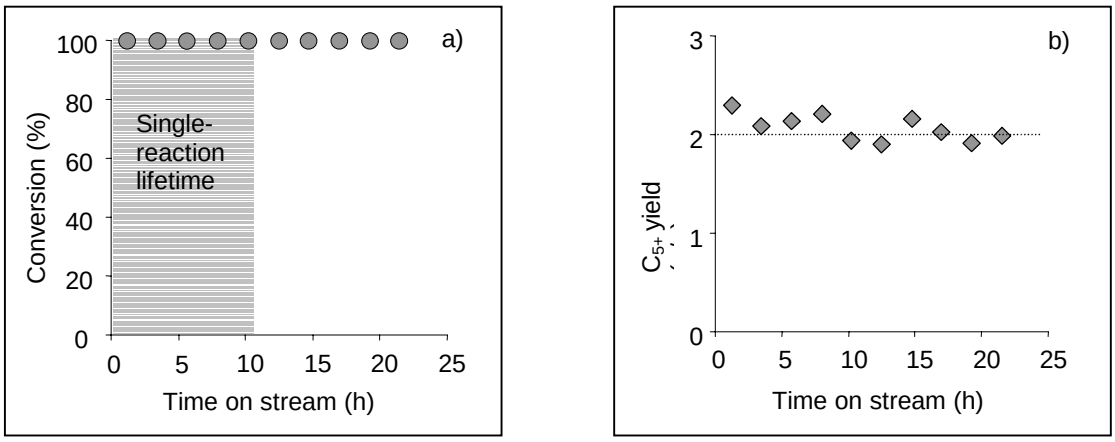

Figure 4.3: Alkylation performance (only reaction time) during a cycle. a) Butene conversion as a function of time-on-stream; b) C_{5+} product yield as a function of time-on-stream.

No decline of butene conversion was observed during the set of reactions/lt-regenerations. The yield was nearly constant during the whole cycle, with a value close to the theoretical value of 2.04 g/g. Figure 4.4 (a) compiles the product group selectivity for the three main groups of reaction products, *i.e.* alkanes with 5 to 7 carbon atoms, octane isomers and alkanes with 9 and more carbon atoms (heavy fraction) as a function of time-on-stream. The selectivity to octanes slightly decreased from approximately 82 wt.% in the first reaction to a value close to 79 wt.% in the last reaction. The light alkanes (C_5-C_7) generated by cracking and hydride transfer and the heavy fraction (C_{9+}) slightly increased, reaching maximum values of approximately 11 wt.% and 7 wt.% in the last reaction, respectively. The selectivity to n-butane was approximately constant along the cycle with values between 3 and 4 wt.%.

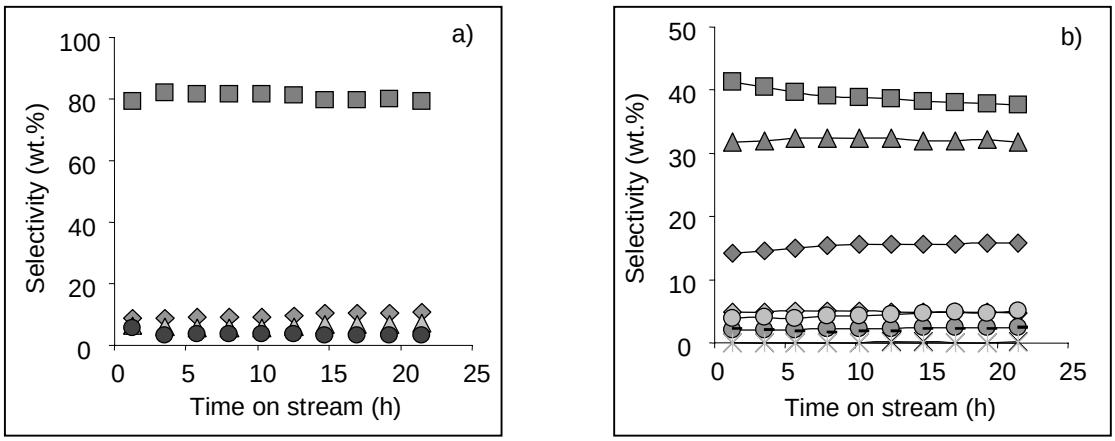

Figure 4.4: Alkylation performance of catalyst Me-RE-FAU. a) Product group selectivities with time-on-stream (● n-C_4, ◆ C_5-C_7 products, ■ C_8 products, △ C_{9+} products); b) selectivities in the C_8 fraction with time-on-stream (■ 2,3,3-TMP, ◆ 2,2,4-TMP, ▲ 2,3,4 TMP, ◇ 2,5-DMH/2,2,3-TMP, ○ 2,3-DMH, - 4-MHP/3,4-DMH, ● 2,4-DMH, × 3,4-DMH, ✳ Octenes).

The selectivity within the C_8 fraction is depicted in Figure 4.4 (b). Trimethylpentanes were the dominating isomers. Among the trimethylpentanes, 2,3,3-TMP, 2,2,4-TMP and 2,3,4-TMP dominated and constituted together more than 85 wt.%. The selectivity to 2,2,4-TMP continuously increased with values of 14 wt.% in the first reaction to 16 wt.% in the last reaction. The combined selectivity to 2,2,3-TMP and to 2,5-DMH was constant for all reactions with values of ca. 5 wt.%. The selectivity to 2,3,3-TMP continuously decreased from values close to 41 wt.% in the first reaction to values close to 38 wt.% in the last one. The selectivity to 2,3,4-TMP was constant for all reactions, with values always close to 32 wt.%. The other octanes observed, 2,3-DMH, 2,4-DMH, 3,4-DMH and 4-MHP, showed selectivities lower than 5 wt.% for all reactions. Octenes, which are a clear indicator of deactivation in the alkylation reaction, were not detected.

4.3.2 *Mild-regeneration step during the long-term experiment*

The selectivities to the three main group product fractions (C_5-C_7, C_8 and C_{9+}) and the selectivity to n-butane as a function of time during mild-regeneration are shown in Figure 4.5 (a).

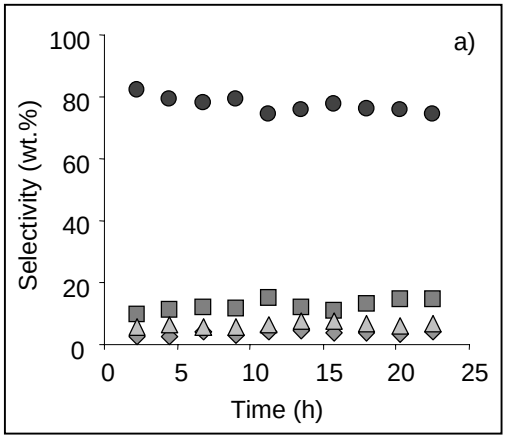

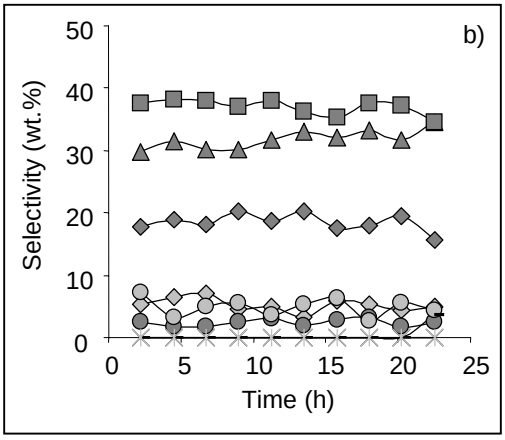

Figure 4.5: Product distribution during the mild-regeneration step. a) Product group selectivities with time-on-stream (● n-C_4, ◇ C_5-C_7 products, ■ C_8 products, △ C_{9+} products); b) selectivities in the C_8 fraction with time-on-stream (■ 2,3,3-TMP, ◆ 2,2,4-TMP, ▲ 2,3,4 TMP, ◇ 2,5-DMH/2,2,3-TMP, ○ 2,3-DMH, - 4-MHP/3,4-DMH, ● 2,4-DMH, × 3,4-DMH, ✳ Octenes).

As shown in Figure 4.5 (a), n-butane showed the highest selectivity during lt-regeneration with values from 82 wt.% in the fist lt-regeneration to 75 wt.% in the last lt-regeneration. The selectivity to the C_8 fraction increased continuously from ca. 10 wt.% in the first lt-regeneration to approximately 15 wt.% in the last one. The selectivity to the C_5-C_7 fraction and to the C_{9+} fraction was approximately constant for all lt-regenerations with values ranging from 3 wt.% to 4 wt.% for the C_5-C_7 fraction and from 6 wt.% to 7 wt.% for the C_{9+} fraction. Thus, a higher selectivity to the C_5-C_7 fraction and, in particular, to the C_{9+} fraction as compared to the C_8 fraction was obtained during lt-regeneration with respect to the reaction time.

The selectivity within the C_8 fraction is depicted in Figure 4.5 (b). Trimethylpentanes were the dominating isomers. Among the trimethylpentanes, 2,3,3-TMP, 2,2,4-TMP and 2,3,4-TMP dominated and constituted together more than 85 wt.%. The selectivity to 2,2,4-TMP showed values between 15 wt.% and 20 wt.%. The combined selectivity to 2,2,3-TMP and to 2,5-DMH was approximately constant for all reactions with values of ca. 6 wt.%. The selectivity to 2,3,3-TMP showed values from 35 to 38 wt.% and the selectivity to 2,3,4-TMP slightly increased with values from 30 to 35 wt.%. The other octanes observed, 2,3-DMH, 2,4-DMH, 3,4-DMH and 4-MHP, showed selectivities lower than 6 wt.% for all lt-regenerations.

4.3.3 *Hard-regeneration step during the long-term experiment*

The catalyst was ht-regenerated after a set of reaction/lt-regeneration was repeated usually 10 times. The hard-regeneration step was performed in the gas phase using H_2 at 20 bars. The temperature was kept at reaction temperature during 2 hours and then it was increased at a slow rate up to 350°C with a dwell-time of 7 hours at this temperature, as shown in Figure 4.6. The evolution of the cracked products during the hard-regeneration step was monitored *on-line* by CG. Iso-butane was the main compound detected during ht-regeneration. It was not possible to differentiate between iso-butane as a remainder from the lt-regeneration step and iso-butane as a cracking product from the ht-regeneration step. Therefore, iso-butane will not be considered in the following discussion. The amount of product from cracking passed through three main maxima at temperature values of approximately 160°C, 290°C and 350°C.

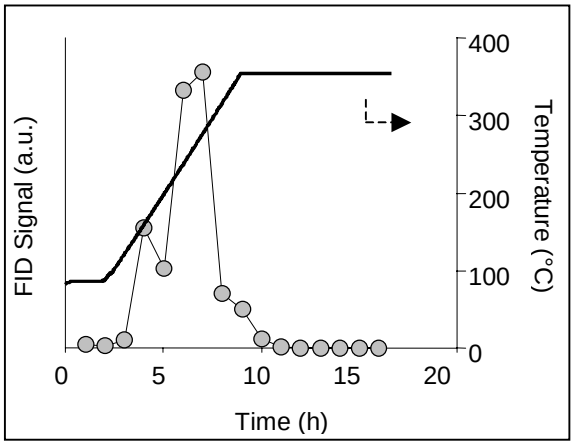

Figure 4.6: Product and temperature profile as a function of time

Six main fractions were grouped within the cracked products: C_1-C_3, n-C_4, iso-C_5, n-C_5, C_6-C_7, C_8 and C_{9+} as it can be seen in Figure 4.7. At the early stages of the ht-regeneration step, the selectivity to n-butane was 100 wt.% and it dropped sharply to values close to 12 wt.% at a temperature of 160°C. Afterwards, it showed 2 maxima, one at 200°C and a second one after 1 hour at 350°C with values close to 20 and 40 wt.%, respectively. It was not possible to determine the fraction of n-butane as a result of isomerization of the remaining iso-butane or as a result of cracking from heavier compounds. The other ht-regeneration products showed different selectivity maxima during the temperature ramp: the C_1-C_3 fraction passed through a maximum of 7 wt.% at 200°C and through a second one of ca. 32 wt.% after 1 h at 350°C, iso-C_5 passed through a maximum of ca. 85 wt.% at 160°C and through a second maximum of 30 wt.% after 1 h at 350°C, the C_6-C_7 fraction passed though a maximum of ca. 60 wt.% at 200°C, C_8 through a maximum of ca. 65 wt.% at 235°C and C_{9+} through a maximum of ca. 42 wt.% at 275°C.

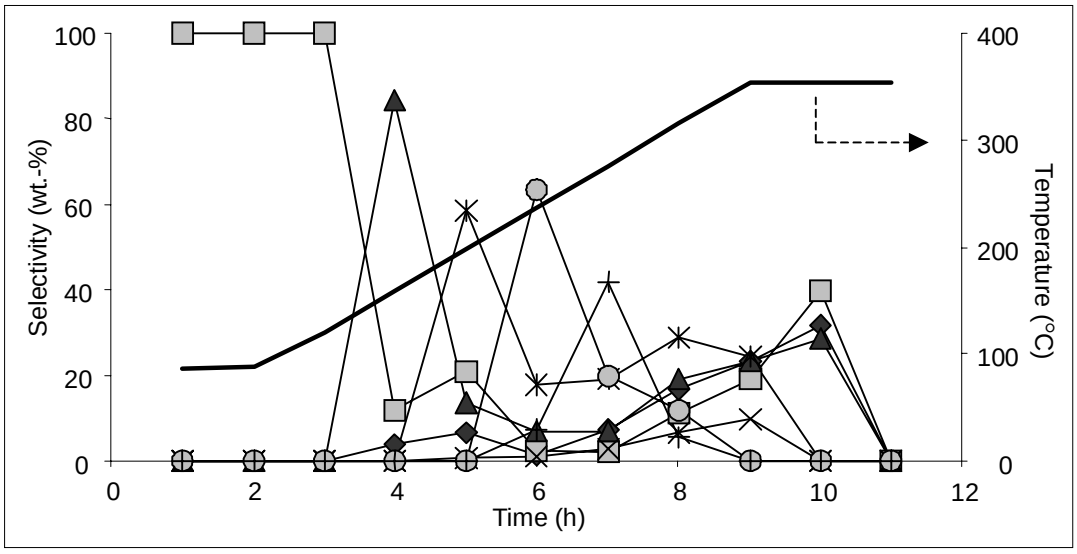

Figure 4.7: Product selectivities during the hard-regeneration step (◆C_1-C_3, □ n-C_4, ▲ iso-C_5, × n-C_5, ✳ C_6-C_7, ○ C_8, + C_{9+}, — Temperature).

4.3.4 *Overall alkylation reaction over more cycles*

The evolution of the alkylate produced, as well as the products of lt- and ht-regeneration, are shown for an interval of 5 cycles (each cycle is made up of a set of 10 reaction/lt-regenerations and 1 ht-regeneration). The catalyst was therefore five times ht-regenerated. The total lifetime after the 5 cycles amounted to approximately 10 times the lifetime of the catalyst in a single reaction.

The group fraction selectivities along the five cycles are shown in Figure 4.8 (a). The selectivity to the C_8 fraction was constant and close to 82 wt.% during the first cycle. Its selectivity slightly decreased for the other cycles with values close to 78 wt.% in the first reaction of every cycle to ca. 75 wt.% in the last reaction of every cycle. The selectivity to the light alkanes (C_5-C_7) moderately increased within every cycle with a value close to 8 wt.% in the first reaction and between 10 wt.% and 12 wt.% in the last reaction. No remarkable differences in the selectivity of the light alkanes were seen among the cycles. . The selectivity to the C_{9+} fraction increased moderately within every cycle but never exceeded 10 wt.%. The selectivity to n-butane was approximately constant within a cycle with values between 3 and 4 wt.% for the first cycle and between 2.5 and 3 wt.% for the next cycles.

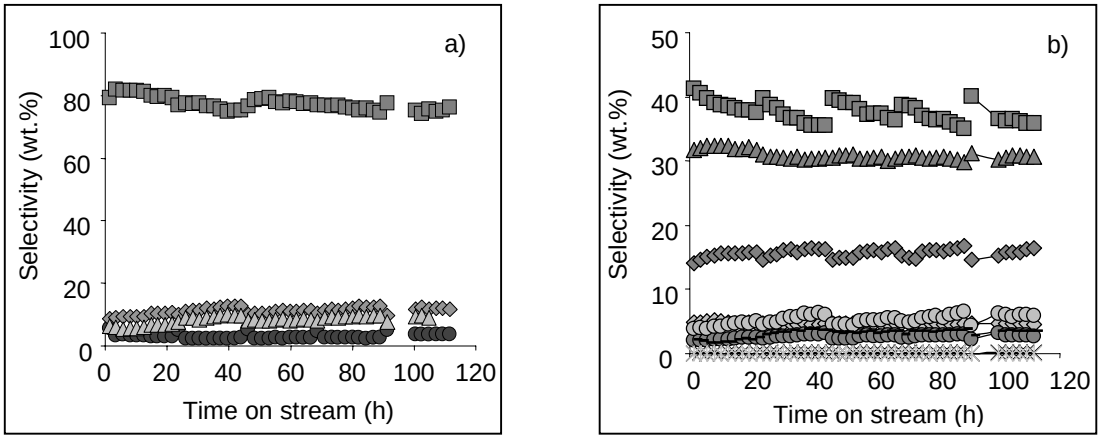

Figure 4.8: Alkylation performance of catalyst Me-RE-FAU. a) Product group selectivities with time-on-stream (● n-C_4, ◇ C_5-C_7 products, ■ C_8 products, △ C_{9+} products); b) selectivities in the C_8 fraction with time-on-stream (■2,3,3-TMP,◆2,2,4-TMP,▲ 2,3,4 TMP, ◇ 2,5-DMH/2,2,3-TMP, ○2,3-DMH, - 4-MHP/3,4-DMH, ● 2,4-DMH, × 3,4-DMH, ✳ Octenes).

The selectivity within the C_8 fraction is depicted in Figure 4.8 (b). Trimethylpentanes were the dominating isomers. Among the trimethylpentanes, 2,3,3-TMP, 2,2,4-TMP and 2,3,4-TMP dominated and constituted together more than 80 wt.%. The selectivity to 2,2,4-TMP continuously increased with values of 14 wt.% in the first reaction to 16 wt.% in the last reaction for all cycles. The combined selectivity to 2,2,3-TMP and to 2,5-DMH was constant for all reactions with values of ca. 5 wt.%. The selectivity to 2,3,3-TMP continuously decreased from values close to 41 wt.% in the first reaction to values close to 37 wt.% in the last one for all cycles. The selectivity to 2,3,4-TMP was approximately constant for all reactions, with values close to 32 wt.%. The other octanes observed, 2,3-DMH, 2,4-DMH, 3,4-DMH and 4-MHP, showed individual selectivities lower than 5 wt.% for all reactions. No octenes, which are a clear indicator of deactivation in the alkylation reaction, were detected.

The selectivities to the different fractions, for the lt-regeneration steps along the five cycles, are shown in Figure 4.9 (a). The selectivity to n-butane showed values between 75 and 80 wt.% for all cycles. The selectivity to the C_8 fraction slightly varied along the cycles with values between 10 and 20 wt.%. The selectivity to the C_5-C_7 fraction remained approximately

constant, with values between 2.5 and 3.5 wt.% for all cycles, and the C_{9+} fraction showed values between 6 and 8 wt.% for all cycles.

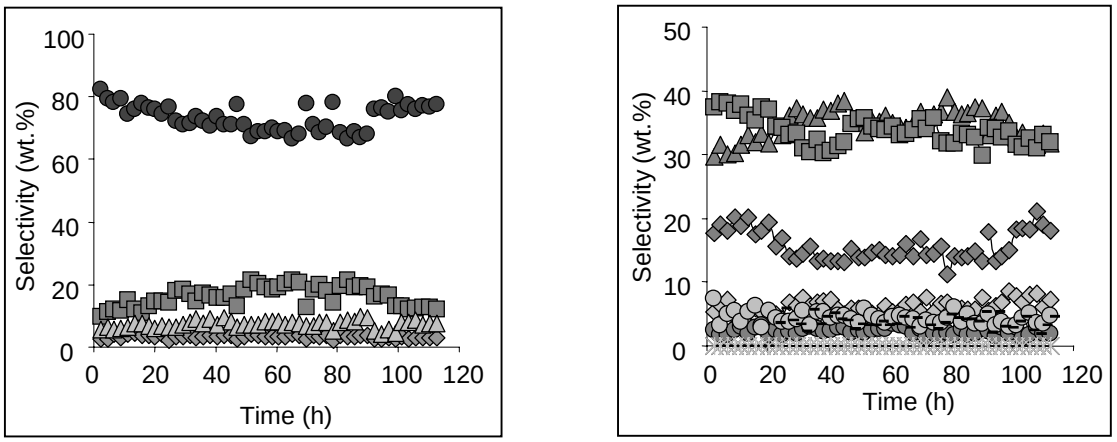

Figure 4.9: Mild-regeneration selectivities along 5 cycles: a) Product group selectivities with time-on-stream (● n-C_4, ◆ C_5-C_7 products, ■ C_8 products, △ C_{9+} products); b) selectivities in the C_8 fraction with time-on-stream (■ 2,3,3-TMP, ◆ 2,2,4-TMP, ▲ 2,3,4 TMP, ◇ 2,5-DMH/2,2,3-TMP, ○ 2,3-DMH, - 4-MHP/3,4-DMH, ● 2,4-DMH, × 3,4-DMH, ✳ Octenes).

The selectivity within the C_8 fraction is depicted in Figure 4.9 (b). Trimethylpentanes were the dominating isomers. Among the trimethylpentanes, 2,3,3-TMP, 2,2,4-TMP and 2,3,4-TMP dominated and constituted together more than 85 wt.%. The selectivity to 2,2,4-TMP showed values between 15 wt.% and 20 wt.%. The combined selectivity to 2,2,3-TMP and to 2,5-DMH was ca. 7 wt.% for all reactions. The selectivity to 2,3,3-TMP showed values from 31 to 37 wt.% and the selectivity to 2,3,4-TMP showed values from 30 to 38 wt.%. The other octanes observed, 2,3-DMH, 2,4-DMH, 3,4-DMH and 4-MHP, had selectivities lower than 5 wt.% for all reactions.

The amount of cracked products, during ht-regeneration after each of the five reactions/lt-regenerations sets, is shown in Figure 4.10. For reasons not clear yet, the amount of cracked product was much higher after the first set of reactions/lt-regenerations than in the next ones, although the profile for every group of compounds was similar for all ht-regenerations. On the other hand, the amount of cracked product remained constant from the second to the fifth

cycle. In all cases, the three main maxima observed appeared at: 160°C, 290°C and after 1 hour at 350°C. Minimal amount of compounds were released after 2 hours at 350°C.

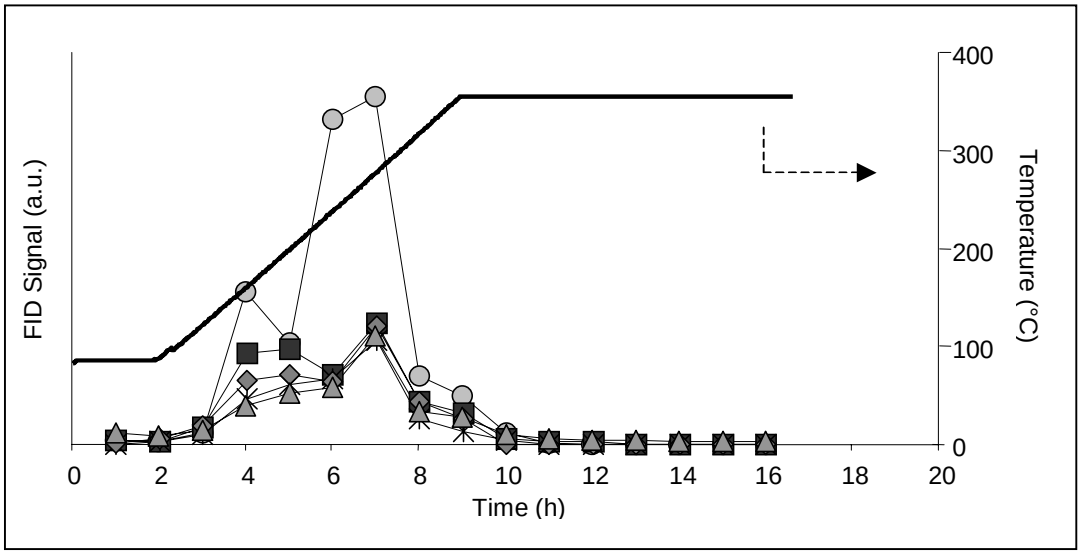

Figure 4.10: Product and temperature profile during hard-regeneration as a function of time (○after cycle 1 , ■ after cycle 2, ✕ after cycle 3, ◆ after cycle 4 and △ after cycle 5).

The selectivity to the main fractions is depicted in Figures 4.11, 4.12 (a, b), 4.13 (a, b) and 4.14 (a, b) for all cycles. Iso-butane is not included as it was not possible to differentiate between the iso-butane produced from cracking and the iso-butane remaining from the lt-regeneration step.

The selectivity to the n-butane is shown in Figure 4.11. Its selectivity was 100 wt.% at the beginning of hydrocracking decreasing to values close to 5 wt.% while ramping up to 350°C. Then, it increased again with maximum after a few hours at 350°C. Note that n-butane could be a cracking product as well as a product of isomerization of iso-butane.

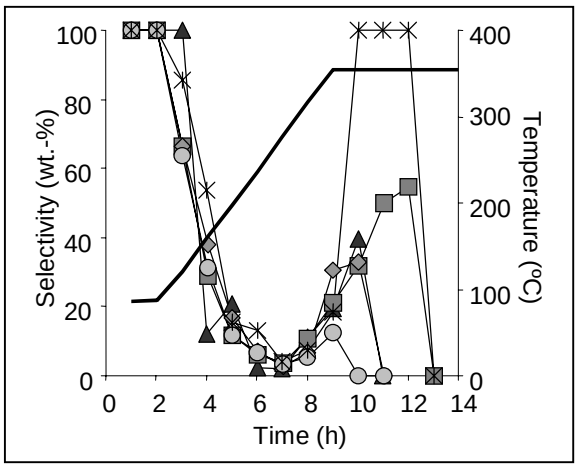

Figure 4.11: n-C_4 selectivity during hard-regeneration (▲ cycle 1, ■ cycle 2, ◆ cycle 3, ● cycle 4 and ✕ cycle 5)

Figure 4.12 shows the selectivity to the C_1-C_3 (a) and to the n-C_5 fraction (b) during ht-regeneration for all cycles. As shown in Figure 4.12 (a), the selectivity to the C_1-C_3 fraction followed a profile with two maxima: the first one at 120°C and the second one at 350°C. In both cases, the maximum selectivity was approximately the same, with values close to 40 wt.%. The selectivity to n-C_5 is shown in Figure 4.12 (b). In this case, only a high temperature peak with selectivity of ca. 10 wt.% was observed.

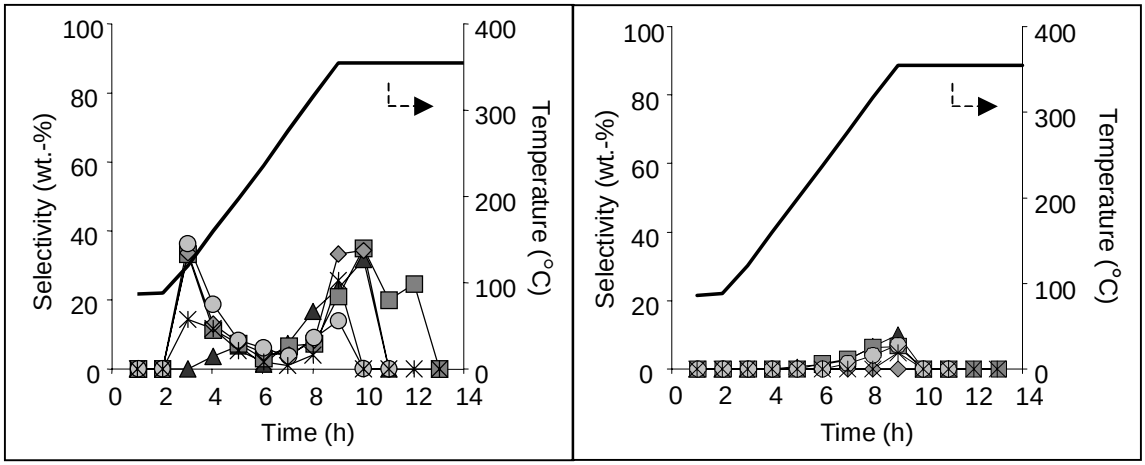

Figure 4.12: C_1-C_3 (a) and n-C_5 (b) selectivity during the hard-regeneration (▲ cycle 1, ■ cycle 2, ◆ cycle 3, ● cycle 4 and ✕ cycle 5).

Figure 4.13 shows the selectivity to the iso-C_5 fraction (a) and to the C_6-C_7 fraction (b) during ht-regeneration for all cycles. As shown in Figure 4.13 (a), the selectivity to iso-C_5 followed a similar profile as the one for the C_1-C_3 fraction. Two main peaks were observed with maxima at 160°C and 350°C and with values between 50 and 85 wt.% and between 20 and 30 wt.% selectivity, respectively. The iso-C_5 selectivity decreases from the first ht-regeneration to the fifth ht-regeneration. The selectivity profile for the C_6-C_7 fraction is shown in Figure 4.13 (b). It showed two overlapped peaks with maxima at ca. 200°C and 300°C and with selectivity values between 60 and 80 wt.% and between 30 and 45 wt.%, respectively. The selectivity to this fraction was lower for the first ht-regeneration and remained approximately constant for the next ht-regenerations.

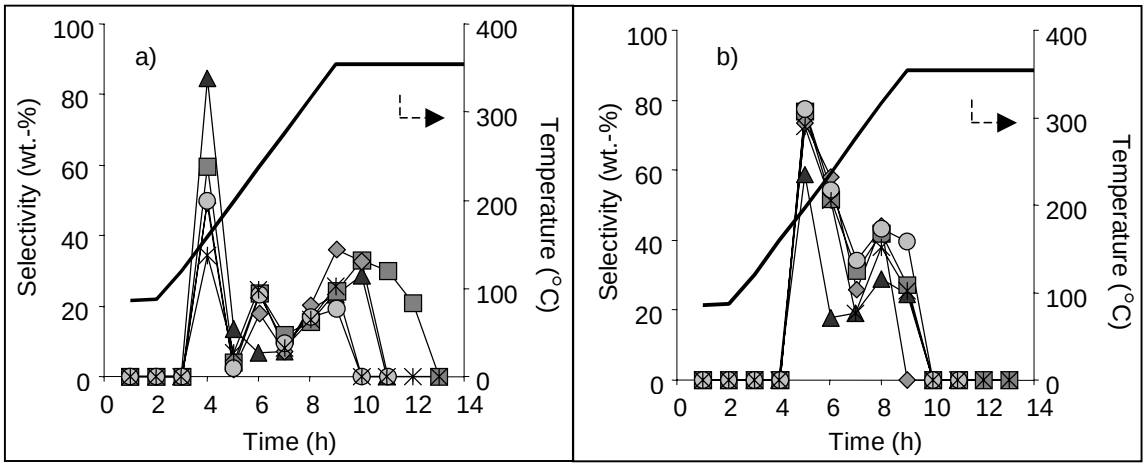

Figure 4.13: iso-C_5 (a) and C_6-C_7 (b) selectivity during the hard-regeneration (▲cycle 1, ■ cycle 2,◆ cycle 3, ○ cycle 4 and ✳ cycle 5).

Figure 4.14 shows the selectivity to the C_8 fraction (a) and to the C_{9+} fraction (b) during ht-regeneration for all cycles. As shown in Figure 4.14 (a), the selectivity to the C_8 fraction showed a single peak with a maximum at ca. 240°C for the first ht-regeneration and at ca. 280°C for the other ht-regenerations. The maximum selectivity value for the C_8 fraction varied between 30 and 60 wt.%, the latter being the highest value for the first ht-regeneration. No clear trend was observed within the other ht-regenerations. The selectivity to the C_{9+} fraction showed one peak at 280°C with selectivity of 40 wt.% for the first cycle and between 10 and 20 wt.% for the following ones.

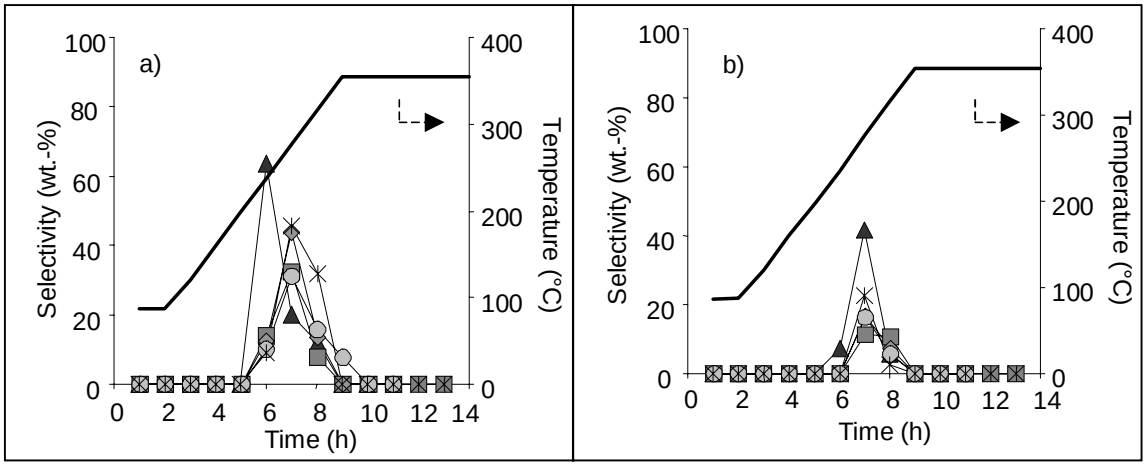

Figure 4.14: C_8 (a) and C_{9+} (b) selectivity during the hard-regeneration (▲cycle 1, ■cycle 2, ◆cycle 3, ●cycle 4 and ✕cycle 5).

4.4 Discussion

4.4.1 Catalyst performance

A stable performance was achieved by a cycled process based in a series of 10 reaction/lt-regeneration with a final ht-regeneration (Figure 4.8). All reactions run with a constant productivity close to the maximum theoretical value of 2.04 $g_{alkylate}$ / (g_{olefin} h). a constant product quality was achieved over 5 cycles, which amounted to 10 times the usable lifetime of the catalyst in a single reaction, without signs of deactivation of the catalyst.

In a reaction/lt-regeneration set, the catalyst could be partly regenerated by simple washing with H_2 dissolved in iso-butane at 75°C and 20 bars. By using a single set of reactions/lt- regenerations the lifetime of the catalyst, and therefore its productivity, could be at least doubled. Moreover, no signs of deactivation within a set were observed and therefore it would be probably possible to extend the lifetime of the catalyst even longer by this method. Van Broekhoven *et al.* [11] found the time at which the catalyst is lt-regenerated as the crucial step, being in principle the farther from the usable lifetime of the catalyst the better. In the series of experiments presented in this chapter the catalyst was arbitrarily lt-regenerated after 20% of its usable lifetime. After doing once the regeneration with iso-butane at 180°C and 111 bars, Ginosar *et al.* [6] achieved in the next reaction C_{5+} and C_8 yield values close to 80% of the initial ones, which are far below the stable yield presented in this chapter.

A stable mode of operation was found by He *et al.* [2] when doing lt-regeneration of the catalyst with dissolved H_2 in iso-butane at a temperature of 70°C and a pressure of 50 bars. A series of 4 reactions/lt-regenerations was performed by these authors showing a stable performance and product quality. A similar temperature to the one used by He *et al.* was used, but a milder pressure of 20 bar was used. A ht-regeneration procedure at 350-440°C and 20 bar of H_2 was established which allowed a stable performance over long periods. Weitkamp *et al.* [12] found that the alkylation catalyst was fully regenerated (the carbon content after regeneration was lower that 0.1 wt.% as measured by elemental analysis) at ht-regeneration conditions similar to those presented in this chapter.

4.4.2 Comparison of the quality of the product between a single reaction and a set of reactions/mild-regenerations

Figures 4.2 and 4.4 display the selectivity to the different products for a single reaction and for the reactions within a set of 10 reactions/lt-regenerations. It is noticeable that the total time-on-stream for the set of reaction/lt-regeneration was approximately double than the time-on-stream for the single reaction. The quality of the alkylate was slightly better (higher selectivity to the C_8 fraction and higher selectivity to the TMPs within the C_8 fraction) during a set of reaction/lt-regenerations that during a single-reaction. Thus, the selectivity to the C_8 fraction remained constant and close to 80 wt.% during a set of reactions/lt-regenerations, whereas it decreased to values of about 70 wt.% at the end of the usable lifetime of the catalyst for a single reaction. Within the C_8 fraction, a higher selectivity to trimethylpentanes as compared to dimethylhexanes was obtained when performing the set of reactions/lt-regenerations in comparison to the single reaction, which enhances the quality of the alkylate produced. A more rapid decrease of the 2,3,3-TMP selectivity and similar 2,3,4-TMP and 2,2,4-TMP selectivities with time-on-stream was observed for the single reaction as compared to the set of reactions/lt-regenerations. The selectivity to dimethylhexanes increased with time-on-stream for the single reaction, whereas it was practically constant during the set of reactions/lt-regenerations, which is also a sign of better product quality.

The quality of the product was continuously deteriorated with time-on-stream for a single reaction while it stayed constant during a set of reactions/lt-regenerations. Therefore, the catalyst was partly regenerated by simple washing with H_2 dissolved in iso-butane at 75°C and 20 bars of pressure. During the lt-regeneration step the main products were n-butane and

the typical products from alkylation reaction. As shown in Figure 4.5, the selectivity to the light and heavy fractions as compared to the C_8 fraction was higher during lt-regeneration than during reaction. Therefore, during the lt-regeneration step, not only washing of the typical alkylation compounds is performed but also accumulated heavier compounds are released.

4.4.3 Cracked products during the hard-regeneration step

As seen in chapter 2, most of the deposited coke species in iso-butane/butene alkylation are paraffin molecules with molecular weights ranging approximately from 130 to 560 g/mol. Therefore, cracking of paraffins is considered to be the main reaction involved in regeneration cycles. Two simultaneous mechanisms are proposed for the ht-regeneration procedure: catalytic (hydro-) cracking based in a bimolecular route and catalytic cracking based in a monomolecular route.

The mechanism of catalytic cracking of hydrocarbons has been studied by many authors over the last years [13-26]. Several studies have shown that paraffinic cracking occurs through two well-differentiated mechanisms [25, 26]. The first one is a bimolecular mechanism and involves a hydride transfer step from a neutral molecule to an adsorbed carbenium species to form the adsorbed carbenium ion of the former, followed by its β-scission. The process generates an olefin and a carbenium ion. Hydride transfer from a feed molecule to the latter generates a paraffin molecule, which subsequently desorbs. In the case of hydrocracking, the catalysts used are typically bifunctional catalysts with a hydro-dehydrogenating function (noble metals or sulphides of groups VI and VIII metals) and with an acidic function [23, 27]. The alkane hydrocracking is explained on the basis of a classical bifunctional mechanism that starts when a metal site dehydrogenates alkanes into alkenes, an acid site converts the alkene into another isomer or into a cracking product through carbenium ion intermediates and finally a metal site hydrogenates the converted alkene back into an alkane [23, 28, 29]. As already shown by several authors, the hydrocracking activity, stability and selectivity are found to be a function of the balance between the acid and the hydrogenating functions and also a function of pore size [23, 27, 29-31]. Over the last few years, it was postulated that the probability for a molecule to hydrocrack increases with the increase in the degree of branching as more stable carbocationic transition states are produced by more extensively branched isomers [27, 29, 32]. Isomerization can occur through non-branching

rearrangements (type A) or through branching rearrangements (type B), the latter being slower than the former. Branching isomerization can take place *via* protonated cyclopropane and cyclobutane intermediates. Cracking can occur through type A, B and C β-scission. As already shown by Weitkamp *et al.* [4], type A β-scission implies starting from a tertiary carbenium ion to give another tertiary carbenium ion, type B β-scission implies starting from a secondary carbenium ion to give a tertiary carbenium ion or *vice versa* and type C β-scission implies starting from a secondary carbenium ion to give another secondary carbenium ion. Guisnet *et al.* [28] found the rate constants for n-decane hydrocracking at 200°C in the following order: A cracking > A isomerization > B isomerization > B cracking >> C cracking. Under the conditions used by these authors, type C β-scission was found to be almost negligible. A different distribution between isomerization and cracking products can be obtained depending on the acid site concentration of the catalyst, on the amount of hydrogenating function contained in the catalyst and on the hydrocracking conditions (pressure, temperature…).

The second mechanism for catalytic cracking of hydrocarbons is monomolecular and requires the attack of a proton on a C-C bond of a paraffin molecule, forming a pentacoordinated carbocation, and its posterior cracking to give a paraffin molecule and the complementary adsorbed carbenium ion [26].

The two mechanisms for catalytic cracking of hydrocarbons coexist. The activation energy was found to be higher for the protolytic scission than for the β-scission [25] and, therefore, the importance of protolytic cracking processes increases with temperature at the expense of β-scission [20]. Moreover, the product distribution will depend on the relative contribution of protolytic and β-scission mechanisms. When the protolytic cracking is the predominant mechanism more lineal paraffins, methane, ethane and even ethylene and H_2 will be produced. On the other hand, when β-scission dominates high yields of branched products will be obtained [13].

In the case studied in this chapter, ht-regeneration of the deposited hydrocarbons was performed with 20 bar H_2 using a slow temperature ramp () from reaction temperature (75°C) to 350°C and a final dwell-time of 7 h. Most of the cracked products were desorbed at 290°C. No attempt to characterize the single compounds produced during the ht-regeneration was made due to the large number of single compounds detected. The cracked compounds observed were grouped in C_1-C_3, C_4 (iso-C_4 and n-C_4), C_5 (iso-C_5 and n-C_5), C_6-C_7, C_8 and

C_{9+} as shown in Figure 4.7. Interestingly, marked differences in the profile between short and long chain compounds occurred. Short chain products (with the exception of n-C_5) showed two well-differentiated maxima during ht-regeneration while long-chain (C_6-C_7, C_8 and C_{9+}) compounds showed a single peak or two overlapped peaks. The amount of cracked compounds during the first cycle was higher than during the next ones, but the selectivity to the different fractions within the products of ht-regeneration was approximately constant for all cycles as well as the temperatures were constant for the selectivity maxima.

The selectivity to the C_1-C_3 fraction showed two well-differentiated maxima at 120°C and at 350°C with values close to 40 wt.%. Smirniotis *et al.* [33] found no CH_4 and a very small fraction of C_2H_6 during octane hydrocracking. The formation of those compounds through a bimolecular mechanism would require a type D β-scission (secondary to primary carbenium ion), which is energetically very unfavourable. C_3H_8 hydrocarbons can be formed through a type B β- scission that, although less favourable than type A β-scission, is likely to happen under the cracking conditions used. On the other hand, the formation of light alkanes is typical of protolytic cracking reactions, being favoured at high temperatures. A typical scheme for protolytic cracking of an arbitrary alkane is depicted in Figure 4.15. Three main different routes to give light alkanes are shown for the exemplary depicted molecule. Route 1 leads to the formation of methane, route 2 leads to the formation of propane and route 3 leads to the formation of hydrogen.

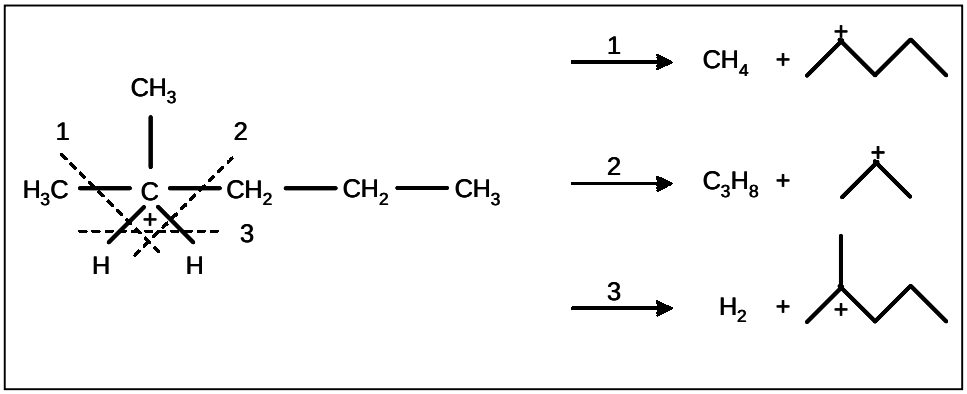

Figure 4.15: Protolytic cracking of 1-methyl pentane.

The formation of n-C_4 can be either a result of isomerization from iso-C_4, which remains from lt-regeneration, or of cracking of heavier compounds. Isomerization of iso-C_4 to give n-

C_4 occurs *via* a bimolecular route that usually requires strong Brønsted acid sites, long contact time and high temperature [34, 35]. High concentrations of hydrogen would inhibit this bimolecular route due to the decrease in the concentration of tert-butyl carbenium ions though their hydrogenation [36]. Protolytic cracking of long chain paraffins would result in the formation of n-C_4 as already shown by several authors [16, 24, 26, 32, 37].

A high selectivity to iso-C_5 is observed with an initial maximum at 160°C and a second one at 350°C. The large selectivity to iso-C_5 agrees with previous results presented by Smirniotis *et al.,* [33] who found that large pore zeolites as FAU favour the production of iso-C_5 during *e.g.* octane hydrocracking. As shown in Figure 4.12, the selectivity to n-C_5 remains very low and with a unique maximum at 350°C. The formation of n-C_5 is more limited than the formation of iso-C_5, as the former would either require type B β-scission in which a secondary carbenium ion is formed or it would be a product of protolytic cracking, which requires high activation energies.

During hydrocracking a large number of compounds with molecular mass higher than C_5 was detected. No differentiation was made between them. These compounds came from cracking or isomerization reactions. It is remarkable that the low temperature maxima for iso-C_5, C_6-C_7, C_8 and C_{9+} followed a trend with respect to temperature (160 °C for iso-C_5, ca. 200°C for C_6-C_7 , C_8 at ca. 235°C and C_{9+} at ca. 275°C) which can be attributed to transport limitations.

4.5 **Conclusions**

A suitable method for the regeneration of catalysts for iso-butane/butene alkylation is developed.

By lt-regeneration, the catalyst usable lifetime was at least doubled. A high and unaltered product quality was maintained within a set of reactions/lt-regenerations. The catalyst performance was driven back to its (near-) initial activity through ht-regeneration in the gas phase. A broad distribution of products was released during ht-regeneration as a result of cracking of the accumulated deposits.

A stable catalytic performance and product quality was achieved by combining a set of n-reactions/lt-regenerations with a final ht-regeneration in a cycled process. No signs of deactivation were observed.

4.6 **Acknowledgments**

The author wishes to thank Xaver Hecht from TUM for his help in all technical aspects. Financial support from LURGI GmbH is gratefully acknowledged.

4.7 **References**

1. Stell J., *Oil Gas J.* **99 (52)**, 75 (2001).
2. He, Y., He Y., Xie W., Fu Q., U.S. Patent 6,492,571 B1 (2002).
3. Feller A., Zuazo I., Guzmán A., Barth J.O., Lercher J.A., *J. Catal* **216**, 313 (2003).
4. Weitkamp J., Traa Y., *in* "Handbook of Heterogeneous Catalysis" (Ertl G., Knözinger H., Weitkamp J., Eds), Vol. 4, p.2039, VCH, Weinheim, 1997.
5. Querini C.A., *Cat. Today* **62**, 135 (2000).
6. Ginosar D.M., Thompson D.N., Burch K.C., *Appl. Catal. A* (2004).
7. Nassionou G.A.D., Magnoux P., Guisnet M., *Microp. Mesop. Mater.* **22**, 389 (1998).
8. Guisnet M., Magnoux P., *Catal. Today* **36**, 477 (1997).
9. Rørvik T., Mostad H., Ellestad O.H., Stöcker M., *Appl. Catal A* **137**, 235 (1996).
10. Yang C.L., U.S.Patent 3,851,004 (1976).
11. Van Broekhoven E.H., Cabre F.R.M., Bogaard P., Klaver G., Vonhoj M., U.S. Patent 5,986,158 (1999).
12. Josl R., Klingmann R., Traa Y., Gläser R., Weitkamp J., *Catal. Commun.* **5**, 239 (2004).
13. Corma A., Orchillés A.V., *Microp. Mesop. Mater.* **35-36**, 21 (2000).
14. Yaluris G., Madon R.J., Dumesic J.A., *J. Catal.* **165**, 205 (1997).
15. Kissin Y.V., *J. Catal.* **180**, 101 (1998).
16. Corma A., Miguel P.J., Orchillés A.V., *J. Catal.* **145**, 171 (1994).
17. Narbeshuber T.F., Brait A., Seshan K., Lercher J.A., *Appl. Catal. A* **146**, 119 (1996).
18. Wojciechowski B.W., Corma A., *in* "Catalytic cracking – Catalysts, Chemistry, and Kinetics", Vol. 25, Marcel Dekker, Inc., 1986.
19. Guerzoni F.N., Abbot J., *J. Catal.* **139**, 289 (1993).
20. Groten W.A., Wojciechowski B.W., *J. Catal.* **140**, 262 (1993).
21. Mota C.J.A., Esteves P.M., Ramirez-Solis A., Hernandez-Lamoneda R., *J. Am. Chem. Soc.* **119**, 5193 (1997).
22. Whitmore F.C., *Ind. Eng. Chem.* **26**, 94 (1934).

23. Guisnet M., Thomazeau C., Lemberton J.L., Mignard S., *J. Catal.* **151**, 102 (1995).
24. Brait A., Koopmans A., Weinstabe H., Ecker A., Seshan K., Lercher J.A., *Ind. Eng. Chem. Res.* **37**, 873 (1998).
25. Haag W.O., Dessau R.M., Proceedings of the 8th International Congress on Catalysis, Dechema, Berlin **2**, 305 (1984).
26. Corma A., Mighel P.J., Orchillés A.V., *Ind. Eng. Chem. Res.* **36**, 3400 (1997).
27. Guisnet M., Alvarez F., Gianetto G., Perot G., *Catal. Today.* 1, 415 (1987).
28. Maesen T.L.M., Calero S., Schenk M., Smit B., *J. Catal.* **221**, 241 (2004).
29. Alvarez F., Ribeiro F.R., Perot G., Thomazeau C., Guisnet M., *J. Catal.* **162**, 179 (1996).
30. Weitkamp J., *Ind. Eng. Chem. Prod. Res. Dev.* **21**, 550 (1982).
31. Taylor R.J., Petty H.P., *App. Catal. A* **119**, 121 (1994).
32. Martens G.G., Marin G.B., Martens J.A., Jacobs P.A., Baron G.V., *J. Catal.* **195**, 253 (2000).
33. Zhang W., Smirniotis P.G., *J. Catal.* **182**, 400 (1999).
34. Guisnet M., Gnep N.S., *Appl. Catal. A* **146**, 33 (1996).
35. Fogash K.B., Larson R.B., González M.R., Kobe J.M., Dumesic J.A., *J.Catal.* **163**, 138 (1996).
36. Tran M.T., Gnep N.S., Guisnet M., Nascimiento P., *Catal. Lett.* **47**, 57 (1997).
37. Blomsma E., Martens J.A., Jacobs P.A., *J. Catal.* **155**, 141 (1995).

Summary

The aim of this thesis was to understand the routes of deactivation of iso-butane / 2-butene alkylation on faujasitic zeolites and to correlate the alkylation performance with the physicochemical properties of the zeolite used. It was also under the scope of this thesis, to propose a reaction/regeneration mechanism that ensures a successful and continuous operation.

It could be shown that the avoidance of structural damage occurring during the modification procedure is the key factor for suitable alkylation catalyst. A high Na^+ exchange and a low dealumination degree is a major importance to ensure a catalyst with high performance. A high concentration of strong Brønsted acid sites is mandatory to favor the alkylation reaction and achieve a high hydride transfer rate. High concentration of weak Brønsted acid sites catalyze dimerization. Na^+ cations weaken neighboring Brønsted acid sites. Dealumination of the catalyst led to the transformation of Brønsted into Lewis acid sites, which increased the concentration of olefins near the Brønsted acid sites accelerating the deactivation. A successful catalyst for alkylation has to posses a high concentration of strong Brønsted acid sites and a low concentration of Lewis acid sites.

It could be shown that during the alkylation reaction a high quality alkylate was produced that was practically free of unsaturated compounds and aromatics, even at times close to deactivation. A higher quality alkylate was produced by superior catalysts. Unsaturated compounds and aromatics appeared in higher concentration and at shorter times-on-stream in the alkylate produced by the inferior catalyst, although their concentration was very low in all cases. Trimethylpentanes amounted for approximately 80 wt.% of the produced alkylate by good performing catalysts what provided a high RON number.

It could be shown that the accumulated deposits in the pores of the catalyst were mainly formed by highly branched paraffinic compounds following a $(CH_2)_3$ series and with molecular weights from 128 g/mol to 548 g/mol. The deposits formed inside the pores of the catalyst were a result of propene oligomerization. Superior catalysts showed lower masses in the deposits with a maximum at C_{12}-C_{15} while inferior catalysts showed a maximum at C_{24}-C_{27}. Low amounts of olefins and aromatics were also found in the deposits. Small amounts of $C_{12}H_{26}$ and $C_{16}H_{34}$ from multiple alkylation were also detected in the deposits. Cyclic compounds and aromatics were formed on the surface of the catalyst as observed by MALDI-TOF. These types of compounds were not detected when the zeolite was dissolved in HF and

the coke molecules extracted with methylene chloride. Therefore, their concentration was low within the total concentration of deposits. These types of molecules were responsible for pore mouth plugging on the surface of the catalyst. The size of the molecules detected by MALDI-TOF increased with time-on-stream for all catalyst. They were of a C_nH_{2n-4} and C_nH_{2n-18} nature with molecular masses ranging from 150 to 360.

A suitable method for the regeneration of catalysts for iso-butane/butene alkylation was developed. The method was based on cycles containing reaction, mild-regeneration by washing in the liquid phase and hard-regeneration in the gas phase. By mild-regeneration, the catalyst usable lifetime was at least doubled. A high and unaltered product quality was maintained within a set of reactions-mild regenerations. The catalyst performance was driven back to its (near-) initial activity through its hard-regeneration in the gas phase. A broad distribution of products was released during hard-regeneration as a result of cracking of the accumulated deposits. A stable catalytic performance and product quality was achieved by combining a set of n-reactions/mild-regenerations with a final hard-regeneration in a cycled process. No signs of deactivation were observed.

Zusammenfassung

Das Ziel dieser Doktorarbeit war die Deaktivierungswege während der Iso-butan / 2-Buten Alkylierung mit faujasiten Zeolithen zu verstehen, und die Alkylierungsleistung mit den physikalisch-chemikalischen Eigenschaften vom Katalysator zu korrelieren. Ein weiteres Ziel der Arbeit war ein Reaktion/Regenerations Mechanismus vorzuschlagen, welcher eine kontinuierliche und erfolgreiche Operation sicherstellt.

Es konnte bewiesen werden, dass das Meiden von strukturellen Schäden, die während dem Modifikationsprozess enstehen können, die Schlüssel zur Herstellung von einem geeigneten Katalysator sind. Ein hohes Na^+ Austauschniveau und ein niedriger Dealuminierungsgrad sind von enormer Wichtigkeit um einen Katalysator mit hoher Aktivität zu garantieren. Eine hohe Konzentration von starke Brønsted Säurezentren begünstigt die Alkylierungsreaktion, sowie die Erreichung von einem hohen Hydridtransfer. Eine hohe Konzentration von schwachen Brønsted Säurezentren katalysiert die Dimerisierung. Na^+ Kationen schwächen die benachbarten Brønsted Säurezentren. Die Dealuminierung vom Katalysator führt zu der Umwandlung von Brønsted zu Lewis Säurezentren, welche die Konzentration von Olefinen in der Nähe der Brønsted Säurezentren erhöhen und die Deaktivierung beschleunigen. Ein erfolgreicher Katalysator für die Alkylierung muss eine hohe Konzentration an starken Brønsted Säurezentren und eine niedrige Konzentration an Lewis Säurezentren haben.

Es konnte gezeigt werden, dass während der Alkylierung ein Alkylat von hoher Qualität hergestellt wurde, diesen enthielt nur geringe Mengen an ungesättigte Komponenten und Aromaten war, sogar bis knapp vor der Deaktivierung. Ein Alkylat mit höherer Qualität wurde mit den besseren Katalysatoren erreicht. Spuren von ungesättigten Komponenten und Aromaten erschienen in grösserer Konzentration und mit kürzerer Reaktionszeit in dem Alkylat welches mit den schlechteren Katalysatoren, produziert wurde. Trimetylpentankomponenten haben einen Gewichtsanteil von ca. 80% des Alkylkates die mit Katalysatoren hoher Qualität hergestellt wurden, was einer hohen RON Nummer entspricht.

Es wurde bewiesen, dass der angesammelte Koks in den Mikroporen des Katalysators hauptsächlich von stark verzweigten Parafinnkomponenten, die einer $(CH_2)_3$ Serie folgen und Molmassen von 128 g/mol bis 548 g/mol besitzen. Der Koks, welcher im Inneren der Poren des Katalysators enstehet, ist ein Produkt der Propen Oligomerisierung. Die besseren Katalysatoren zeigten Koks niedrigerer Massen, mit einem Maximum von C_{12}-C_{15}, während die schlechteren ein Maximum von C_{24}-C_{27} zeigten. Niedrigere Mengen an ungesättigten

Komponenten und Aromaten wurden auch im Koks gefunden. Kleinere Mengen von $C_{12}H_{26}$ und $C_{16}H_{34}$, von Mehrfachalkylierungen, wurden auch im Koks nachgewiesen. Zyklische Komponenten und Aromaten wurden auf der Oberfläche des Katalysators gebildet, dieses konnte mit MALDI-TOF gezeigt werden. Diese Art von Komponenten konnten nicht nachgewiesen werden nachdem der Katalysator mit HF aufgelöst wurde, und der Koks mit Methylenchlorid extrahiert wurde. Deswegen war ihre Konzentration imgesamten Koks sehr gering. Diese Art von Molekülen sind für die Blockierung der Mikroporen an der Obefläche vom Katalysator verantwortlich. Die Grösse der mit MALDI-TOF nachgewiesenen Molekülen steigt mit der Reaktionszeit, für alle Katalysatoren. Diese sind C_nH_{2n-4} und C_nH_{2n-18} Moleküle, mit Molare Massen von 180 bis 360.

Zusätzlich wurde eine geeignete Methode für die Regenegierung von Katalysatoren für Isobutan/Buten Alkylierung entwickelt. Die Methode basierte auf Zyklen bestehend aus eine Reaktion, einer milden-Regenerierung in der flüssigen Phase, und einer harten Regenerierung in der Gas Phase. Bei der milden Regenerierung wurde die Lebenszeit verdoppelt. Eine hohe und unveränderte Produktqualität wurde auch nach mehreren Zyklen erreichen. Mittels harten Regenerierung wurde die Anfangsactivität des Katalysators wieder erreicht. Es wurde eine breite Verteilung von Produkten während der harten Regenegierung als Ergebniss des Crackens des Koks erhalten. Eine stabile Leistung und Produktqualitätwurde mit einer Kombination aus n-Reaktionen + n-milder Regenegierungen und einer anschliessenden harten Regenegierung erreicht. Es zeigte sich keine Deaktivierung.

Resumen

El objetivo de esta tesis ha sido entender las rutas de desactivación durante la alquilación de iso-butano / 2-buteno con zeolitas faujasíticas y correlacionar la actividad de éstas durante la alquilación con sus propiedades fisicoquímicas. Ha estado también dentro del objetivo de esta tésis, el proponer un procedimiento de reacción/regeneración que asegure una operación continua y exitosa.

Se ha mostrado que la supresión de daños estructurales, que pueden tener lugar durante el procedimiento de modificación, es el factor clave para obtener un catalizador adecuado para la alquilación. Un alto intercambio catiónico de Na^+ y un bajo nivel de desaluminación es de importancia vital para favorecer la reacción de alquilación y alcanzar una alta velocidad de transferencia de hidrógeno. Una alta concentración de sitios ácidos de Brønsted débiles cataliza la dimerización. Los cationes Na^+ debilitan sitios Brønsted ácidos adyacentes. La desaluminación del catalizador conduce a la transformación de sitios ácidos de Brønsted en sitios ácidos de Lewis, lo que incrementa la concentración de olefinas cerca de los sitios ácidos de Brønsted accelerando la desactivación del catalizador. Un catalizador exitoso para la alquilación tiene que poseer una alta concentración de sitios ácidos de Brønsted fuertes así como una baja concentración de sitios ácidos de Lewis.

Se ha mostrado que durante la reacción de alquilación se produce un alquilado de alta calidad que permanence prácticamente libre de compuestos insaturados y aromáticos, incluso a tiempos de reacción cercanos a la desactivación. Un alquilado de mayor calidad fué producido por los catalizadores de nivel superior. Compuesto insaturados y aromáticos aparecieron en mayor concentración y a menores tiempos de reacción en el alquilado producido por catalizadores de inferior calidad, aunque su concentración fue muy baja en todos los casos. Trimetilpentanos constituyeron aproximadamente el 80 % en peso del alquilado producido por un catalizador de alta calidad lo cual proporciona un alto índice de RON.

Se ha mostrado que los depósitos acumulados en los poros del catalizador fueron mayoritariamente formados por compuestos altamente parafínicos siguiendo una serie $(CH_2)_3$ y con pesos moleculares desde 128 g/mol hasta 548 g/mol. Los depósitos formados en el interior de los poros del catalizador fueron el resultado de oligomerización de propeno. Los catalizadores superiores mostraron depósitos de menor masa molecular con un máximo en su distribución en C_{12}-C_{15} mientras que catalizadores inferiores mostraron un máximo en C_{24}-

C_{27}. Se encontraron también pequeñas cantidades de olefinas y aromáticos en los depósitos. A su vez, se encontraron pequeñas cantidades de $C_{12}H_{26}$ y $C_{16}H_{34}$ en los depósitos, como resultado de alquilación multiple. Compuestos cíclicos y aromáticos fueron formados en la superficie del catalizador como se observó con MALDI-TOF. Estos tipos de compuestos no fueron detectados cuando el catalizador fue disuelto en HF y los depósitos extraídos con diclorometano. Por lo tanto, su concentración fué baja dentro del total. Estos tipos de compuestos fueron responsables del taponamiento de poros en la superficie del catalizador. El tamaño de las moléculas detectadas con MALDI-TOF incrementó con el tiempo de reacción para todos los catalizadores. Estas fueron de naturaleza C_nH_{2n-4} y C_nH_{2n-18} con pesos moleculares desde 150 a 360.

Se desarrolló un método adecuado para la regeneración de catalizadores para la alquilación de isobutano con buteno. Este método fué basado en ciclos conteniendo reacción, regeneración-moderada a través de lavado en fase líquida y regeneración-dura en fase gas. A través de la regeneración-moderada, el tiempo de vida del catalizador fué por lo menos doblado. Se mantuvo una alta e inalterada calidad del producto dentro de un conjunto de reacciones- regeneraciones moderadas. El catalizador fué llevado a su actividad (quasi-) inicial a través de regeneraciones-duras en fase gas. Se obtuvo una amplia gama de productos durante la regeneración dura como resultado del cracking de los depósitos acumulados. Se obtuvo un catalizador y una calidad de alquilado estable combinando un conjunto de n-reacciones/n-regeneraciones-moderadas con una regeneración-dura final en un proceso cíclico. No se observaron señales de desactivación.